Francisco Maria Baltazar Alçada Xara Brasil
Licenciatura em Ciências de Engenharia Mecânica

Samples Certification in Colorimetry for CIELAB Color Space

Dissertação para obtenção do Grau de Mestre em
Engenharia Mecânica

Orientador: Prof. Doutora Helena Navas, Professora Associada, NOVA School of Science and Technology

Co-orientador: Doutor Olivier Pellegrino, Responsável dos laboratórios de Fotometria, Radiometria e Radiofrequência, Instituto Português da Qualidade

Jurí:

Presidente: Prof. Doutor Rui Fernando dos Santos Pereira Martins
Arguente: Doutora Maria Isabel de Araújo Godinho
Vogal: Prof. Doutora Helena Víctorovna Guitiss Navas

NOVA SCHOOL OF SCIENCE & TECHNOLOGY

September, 2021

Samples Certification in Colorimetry for CIELAB Color Space

Acknowledgments

I want to express my acknowledgments to everyone that somehow cooperated directly and indirectly in the elaboration of this dissertation.

A special thanks to my advisers, Dr. Olivier Pellegrino, and Prof. Dr. Helena Navas, for all the availability, concern, and attention given along this process and to IPQ for the opportunity to do this internship in their facilities.

To my family for all the support given, especially to my sister and parents, who have always supported, backed me and my choices over the years, and granted that nothing ever missed to me, and my grandparents for always being a source of inspiration for me to do better and to be a better person.

And to all my friends for always being with me in the darkest moments and keeping me sane during this tough last year.

Abstract

The present study was developed in the Metrology Department (DMET) of the Portuguese Institute for Quality (IPQ). The objective was to participate to the development of a field of colorimetry based on spectrophotometry.

Indeed, spectrophotometry ensures high accuracy measurement results, which can be very beneficial for studies in colorimetry, allowing a better quality in the processes of the colors linearization.

As colorimetry only deals with the visible region of the electromagnetic spectrum, it is required to befall the spectrophotometry measurements along all that region of the spectrum. Then using the reflectance or the transmittance measured by the spectrophotometer, the data collected can be used to determine the chromaticity coordinates of a sample in diverse color spaces.

In this work, the CIELAB color space was chosen to be explored due to being a uniform color space, facilitating comparisons between different colors, due to equal distances in this color space, representing equal perceived color differences and to establish a correspondence with the RAL system, which is an European color matching system, developed by the RAL German Institute for Quality Assurance and Labeling.

Keywords: Colorimetry, Spectrophotometry, CIELAB, Reflectance, Transmittance, RAL

Resumo

O presente trabalho foi realizado no Laboratório de espectrofotometria Departamento de Metrologia do Instituo Português de Qualidade. O objetivo traçado visava o desenvolvimento de um estudo ligado à colorimetria baseado na espectrofotometria.

A espectrofotometria garante elevado rigor nas medições, o que pode ser benéfico para estudos na colorimetria, permitindo um aumento de qualidade nos processos de linearização das cores.

Como a colorimetria apenas se dedica ao estudo da região visível do espectro eletromagnético, é necessário que as medições espectrofotométricas ocorram apenas nessa região. Usando o fator de reflexão ou transmissão medido pelo espectrofotómetro, os dados recolhidos podem ser depois usados para determinar coordenadas cromáticas de amostras em diversos espaços de cores.

Neste trabalho, o espaço de cores CIELAB foi escolhido para ser explorado enquanto um espaço de cores uniforme, facilitando comparações entre cores diferentes, devido às distâncias observadas neste espaço de cores representarem as mesmas diferenças de cores percecionadas pelo observador e para estabelecer uma correspondência com o sistema RAL , que é um sistema europeu de correspondência de cores, desenvolvido pelo *German Institute for Quality Assurance and Labeling*.

Palavras-chave: Colorimetria, Espectrofotometria, CIELAB, Reflexão, Trasnmissão, RAL

Contents

List of Figures

List of Tables

Abbreviations and Acronyms

BIPM - *Bureau International des Poids et Mesures*

CIE – International Commission on Illumination

CMF – Color Matching Function

DMET – *Departamento de Metrologia*

EURAMET – European Association of National Metrology Institutes

IPQ – *Instituto Português de Qualidade*

NPL - National Physics Laboratory

SPD - Spectral Power Distribution

Symbols

a – Ordinate in the origin

A – Absorptance

$a*$ – $a*$ coordinate from CIELAB

${a^*}_{\frac{1}{0}}$ – $a*$ CIELAB coordinate from object $\frac{1}{2}$

b – Slope of the straight line

$b*$ – $b*$ coordinate from CIELAB

${b^*}_{\frac{1}{0}}$ – $b*$ CIELAB coordinate from object $\frac{1}{2}$

c – Speed of light

$[C]$ – Unknown Stimulus

${C^*}_{ab}$ – CIELAB chroma

${C^*}_{ab,\frac{1}{0}}$ – Chroma from object ½

$cov_{a,b}$ – Covariance associated to the calibration model involving variables a and b of equation 5.21

E_r – Relative error

f – Frequency

h – Uncertainty quoted by the external source

h_{ab} – CIELAB hue angle

${h^*}_{ab,\frac{1}{0}}$ – Hue angle from object $\frac{1}{2}$

J – Jacobian matrix associated to the CIELAB color space

k – Coverage factor

$L*$ – CIELAB lightness

$L^*_{\frac{1}{0}}$ – CIELAB lightness from object $\frac{1}{2}$

n – Number of repetitions

$P(\lambda)$ – Function of nonmonochromatic test color stimulus

$\bar{q}$ – Arithmetic mean

q_k – Value observed in the k^{th} repetition

R – Reflectance

R, G, B – Amount of each stimuli

$[R], [G], [B]$ – Units of matching stimuli

$R(\lambda)$ – Spectral reflectance

R_{c} – Corrected reflectance of the sample

$R'_{\text{c}}(\lambda)$ – Reflectance of the sample intended to measure

$R'_{\text{ref}}(\lambda)$ – Reflectance of 100 % using a certified sample where the light is totally reflected

$R_{\text{s}}(\lambda)$ – Sample´s reflectance

$R_s^*(\lambda)$ – Arithmetic mean of the 2 measurements´ days of the sample´s reflectance

$R^*_{\text{ref}}(\lambda)$ - Arithmetic mean of the 2 measurements´ days of the sample´s corresponding to 100 % Reflectance

$R'_0(\lambda)$ – Reflectance of 0% using a light trap, where photons are lost

$R^*_0(\lambda)$ – Arithmetic mean of the 2 measurements´ days of the sample´s corresponding to 0 % reflectance;

$s^2(q_k)$ – Experimental variance

$s^2(\bar{q})$ – Experimental variance of the mean

S_{Mi} – Standard deviation of the mean

S_{Ri} – Reproducibility uncertainty;

S_{ri} – Repeatability uncertainty;

$S(\lambda)$ – Relative SPD of the illuminant

$s(\lambda)_1$ – Standard deviation of the values obtained in the first day of measurements for each sample

$s(\lambda)_2$ – Standard deviation of the values obtained in the second day of measurements for each sample

T – Transmittance

$T(\lambda)$ – Spectral transmittance

T_{c} – Corrected transmittance of the sample

$T_{\text{f}}(\lambda)$ – Samples´ transmittance

$T'_{\text{f}}(\lambda)$ – Transmittance of the sample intended to measure

$T^*_{\text{f}}(\lambda)$ – Arithmetic mean of the transmittance measured in the two days of measurements;

$T^*_{\text{f}}(\lambda)_1$ – Arithmetic mean of the transmittance measured in the first day of measurements

$T^*_{\text{f}}(\lambda)_2$ – Arithmetic mean of the transmittance measured in the second day of measurements

$T_0(\lambda)$ – Arithmetic mean of the two measurements days of the sample´s corresponding to 0 % transmittance;

$T_{100}(\lambda)$ – Arithmetic mean of the two measurements days of the sample´s corresponding to 100 % transmittance;

$T'_0(\lambda)$ – 0 % transmittance, obtained with an opaque sample

T_i – Transmittance value of the sample measured in wavelength i

$T'_{100}(\lambda)$ – 100 % transmittance, obtained without any sample in the light path

U – Expanded uncertainty

$u(A)$ – Uncertainty associated to absorptance

$u(T)$ – Uncertainty associated to transmittance

$u(a)$ – Uncertainty associated to the ordinate in the origin (*a*) of the calibration equation 5.21

$u_A(T_i)$ – Type A uncertainty associated with the measurement of a sample´s transmittance (T_i)

$u_{acc}(\lambda)$ – Uncertainty of the wavelength associated to its accuracy

$u(b)$ – Uncertainty associated to the slope (*b*) of the calibration equation 5.21

$u_B(T_i)$ – Type B uncertainty associated with the measurement of a sample´s transmittance

$u_c(y)$ – Combined standard uncertainty associated to *y*

$u_{L^*}, u_{a^*}, u_{b^*}$ – Uncertainties associated to L*, a* and b* values of the CIELAB color space

$u_{non.\ lin}$ – Uncertainty associated to the non-linearity of the detectors;

$u_{phot.\ acc}$ – Uncertainty associated to the photometric accuracy;

$u_{photo.\ lev}$ – Uncertainty associated to photometric levelling

$u_{phot.\ noise}$ – Uncertainty associated to photometric noise

$u_{phot.\ rep}$ – Uncertainty associated to the photometric reproducibility;

u_{R_c} – Uncertainty associated to the corrected reflectance after the calibration model is applied

u_{repr} – Uncertainty of the wavelength associated to its reproducibility

u_{res} – Uncertainty of the wavelength associated to its resolution

$u_{R_{ref}}$ – Uncertainty associated to $R_{ref}(\lambda)$

u_{R_s} – Combined standard uncertainty associated to the sample reflectance

$u_{R_s^*}$ – Uncertainty associated to $R_s(\lambda)$

u_{R_0} – Uncertainty associated to $R_0(\lambda)$

$u_{stray\ light}$ – Uncertainty associated to the stray light

u_{T_f} – Uncertainty associated to $T_f(\lambda)$

$u_{T_f^*}$ – Uncertainty associated to $T^*{}_f(\lambda)$

$UT_f(\lambda)$ – Expanded uncertainty of the sample´s transmittance in function of the wavelength

u_{T_i} – Uncertainty associated to a sample by combining type A and type B

$u_X(\lambda), u_Y(\lambda), u_Z(\lambda)$ – Uncertainty associated to the tristimulus value X, Y, Z

u_x, u_y, u_z – Uncertainties associated to the chromaticity coordinates

u_X, u_Y, u_Z – Uncertainties associated to the tristimulus values

u_{T_0} – Uncertainty associated to $T_0(\lambda)$

$u_{T_{100}}$ – Uncertainty associated to $T_{100}(\lambda)$

u_λ – Uncertainty associated to the wavelength;

$u_{\rho'}$ – Uncertainty associated to ρ'

$V_{(L*,a*,b*)}$ – Variance and covariance matrix of CIELAB color space

V_m – Measured quantity value

V_r – Reference quantity value

$V_{(X,Y,Z)}$ – Variance and covariance matrix of the tristimulus values

Xi – i^{th} quantity that the measurand Y is dependent of

x_i – Estimate of the quantity X_i

X, Y, Z – Tristimulus Values

X_n, Y_n, Z_n – Tristimulus Values of specified white object (perfect reflecting diffuser)

$\bar{x}(\lambda), \bar{y}(\lambda), \bar{z}(\lambda)$ – CMF of the CIE 1931 standard observer.

Y – Measurand

$\frac{\partial f}{\partial x_i}$ – Sensitivity coefficient

Δa^* – CIELAB *a** difference

Δb^* – CIELAB *b** difference

ΔC^*_{ab} – CIELAB chroma difference

ΔE^*_{ab} – CIELAB color difference

ΔH^*_{ab} – CIELAB hue difference

Δh^*_{ab} – CIELAB hue angle difference

λ – Wavelength

λ_i – Wavelength i to be analyzed

$\rho'(\lambda)$ – Certified value of a sample with a reflectance near 100%

ϕ_i – Incident light flux

ϕ_r – Reflected light flux

ϕ_t – Transmitted light flux

ϕ_λ – Color stimulus function of the light seen by the observer

1. Introduction

This chapter presents the theoretical framework, the followed methodology, and the structure of the dissertation.

1.1. Thematic Framework, Motivations, and Objectives

The preservation and restitution of the colors have substantial economic importance, both in production (visualization, projection, print) and capture (digitalization, filming) of the images.

In the Spectrophotometry Laboratory of the *Instituto Português de Qualidade* (IPQ), colorimetry is an area in developing process through the development of measuring technical procedures of the regular transmittance and regular reflectance.

Colors are classified using color systems, which were developed with the idea of creating an uniform way to measure and compare colors. There are multiples color systems created along the years, and each one has its own vantages and disadvantages, one of the most utilized ones and also the one explored in this work is the CIELAB color space, that is known for being a uniform color space, this means that the color differences we perceive with raw eye are uniformimly similars to the differences in this color space.

The objective of this work consists of establishing a connection between the conceptual tools of spectrophotometry and colorimetry. The high accurate measurements in spectrophotometry grants rigor in obtaining the required data, for processes of the color linearization used in colorimetry.

This document results from a training realized in the Metrology Department (DMET) of the IPQ in the Laboratory of Spectrophotometry, belonging to the *Laboratório Nacional de Metrologia* (National Metrology Laboratory, LNM). The DMET mission is to secure the rigor and the traceability of the measurements in the national territory [1].

In the domain of spectrophotometry, the lab is responsible for developing the national metrology standards of photometry, entrusting it namely to maintain the national pattern of candela, calibrations, participation, and coordination of interlaboratory comparisons, and support the legal metrology [1].

The initially proposed program was:

- Integration in the activities developed in the Spectrophotometry Laboratory of the IPQ
- Introduction to colorimetric systems and study of the processes of color linearization
- Application of the colorimetric systems studies to determine relevant spectrophotometric quantity values in transmission and reflection mode in order of the color linearization process
- Redaction of report summarizing the work developed during the internship

1.2. **Study Methodology**

In this work, samples with known RAL Colours are analyzed and certified following a procedure that has been developed and improved in previous works realized in the spectrophotometry laboratory of IPQ and leading to colorimetry carachetrization within the CIELAB color space.

All the measurement results displayed along this work, include uncertainties associated to the quantities according to international recommendations, uncertainties are estimated by type A and type B methods, the combined standard uncertainty leading to the expanded uncertainty.

First it is necessary to calibrate the spectrophotometer~~,~~. ~~to~~ To this purpose, samples certified by the NPL in 2015, were measured. Combining the results obtained with the values from the certificate is deduced a calibration line following the document ISO/TS 28037:2010 that is applied to the data experimentally collected, originating corrected values of the results observed initially. These values should be closer to those referred to in the certificates reducing the errors associated with this procedure.

To correctly analyze and certify the samples of RAL colors, is followed the same procedure. Nine certified ceramic samples from NPL with 102 mm² area and 9 mm thick are measured in regular reflectance mode in all the visible spectrum with a 10 nm interval. The reflectance obtained by the spectrophotometer measurements combined with the values from the certificates are used to trace the calibration line following the standard ISO/TS 28037:2010.

This calibration line is later applied to the results obtained by measuring the reflectance of the samples from RAL colours, with the output of this operation being a corrected value of the reflectance measured initially.

The first step to analyze and certify the samples in colorimetry is to convert the corrected values of the reflectance along the visible spectrum to the tristimulus values. A combination involving an integral function of the reflectance, the spectral power distribution (SPD) of the illuminant, and the color matching function (CMF) of the colorimetric system utilized are necessary to realize this operation.

Once obtained the tristimulus values, it is possible to calculate the chromaticity coordinates and the CIELAB color space values of each sample.

1.3. **Structure of the Dissertation**

The present dissertation is divided into four main chapters, divided into subchapters and sections when necessary. A brief resume from each chapter follows:

Chapter 1, named “Introduction”, presents the theoretical framework, motivation, objectives, and the methodology that this work follows.

Chapter 2, named "Metrology, Colorimetry and Spectrophotometry", is divided in three subchapters the first one "Metrology" and it is presented a brief introduction to metrology, how it is divided, and some relevant concepts related to it that are important for the realization of this work. It is also approached the institutions responsible for developing metrology in Portugal and its duties.

In the second subchapter "Spectrophotometry", is done a small introduction to this topic, presented its importance in diverse applications, the themes of light behavior and electromagnetic spectrum are also approached, and it is explained how a spectrophotometer works.

In the third and last subchapter, "Colorimetry", is dedicated to this science. It is also succinctly explained how the human eye perceives color, the two different processes of creating color stimuli, and the color measuring systems.

In chapter 3, named "Case Study", the working conditions are presented, it is explained the followed methodology, invoving, the procedure used to collect trustfull results in trasmittance and in reflectance mode, the uncertainties calculation and the colorimetric analyzis of the samples from RAL Classic collection following the CIE recommendations including using the CIELAB color space.

Chapter 4, named "Conclusion", presents the main conclusions based on the results obtained and in the work developed during these experiments.

2. Metrology, Spectrophotometry and Colorimetry

In this chapter, metrology, spectrophotometry and colorimetry are introduced. These are fundamental concepts used for the realization of this work.

2.1. Introduction to Metrology

Metrology is the science of measurement and its application. It includes all theoretical and practical aspects of measurement, whatever the measurement uncertainty and field of application. Nowadays Europe, we measure and weigh at a cost equivalent to 6 % of our combined Gross National Product, so metrology has become a natural and vital part of our everyday life [2] [3].

Metrology covers three main activities. The definition and the realization of internationally accepted units of measurement, e.g., the meter and establishment of chains by determining and documenting the value and accuracy of a measurement and disseminating that knowledge, e.g., the documented relationship between the micrometer screw in a precision engineering workshop and a primary laboratory for optical length metrology.

And it is divided in also in three categories with different levels of complexity and accuracy:

1. **Scientific metrology** has the responsibility to organize and develop the measurement standards and their maintenance.

2**. Industrial metrology** has to guarantee that the instruments used in industry measurements have adequate functioning so that their procedures, measuring equipment and products can be trustworthy and safe.

3. **Legal Metrology** has to ensure that the measuring instruments and standards used for economic transactions meet all the legal requirements, which may be performed by a metrological operator [3].

Scientific Metrology

Conventionally it is divided into 9 main technical fields by *Bureau International des Poids et Mesures* (BIPM): Acoustics, amount of substance, electricity, and magnetism, ionizing radiation and radioactivity, length, mass, photometry and radiometry, thermometry, time, and frequency. With the European Association of National Metrology Institutes (EURAMET) three additional fields are considered: flow, interdisciplinary metrology, and quality [3].

Legal Metrology

The origin of legal metrology comes from the necessity to ensure fair trades, especially when involving weights and measures. The focus is to guarantee to citizens, in official and commercial transactions, a correct measurement result while assuring that the instruments used to do so are legally certified [3].

2.1.1. Portuguese System for Quality

The SPQ is the integrated set of entities and organizations interrelated and interacting that, following rules, principles, and procedures internationally acceptable, gathers efforts to dynamize the quality in Portugal and ensure the coordination of the three subsystems - standardization, quality, and metrology - with the purpose of the sustainable development of the country and the increasing of the life quality in the general society [4].

The Subsystem of the standardization is responsible for elaborating the standards in Portugal, mainly following international standards, and tries to guarantee accuracy in that aspect, ensuring that all the projects follow certain principles [4].

The metrology subsystem guarantees that measurements are realized according to proper guidelines, ensuring that the measurement units' patterns are kept and developed according to what is established at an international level [4].

The qualification subsystem fits the activities of accreditation, certification, and others related to the recognition of competencies and evaluation of the conformity [4].

Portuguese Institute for Quality

IPQ is the public institute that, integrated into the indirect State administration, has by mission the coordination of the SPQ, the promotion, and the coordination of activities that aim to contribute to show off the credibility of the action of its economic agents, as well as the development of necessary activities to its functions as the National Institute of Metrology and the National Standardization Organization [1].

IPQ was created in 1986 with the purpose of ensuring “the demand of quality of products and services for the increasing of the life quality of the citizens, increasing of the competitively of the economic activity in a context of progressive liberty of goods circulation” [1].

IPQ is also responsible for coordinating the SPQ and the management and coordination of the financial support programs, intervening in the cooperation with other countries in the domain of the quality [1].

2.1.2. Important Concepts related to Metrology

In this subsection, definitions of the most important terms and concepts of metrology are directly transcribed from the VIM [2].

Quantity is the “property of a phenomenon, body, or substance, where the property has a magnitude that can be expressed as a number and a reference”.

Kind of quantity is the “aspect common to mutually comparable quantities. Width and diameter are quantities of the same kind as it is possible to mutually compare both values unlike, for instance, width and kinetic energy”].

System of quantities is the “set of quantities together with a set of noncontradictory equations relating those quantities.”

Base quantity is the “quantity, in a conventionally chosen subset of a given system of quantities, where no subset quantity can be expressed in terms of the others” .

Table 2.1 – SI Base units each base quantity [1]

Base quantity	Base Unit	
Name	**Name**	**Symbol**
Length	metre	m
Mass	kilogram	kg
Time	second	s
Eletric Current	ampere	A
Thermodynamic Temperature	kelvin	K
Amount of Substance	mole	mol
Luminous Intensity	candela	cd

Derived quantity is the “quantity, in a system of quantities, defined in terms of the base quantities of that system. For example, in a system of quantities that has as base quantity the mass and the length, the pressure is a derived quantity defined by the quotient of mass by an area”.

Base unit is the “measurement unit adopted by convention for a base quantity”.

Quantity Dimension is the “expression of the dependence of a quantity on the base quantities of a system of quantities as a product of powers of factors corresponding to the base quantities, omitting any numerical factor.” The dimension of a quantity *Q* is expressed by equation 2.1 [2].

$$Q = \mathrm{L}^{\alpha}\mathrm{M}^{\beta}\mathrm{T}^{\gamma}\mathrm{I}^{\delta}\Theta^{\varepsilon}\mathrm{N}^{\zeta}\mathrm{J}^{\eta} \quad (2.1)$$

Where:

L - Length

M - Mass

T - Time

I – Electric current

Θ – Thermodynamic temperature

N – Amount of substance

J – Luminous intensity

$\alpha, \beta, \gamma, \delta, \varepsilon, \zeta, \eta$ – Dimensional exponents, its values can be positive, negative, or zero

Measurement is the “process of experimentally obtaining one or more quantity values that can reasonably be attributed to a quantity. It doesn´t apply to properties that haven´t a magnitude, also called nominal properties. It implies a comparison of quantities or counting entities. Measurement presupposes a description of the quantity commensurate with the intended use of a measurement result, a measurement procedure, and a calibrated measuring system operating according to the specified measurement procedure, including the measurement conditions”.

Measurement result is the “set of quantity values being attributed to a measurand together with any other available relevant information. A measurement result is generally expressed as a single measured quantity value and a measurement uncertainty”.

Measurement error is the “measured quantity value minus a reference quantity value. It can be used when there is a single reference quantity value to refer to, which occurs if a calibration is made by means of a measurement standard with a measured quantity value having a negligible measurement uncertainty or if a conventional quantity value is given, in which case the measurement error is known”.

Measurement uncertainty is a “non-negative parameter characterizing the dispersion of the quantity values being attributed to a measurand, based on the information used”.

Repeatability condition of measurement is a “condition of measurement, out of a set of conditions that includes the same measurement procedure, operators, measuring system, operating conditions and location, and replicate measurements on the same or similar objects over a short period of time” .

Reproducibility condition of measurementis a “condition of measurement, related to the precision of the measurement with a set of conditions that includes different locations, operators, measuring systems, and replicate measurements on the same or similar objects”.

2.1.3. Uncertainty and Errors of a Measurement

Every time a measurement is performed, there´s always an amount of uncertainty associated with it, either due to the different surrounding conditions that sometimes are not controllable or some minor mistakes during the preparation of the measure. Even if the conditions are precisely the same, the value obtained in different measures will very likely not be the same, so it´s hugely important to quantify its precision. Although, since the beginning of the scientific study, there was always a preoccupation with the accuracy of measurements, just in the more recent times was created an international procedure in cooperation with laboratories from different countries named GUM - *Guide to the expression of uncertainty in measurement* [5].

2.1.3.1. Uncertainty

In some circumstances, it is impossible to obtain the measurand directly from the measurement device, so when this happens, it is needed to use several input quantities to obtain the pretended measurand. This means that the measurand Y depends on the input quantities X_i $(i = 1, 2, \ldots N)$ as it is shown in equation 2.4 [5]:

$$Y = f\ (X_1, X_2, \ldots, X_i) \tag{2.2}$$

Where:
Y – Measurand
$X_1, X_2, \ldots, X_i - i$ input quantities that the measurand Y is dependent of

To each input quantity, a given uncertainty is associated. The uncertainties obtained by direct measuring or external sources such as materials reference properties, certificate reference materials or manufacturers specifications, or in some cases also other measurands uncertainties previously calculated [5].

Estimate of the Uncertainties

There are two types of evaluations of the uncertainty of measurement. Each one reflects a probability distribution related to the values of the measurand [5]:

Type A – The uncertainty evaluation is calculated by a statistical analysis of a certain number of observations.

Type B – The uncertainty evaluation is determined by different means than the ones used in Type A.

Type A Evaluation of Standard Uncertainty

The best estimate possible to evaluate the quantity q that was measured through a number n of independent observations under the same circumstances is to calculate the **arithmetic mean or average** $\bar{q}$ of the n observations, equation 2.3 [5].

$$\bar{q} = \frac{1}{n}\sum_{k=1}^{n} q_k \qquad (2.3)$$

Where:

$\bar{q}$ - Arithmetic mean

q_k – Value observed in the k^{th} repetition

n – Number of repetitions

The values of q_k always have a slight variation in the repeated observations under the same circumstances, primarily due to random factors. To characterize those variations, the **variance** σ^2 is calculated by equation 2.4, which reflects a probability distribution of the value q [5].

$$s^2(q_k) = \frac{1}{n-1}\sum_{j=1}^{n}(q_k - \bar{q})^2 \qquad (2.4)$$

Where:

$s^2(q_k)$ – Experimental variance

The positive square root of $s^2(q_k)$, $s(q_k)$ the **experimental standard deviation** is what describes the distribution of the mean $\bar{q}$. The best estimate for the **variance of the mean** is $\sigma^2(\bar{q}) = \frac{\sigma^2}{n}$ given by equation 2.5 [5]:

$$s^2(\bar{q}) = \frac{s^2(q_k)}{n} \qquad (2.5)$$

Where:

$s^2(\bar{q})$ – Experimental variance of the mean

Thus, for an input quantity X_i determined from n independent repeated observations $X_{i,j}$, the standard uncertainty $u(x_i)$ of its estimate $x_i = \bar{X}_i$ is $u(x_i) = s(\bar{X}_i)$, with $s^2(\bar{X}_i)$ [5].

Type B Evaluation of Standard Uncertainty

This method calculates de standard uncertainty using means that do not require a repeated number of observations, based on scientific judgment using data provided by certificates, material properties, or manufacturer´s specifications, for example [5].

It uses a probability distribution of the input quantity X_i and the confidence level of that quantity to obtain the standard uncertainty. The most used models of the probability distributions are the normal/Gaussian, triangular, and rectangular distribution which are also the ones approached along with this document [5].

Rectangular Distribution

It is used when it´s not possible to accurately know the quantity X_i but it´s possible to foresee its range of values, this means that it is hard to predict its value, and it is only possible to evaluate in which interval [-*a*,+*a*] it will be. The only conclusion taken is that the probability of X_i to be in the interval [-*a*,+*a*] is equal to 1, therefore is essentially impossible to X_i to be outside of that range of values, figure 2.1 illustrates a graphical example of a rectangular distribution graphically [5].

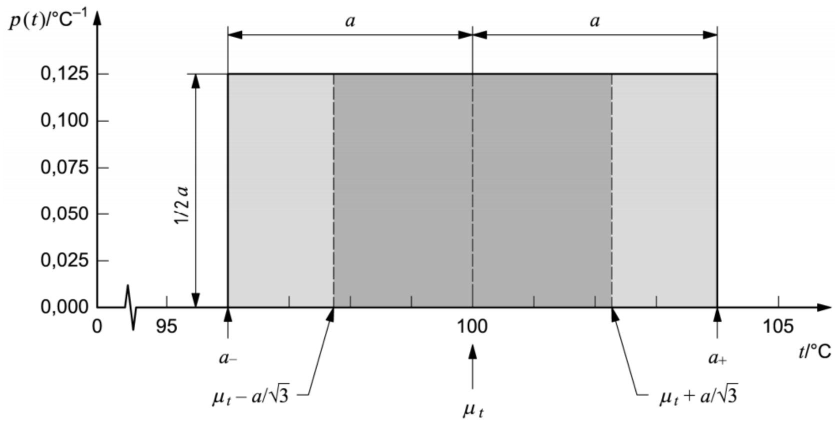

Figure 2.1 – Example of a rectangular distribution [5]

Thus, the midpoint of the interval [*a*-, *a*+] corresponds to the estimate x_i of the quantity X_i, with a variance associated as it is shown in equation 2.6:

$$u^2(x_i) = \frac{(a_+ - a_-)^2}{12} \tag{2.6}$$

Where:

x_i – Estimate of the quantity X_i

In the situation where $a_+ - a_-$ is equal to $2a$, the variance is given by equation 2.7.

$$u^2(x_i) = \frac{a^2}{3} => u(x_i) = \pm\frac{a}{\sqrt{3}} \quad (2.7)$$

Triangular Distribution

Unlike the rectangular distribution, in the triangular, it is known *a priori* that the values closer to the estimate $x_i$of the quantity X_i are more likely than the ones further from it and that there´s an equal probability of its values to be in the interval $[-a, x_i]$ or $[x_i, +a]$, figure 2.2 illustrates a graphical example of a triangular distribution [5].

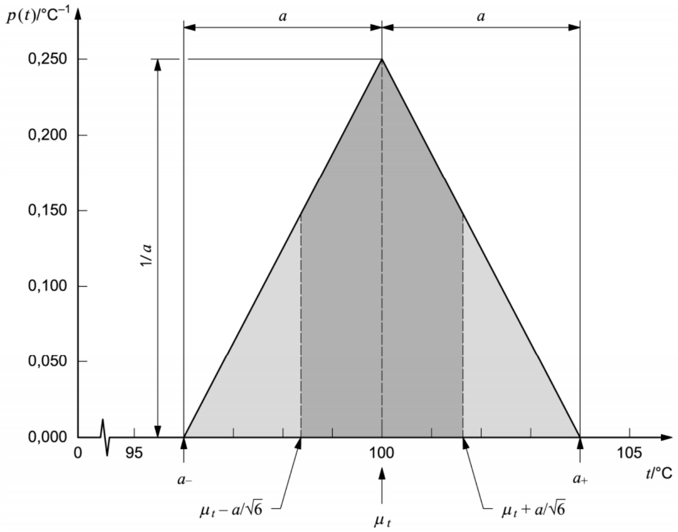

Figure 2.2 – Example of a triangular distribution [5]

The variance $u(x_i)^2$ and the standard deviation $u(x_i)$ are respectively given by equations 2.8 and 2.9.

$$u(x_i)^2 = \frac{a^2}{6} \quad (2.8)$$

$$u(x_i) = \frac{a}{\sqrt{6}} \quad (2.9)$$

Normal or Gaussian distribution

If the estimate of X_i is given by a certificate, a manufacturers specification, or another external source, and if its quoted uncertainty (h) is declared as being a multiple of a standard deviation, σ, its standard uncertainty $u(x_i)$ is given by equation 2.10 [5].

$$u(x_i) = \frac{h}{k} \tag{2.10}$$

Where:

h - Uncertainty quoted by the external source

k – Coverage factor

Figure 2.3 illustrates a graphical example of a normal/gaussian distribution.

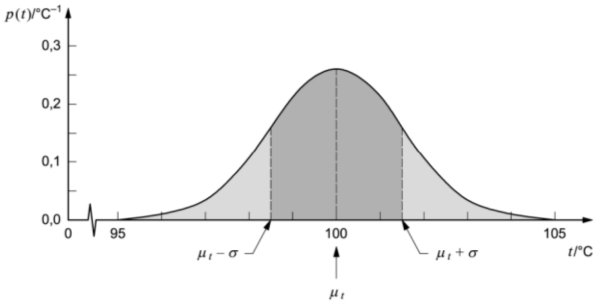

Figure 2.3 – Example of a normal/gaussian Distribution [5]

Combined Standard Uncertainty

Standard measurement uncertainty, denoted by $u_c(y)$ that is obtained using the **individual standard measurement uncertainties** $u(x_i)$ associated with the **input quantities** x_i in a measurement model [5].

The **input quantities** of the function Y can be divided in **correlated**, in case that at least two of them are related to each other and **independent** if none are dependent on another. In this experience, all are independent [5].

When all the **input quantities** are independent of each other, the **combined standard uncertainty** $u_c(y)$ is given by equation 2.11 [5]:

$$u_c^2(y) = \sum_{i=1}^{N} \left(\frac{\partial f}{\partial x_i}\right)^2 u^2(x_i) \tag{2.11}$$

Where:

$\frac{\partial f}{\partial x_i}$ – Sensitivity coefficient

$u_c(y)$ – Combined standard uncertainty

Expanded Uncertainty

It is denoted by U and relates the **combined standard uncertainty** $u_c(y)$ and the **coverage factor** k by multiplying one for another [5].

$$U = k.u_c(y) \tag{2.12}$$

Where:

U – Expanded uncertainty

k – Coverage factor

It is used in applications when it is needed to attribute an uncertainty to the measure of the results that encompasses a significant fraction of values that might be reasonably attributed to the measurand.

Depending on the level of confidence required by the interval $[y - U, y + U]$, a value to the **coverage factor** k is attributed. Usually, a value such as 2 or 3 is good enough to use as it already has a large percentage of the level of confidence. Table 2.2 shows the level of confidence in percentage to each coverage factor k [5].

Table 2.2 – Value of the coverage factor *k* that produces an interval having a level of confidence *p* assuming a normal distribution [5]

Level of confidence *p* (percent)	**Coverage factor *k***
68,27	1
90	1,645
95	1,96
95,45	2
99	2,576
99,73	3

2.1.3.2. Errors

During the calculations of a measurand and its precision, there are always at least small errors, and it is important to understand its origins to obtain a good accuracy in measures being made and possibly avoid them in future situations.

It is characterized by the difference between the **measured quantity value** and the **reference quantity value** [5].

They are divided into two types according to their essence [5]:

Systematic Error is the “component of measurement error that in replicate measurements remains constant or varies in a predictable manner” [2] .

Random Error is the “component of measurement error that in replicate measurements varies in an unpredictable manner” [2] .

In order to evaluate a followed methodology's precision, material reference certificates by accredited institutions, interlaboratory comparisons, or comparative tests can be used [5]. In this study, the material reference certificates are used to verify the quality of the measurements.

The **relative error**, expressed in percentage (%), is used to evaluate a measured value with respect to a reference value: in this study, a measured value is accepted when the relative error is equal to or less than 5 %, given by equation 2.13.

$$E_{\mathrm{r}} = \frac{V_{\mathrm{m}} - V_{\mathrm{r}}}{V_{\mathrm{r}}} \tag{2.13}$$

Where:

E_{r} – Relative error

V_{m} - Measured quantity value

V_{r} - Reference quantity value

2.2. Spectrophotometry

Spectrophotometry is a branch of spectroscopy, which deals with the measurement of the reflection or transmission properties of a body, surface, or material as a function of wavelength. It strongly depends on the geometrical and spectral conditions of the measurement [6].

The first studies related to this subject go back to the XVIII century when Pierre Bouguer, a notorious French scientist, was drinking a glass of wine during a brief vacation in Alentejo, Portugal, and noticed a change in the light when it passed through the wine. By stating that he wrote *Essai d'optique sur la gradation de la lumière,* that he describes the light loss when passing through a certain extent of the atmosphere [7].

This discovery led to, a few years later, Beer-Lambert´s law which describes the beam absorption of electromagnetic radiation (typically, visible light) that propagates through a dissipative medium, establishing a relation between the intensity of the radiation and the optical path within the medium. Figure 2.4 illustrates the Beer-Lambert´s law where the incident beam with passes through a dissipative medium of an optical path and hits the detector with I intensity [8].

.

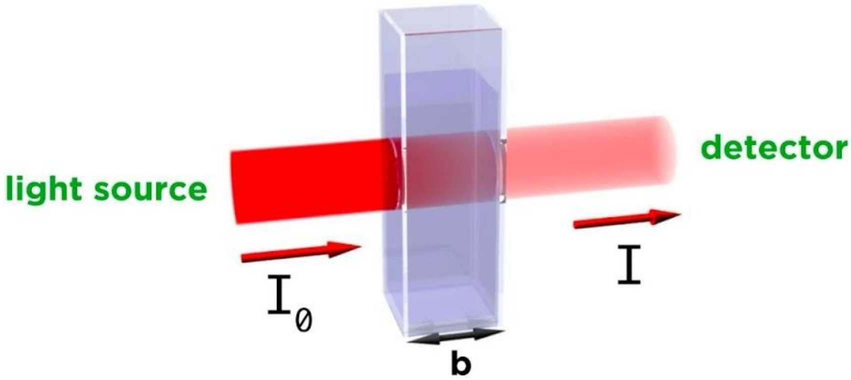

Figure 2.4 – Illustration of Beer-Lambert´s law [9]

Each molecule has its own radiation spectrum. Indeed at given wavelengths radiations are absorbed by given molecules, creating a kind of an identity card based on those wavelengths. Knowing this, molecules are enabled to be identified in other planets by looking at their spectrum and analyzing their composition. Figure 2.5 shows an example of the emission spectrum of some atoms.

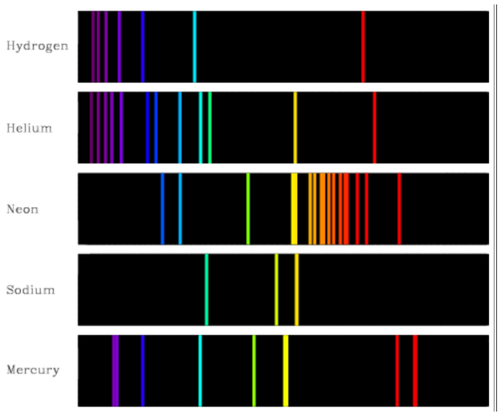

Figure 2.5 – Emission spectrum of several atoms [10]

2.2.1. Electromagnetic Spectrum

The electromagnetic spectrum is the set of all types of electromagnetic radiations. It covers all the radiations with the wavelength ranging from as big as thousands of kilometers to as small as a fraction of the size of atoms. Different wavelengths have different sources and utilities, and they also can carry different types of information [11], [12].

The classification of a radiation may be performed according to its frequency or wavelength, linked by the eq. 2.14 [11]:

$$\lambda = \frac{c}{f} \tag{2.14}$$

Where:

λ – Wavelength

c – Speed of light

f – Frequency

The different spectral domains are designated according to:

Radio waves – These are the ones with the most extensive wavelengths. They are very useful in communications, being used in radio stations and televisions broadcast to transmit its signal from the operator to the user. They used to be known as Hertz waves a century before due to being first produced by this German physicist [13].

Microwaves – With a shorter wavelength and a higher frequency than the radio waves, they are mainly used to warm food, as they force water particles to move and rotate faster and with that increasing the food´s temperature, they are also used in meteorology to provide the images that allow predicting the weather around the globe [13].

Infrared waves (IR) – It is the wavelength range right before the visible light, humans cannot see them, but it´s possible to feel them in the form of heat. There is an extensive range of utilities to use them, from tv remote controls to night vision goggles, and to change information between cell phones, for example [13].

Visible light – It´s the only wavelength range that humans can see from around 380 nm to 700 nm [13].

Ultraviolet – It is also in the border with the visible light. Though humans are not able to see it, some insects like bees can observe them. It´s divided into three types: UV-A, UV-B, and UV-C according to the amount of energy that they transmit while the first ones mentioned can be used to shine fluorescent materials in a darkroom and are harmless, UV-B and UV-C can be pretty dangerous because of the amount of energy they have, UV-B can give humans some tan but also sunburns, in case people don't protect themselves from them, and in last case scenario skin cancer. The UV-C can be very dangerous to our health but luckily is almost entirely captured by the earth's atmosphere due to the ozone layer. That is also one of the reasons why it is so important not to let the ozone hole grow [13].

X-Rays – Mostly known for their use in medicine, it´s a high energized radiation with a tiny wavelength from 0.03 nm to 3 nm [13].

Gamma Rays – It is the most potent kind of radiation produced by the most energetic objects in the Universe. A nuclear explosion or radioactive decay can also create it. With a wavelength of a fraction of atoms, they can pass through almost everything. It is also used in medicine to sterilize objects and cancer treatments [13].

In figure 2.6 the different spectral domains are displayed according to some properties.

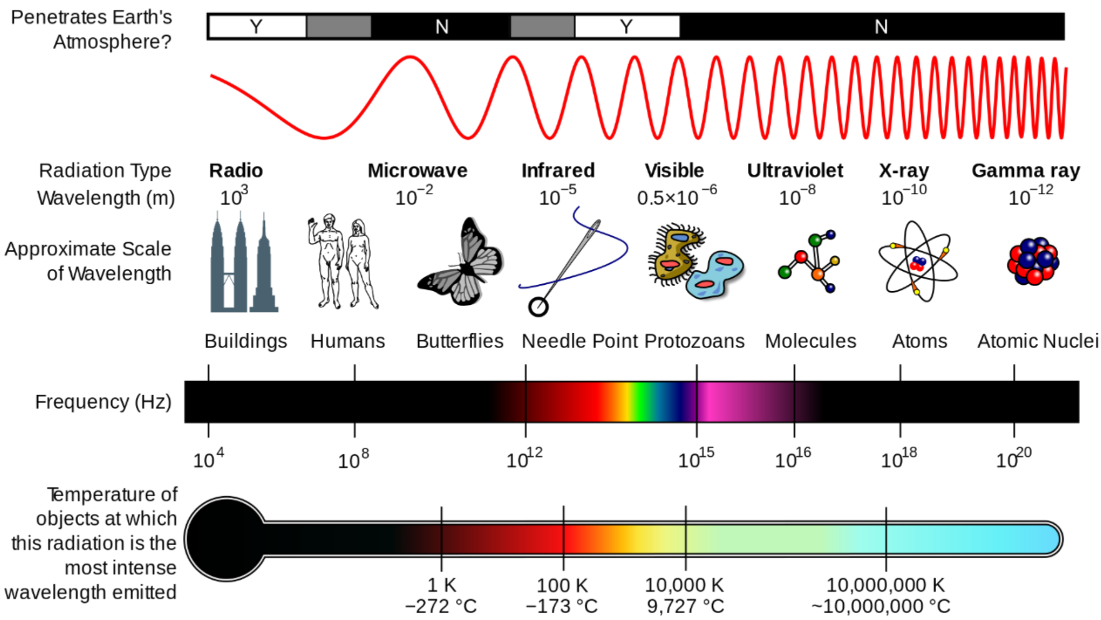

Figure 2.6 – Some properties of the electromagnetic waves [14]

Even though we can only see a minimal set of wavelengths, with the help of technology, it is possible to create images with all the types of radiations to better visualize and understand the phenomena that cannot be spotted with the bare eye. For example, figure 2.7 displayes an image created by combining different kinds of electromagnetic waves.

Figure 2.7 – Crab Nebula spanning nearly the entire breadth of the electromagnetic spectrum

2.2.1. Light Behavior

From the interaction of the light with the propagated medium, three main perceptions are enabled to be distinguished, displayed in figure 2.8:

Transparent – When almost no interaction occurs, leading to an almost maximum regular transmission resulting in a clear vision through the medium.

Translucent – When the light has some interaction with the medium leading to diffuse transmission, not allowing a clear vision, but instead a distortion visualization of the objects behind it.

Opaque – A surface that doesn´t let the light pass through, allowing no transmission at all. The light is reflected or absorbed.

a)  b)  c) 

a) Transparent; b) Translucent; c) Opaque medium

Figure 2.8 – Mediums of the light propagation [15]

When a light beam reaches a surface, three phenomena can occur, absorption, reflection, and transmission, and according to the light beams and surface characteristics, different kinds of reflection and transmission can be observed [16].

Transmission only occurs on a surface that lets the light pass through it. When this happens, similarly to reflection, the light may spread in only one direction, regular transmittance, or in many directions, diffuse transmittance, figure 2.9 [16].

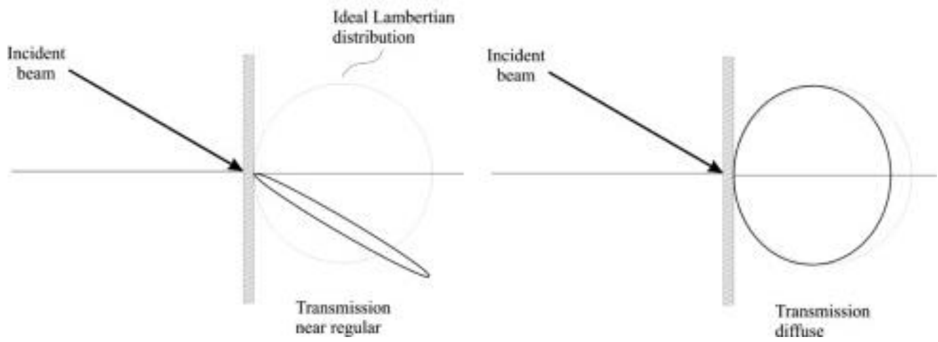

Figure 2.9 – Different kinds of transmission [17]

In spectrophotometry, the transmittance is given by equation 2.15:

$$T = \frac{\phi_t}{\phi_i} \tag{2.15}$$

Where:

T – Transmittance r

ϕ_t – Transmitted light flux

ϕ_i – Incident light flux

If the light beam, when **reflected,** spreads itself in many directions, it´s called diffuse reflection in case that doesn´t happen, and it keeps concentrated in one direction with the same angle as the incident beam, like when a laser beam hits a mirror it´s a specular reflection, and if that reflection goes back to the direction from where it came, it´s called retroreflection figure 2.10 illustrates the different kinds of reflection [16].

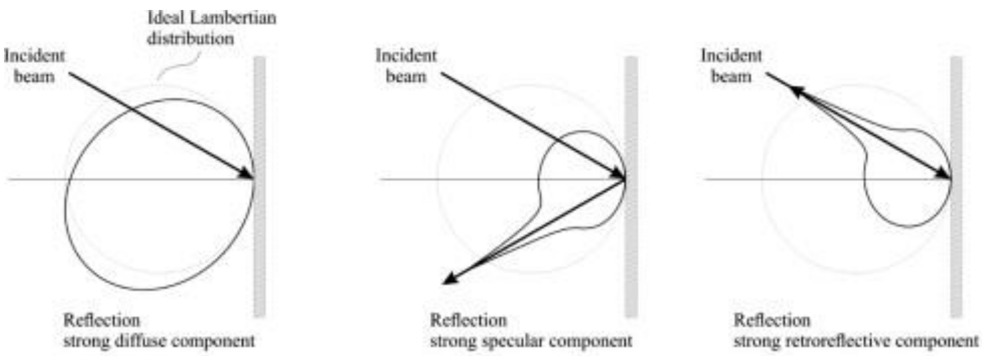

Figure 2.10 – Different kinds of reflection [17]

Similarly to transmittance, the reflectance is calculated according to equation 2.16

$$R = \frac{\phi_r}{\phi_i} \tag{2.16}$$

Where:

R – Reflectance

ϕ_r – Reflected ight flux

ϕ_i – Incident light flux

In table 2.3, a short synthesis of the influence factors involved in the phenomenon of light and its propagation is given, namely in the transmission and the reflection.

Table 2.3 – Regular and diffuse reflection and transmission characteristics [9]

Measurement		Geometric distribution of the light beam	Responsible elements	Characteristics and appearance obtained
Transmission	Regular	Beam transmitted through the sample in the same direction it reaches the surface	Homogenous medium with planar parallel faces	Clear or transparent surface
	Diffuse	Beam transmitted through the sample in many different directions	Dispersion particles or sample refraction (non-opaque) and rough surface.	Translucent or cloudy surface
Reflection	Regular	Beam reflected only in the mirrored direction with respect to the surface perpendicular	Smooth sample surface	Shining surface
	Diffuse	Reflection in all the directions	Rough sample surface	Clear surface

The quantity corresponding to the absorption of light by a sample is the absorptance. Then, the energy associated with the light beam is transformed either into thermic energy or internal energy.

Contrarywise to reflectance and transmittance, the absorptance is evaluated by using a logarithmic function instead of a linear one that is obtained following Beer-Lambert´s law as it is shown in equation 2.17 [16]:

$$\mathrm{A} = -\log_{10}\left(\frac{\phi_t}{\phi_i}\right) = -\log_{10}(T) = \log_{10}\left(\frac{1}{T}\right) \tag{2.17}$$

Where:

A – Absorptance

T – Transmittance

ϕ_t – Transmitted light flux

ϕ_i – Incident light flux

As expected and possible to see in equation 2.17, there is a relation between absorptance and transmittance. The bigger the transmittance, the lower the absorptance, and vice-versa. This is illustrated in figure 2.11 below.

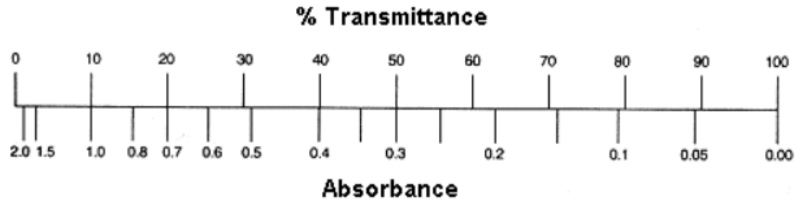

Figure 2.11 – Relation between absorbance and transmittance [18]

2.2.2. Spectrophotometer

The spectrophotometer a the device utilized to measure the transmittance and reflectance in spectrophotometry. It has the capacity to capture wavelengths from 200 nm to 2500 nm, i.e., from the near-infrared (NIR) zone until the ultraviolet (UV) region [9].

The working principle of the spectrophotometer is based on the division in different wavelengths of an incident light beam with the help of a diffraction grating, and quantitantively detects the light beam after its interaction with the sample under analysis. Figure 2.12 displays schematically the main components of a spectrophotometer in analysing a sample solution.

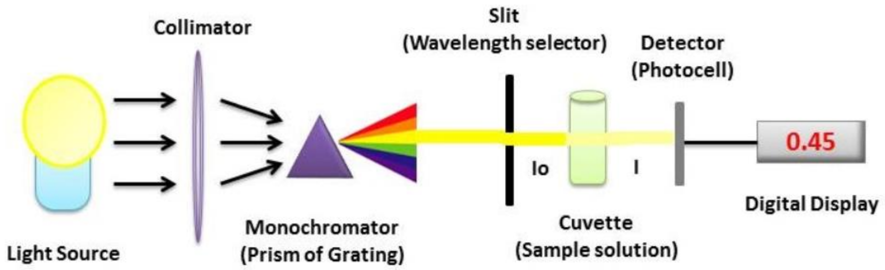

Figure 2.12 – Illustration of the essential components of spectrophotometer [19]

There are two types of spectrophotometers: single beam and double beam. In a single beam spectrophotometer, the radiation follows the path: light source – dispersive system – sample – detector, meaning that once interacted with the sample the beam goes straight to the detector, as displayed in figure 2.13. On the other hand, in the double beam spectrophotometer before reaching the sample, the light beam is divided in two parts, each one following its own path, one goes in the direction of the sample and the other to the reference cell as displayed in figure 2.14 [9].

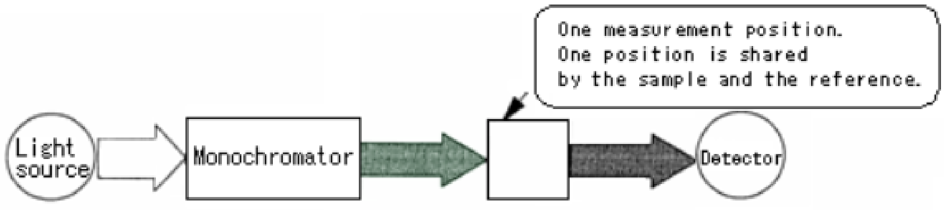

Figure 2.13 – Single beam spectrophotometer graphical scheme [20]

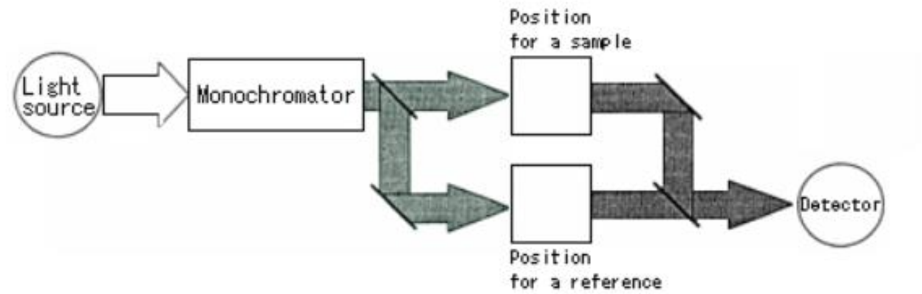

Figure 2.14 – Double beam spectrophotometer graphical scheme [20]

More specifically it can be said that the main components of the spectrophotometer are:

- Light Source
- Dispersive system
- Compartment for the sample
- Signal detector
- Signal processor

Light Source

Ideally, the light source should enable emitting the light beams with enough power and stability for a good measurement in all the spectral interval, with a constant intensity [21].

For these purpose two different kinds of lamps are used in a spectrophotometer.

- **Halogen and Tungsten lamps** that enables measurements in the wavelength interval from 1100 nm until around 350 nm, i.e., between the near-infrared zone (NIR) and the UV region respectively.

- **Deuterium lamp** covers the range of the ultraviolet (UV) zone from around 350 nm to 200 nm.

Figure 2.15 graphically illustrates the energy distribution of both of these light sources.

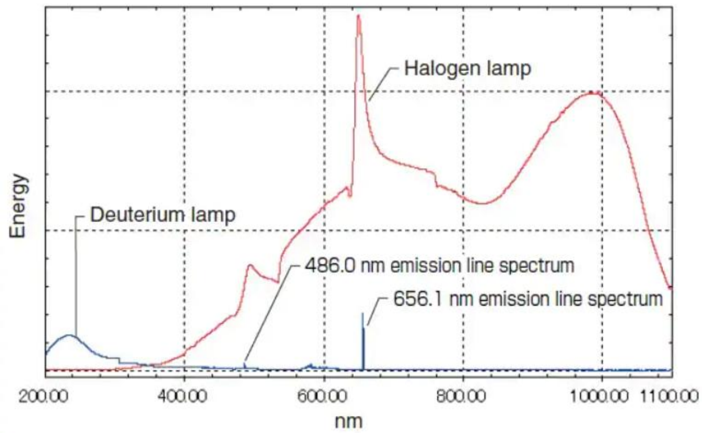

Figure 2.15 – Light Source Energy Distribution [22]

Dispersive System

The function of the dispersive system is to process all the incident light and regulate the wavelength range pretended to be measured. It is constituted by a set of lenses and mirrors, a diffraction grating, and a monochromator [21].

The most known type of monochromator and one of the most utilized ones is the Czerny-Turner monochromator illustrated in figure 2.16.

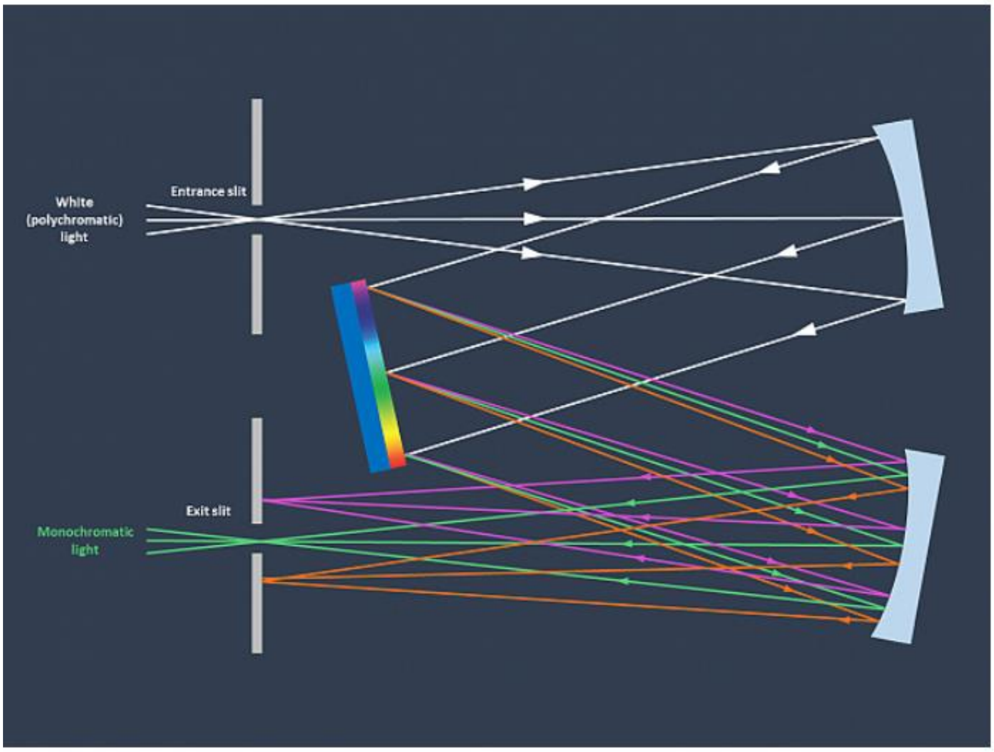

Figure 2.16 – Schematic representation of a Czerny-Turner monochromator [23]

As it is possible to see in the image above, the light beam enters the monochromator by the entrance slit and then reaches the first mirror. Usually, it is utilized concave mirrors, which can collimate the light making all the light beam parallel. If it were possible to look at the light beam after it has passed the first mirror, all that would be seen was white light, which is nothing more than the combination of all the visible wavelengths [22].

In the next stage, this all-parallel light beam reaches the dispersive element. A dispersive element is a component that can separate the light in the different wavelengths by changing its angle and velocity after it reaches a surface, it can be a prism or a diffraction grating, but nowadays, the most common one in spectrophotometers and also the one that is used in the measurements made along this paper is the diffraction grating. The number of lines per meter that the diffraction grating has is related to the resolution of the spectrophotometer in a way that the more lines per meter the diffraction grating, the higher the spectrophotometer resolution [22].

After being reflected by the diffraction grating, the light beam is guided to the second mirror, which has the same properties as the first one, then it reaches the exit slit. In order to control the wavelength that is intended to be measured, it is possible to change the position of the diffraction grating, which allows different wavelengths to pass through the slit. Also, it is possible to change the dimension of the slit by increasing or decreasing it [22].

Chopper

The chopper is an element that is part of a double beam spectrophotometer. Its function is to separate the single beam in two so that after passing through it, they follow different paths, one goes in the direction of the sample, and the other goes to the reference cell [9].

As it can be seen in the image below, the chopper has three different sections:

1. Transparent section – When the light beam passes through this section, it goes in the direction of the reference cell.
2. Mirrored section – When the light beam hits this area of the chopper, it is reflected in the direction of the sample.
3. Black section – This section absorbs the light beam; this allows the spectrophotometer to do minor corrections during the measurement automatically.

Figure 2.17 schematizes a chopper and how it works.

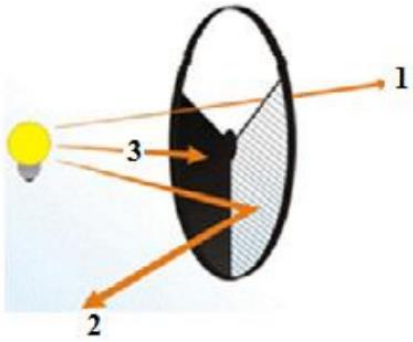

Figure 2.17 – Chopper and its working principles illustration [21]

The chopper is constantly rotating, and its rotational speed should be adjusted to the capacity of the detectors. The beam that passes through the reference cell and the one that passes through the sample cell reaches the detectors simultaneously so that the values can be electronically corrected [22].

Detector

The detector in a spectrophotometer has the function to convert a light signal into an electric signal. It should have a linear response in a wide wavelength range, be extremely sensitive, it also should produce no noise and have a short response time. The type of detector used depends on the wavelength range used in the measurement [24].

The photomultiplier covers the range from 175-900 nm. It is composed of a photoemissive cathode, a series of electrodes (dynodes), and an anode. When a photon hits the cathode, it produces electrons that head towards the series of electrodes, each one keeps producing more and more electrons, amplifying the signal, and then when they reach the anode, the signal is already electronically amplified. The PbS detector is a photoconductive detector and can be used to measure the wavelength range near the infrared zone, from 700 nm to 3300 nm, figure 2.18 schematically demonstrates hoe the photomultiplier tube operates. This laboratory spectrophotometer, a Lambda 950 from Perkin Elmer, has the two kinds of detector [24].

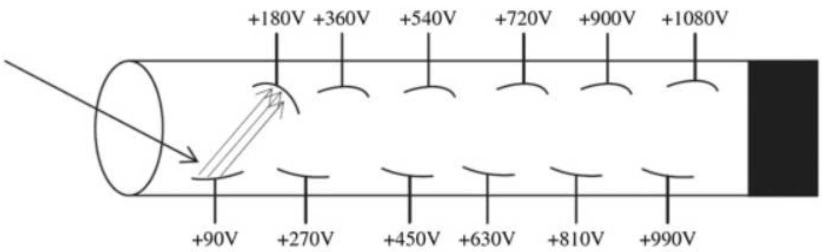

Figure 2.18 – A schematic diagram of a photomultiplier tube [24]

Signal Processor

The signal processor is an electronic device that amplifies the electric signal that came from the detector. It can change the electric current to alternating current (AC) or direct current (DC) and filter the signal by removing unwanted components. After this stage, the data is displayed in an output device. The Lambda 950 software installed in the computer is connected to the spectrophotometer used in this study [9].

Integrating Sphere

The integrated sphere, figure 2.19 is a component that enables the spectrophotometer to measure the reflectance of a sample, although it can also measure the transmittance. Its inner walls are made of a material with a light scattering property, and an extremely high reflectance usually is barium sulfate, which has a reflectance of 99 % and has its own detectors [22].

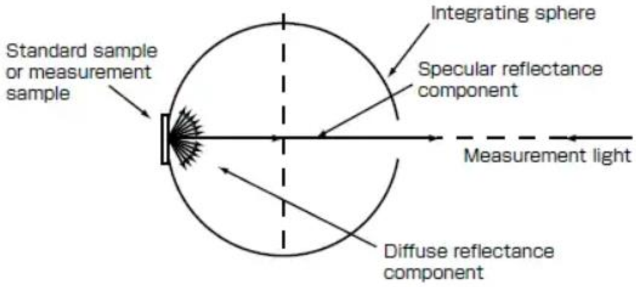

Figure 2.19 – Schematic of a total reflectance measurement [22]

2.3. Colorimetry

According to the vocabulary of the international electrotechnical commission (IEC), the colorimetry is the "measurement of colour stimuli based on a set of conventions" [25]. It has considerable importance in numerous industries such as fashion, wines, and cars, for example. People usually choose cars or clothes by their color, so they must be well identified, Ferrari for instance, has its own type of red, named the Ferrari Red, so they have to make sure that it is always the same [26] [27].

The phenomenon of color is quite complex, people might tend to think that each object or surface has its own color, but that is far from the truth. In fact, it is usually a perception that relates to 3 subjects [17]:

- The interaction of the radiation with the surface – Each surface absorbs and reflects a specific interval of radiations wavelength. The perceived color is nothing more but the reflected radiation from a surface.

- The light source – Depending on the light source, our perception of the surface color varies. This means that different light sources might give us a different perception of the same surface. For example, the light that comes from the sun is different from the one received from most lamps, and both probably make us perceive the same reflected radiations in different ways.

- The human eye – It is only possible for the human eye to capture radiations of given wavelengths in the visible spectrum, between 380 nm and 780 nm, which means that humans do not distinguish radiations of other wavelengths. Also, each person perceives and processes those differently, despite that usually the difference is minimal.

There is also the situation that we look directly to the light source. In this case, the perception of color depends only on the light source and the eye [17].

Within the visible region, the radiation near 700 nm produces the sensation of the red color, while between the 550 nm and 520 nm is green and closer to the 450 nm is blue, as it is shown in figure 2.20 [17].

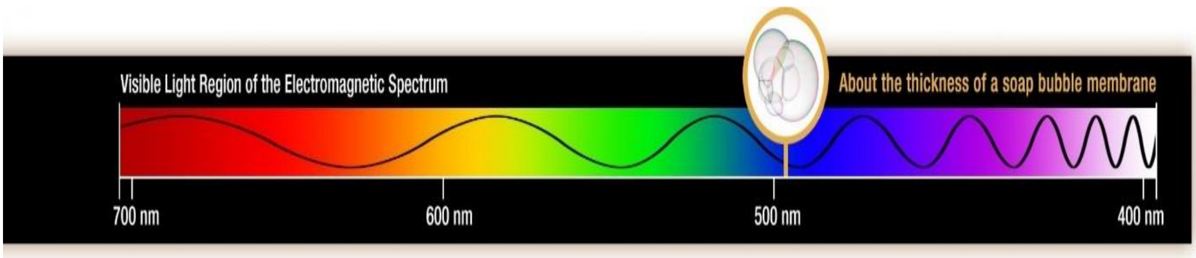

Figure 2.20 – Visible spectrum wavelengths [13]

2.3.1. Perception of the Color by the Human Eye

For the scope of this subsection it is possible to divide the eye components according to their function.

Focusing region

It is responsible for focusing on the image that our eyes are assimilating. The main components are the cornea, iris, pupil, and lens. The first one refracts or bends the light entering the eye towards the pupil, which adapts its size according to the amount of light that it's supposed to pass through it. The iris controls this size variation. Then it reaches the lens that changes shape depending on what is being focused on and sends this information to the retina. Figure 2.21 is a schematic image of the right eye [28].

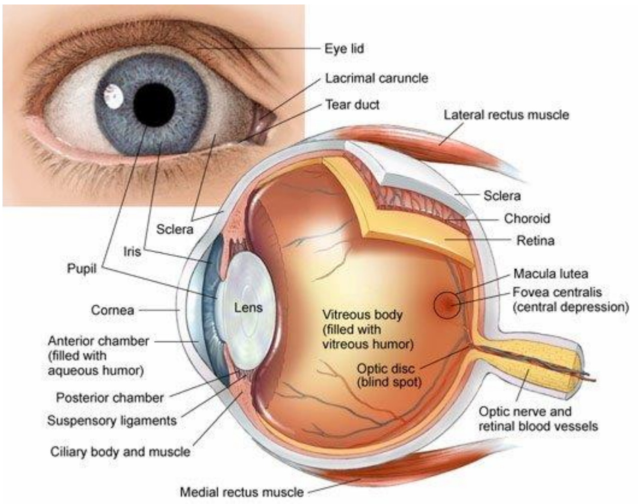

Figure 2.21 – Scheme of the right eye [29]

Transduction Region

The main components are the retina, rods, and cones. Rods and cones, are photoreceptors which are responsible for processing the light that enters the eyesIndeed, under exposition to light, a chemical reaction happens, producing electrical impulses that are sent to the brain.

More specifically, rods are activated when exposed to dark or low intensity light environments, and they process the shades of colors, allowing us to distinguish different tones when there is not much light around.

Contrariwise, cones react to bright environments. They contain photopigments of three different types, red, green, and blue. Each one of them can absorb radiations of different wavelengths giving to the vision system the possibility to distinguish different colors. Some animals, for example, have more than 3 types of cones, which makes it possible for them to see also ultraviolet, or infrared radiations.

The information is then sent to the brain through an electrical signal produced by the optical nerve. Figure 2.22 illustrates the retina structure, where it is possible to see its components [28], [30].

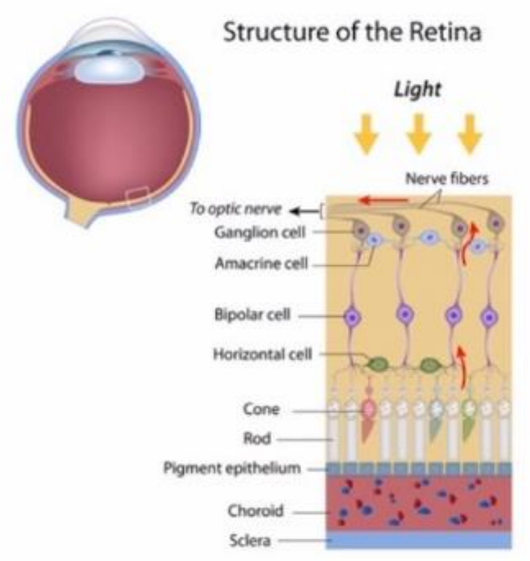

Figure 2.22 – Structure of the retina [28]

2.3.2. Methods for producing color stimuli

The color stimulus, which is the visible radiation entering the eye and producing a sensation of color can be produced by two main methods that are showed in this subsection.

Subtractive color mixing

In this method, the sensation of color is given by removing one of the three primary color pigments: cyan, magenta, or yellow, figure 2.23. The superposing of the two remaining colorants is what creates the color that is seen. This phenomenon happens because when two of these three colors are mixed, they absorb both of their corresponding wavelength radiation. For example, when the magenta and cyan pigments are mixed, the wavelengths of radiation absorbed correspond to the magenta one plus the cyan one. Therefore, the reflected radiations, which are the visible ones, are all the others left in the visible spectrum. This is most used in printers (CMYK system) [31].

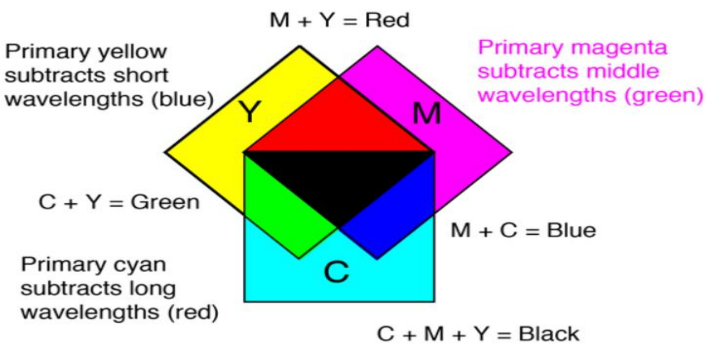

Figure 2.23 – Subtractive color mixing [32]

Additive color mixing

In this kind of color mixing, the sensation of color works in the opposite way of subtractive color mixing, figure 2.24. This means that it is given by the addition of the primary colors (in this case, red, green, and blue).

For example, when all the three primary colors are added, instead of black, the color seen is white because all wavelengths are being emitted.

This system is used in television, where the image is given by putting small pixels of red, green, and blue very close to each other, so close that our eyes can't differentiate them, giving us the perception of colors by adding different amounts of the referred colors, in a specific way. Systems such as RGB and CIELAB, use this kind of method [26] [32].

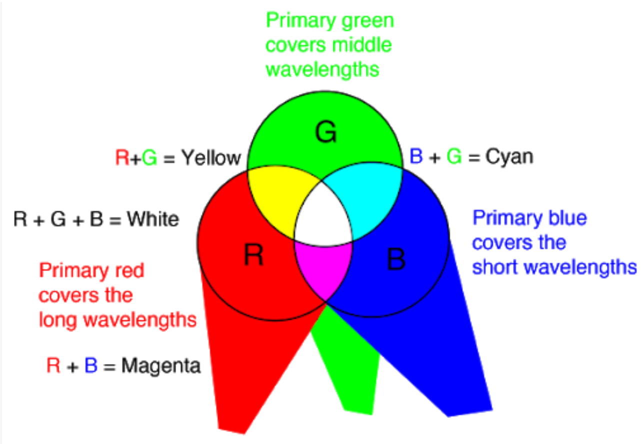

Figure 2.24 – Additive Color Mixing [31]

2.3.3. Illuminants

The chromaticity is the attribute of a color stimulus defined by its trichromatic coordinates or by its dominant or complementary wavelength and purity characteristics taken together [21], [33].

In order to describe the chromaticity of a surface, based on the reflectance or transmittance, the iillumination irradiating the surface needs to be characterised. The illuminants are light sources that irradiate the objects influencing their color perception by the observer, and are represented by the Spectral Power Distribution (SPD). Each one has its own SPD. The International Commission on Illumination (CIE) has chosen some reference sources over the years for their corresponding SPD properties, allowing them to be characterized based on mathematic functions.

The most common and recommended ones are illuminant A and illuminant D65. Others such as illuminant C are still used nowadays.

The illuminant A represents a typical domestic tungsten-filament light. Its relative spectral power distribution is equal to the one of a Planckian radiator at a temperature of approximately 2856 K. It should be used in colorimetric applications that rely on incandescent light sources.

The illuminant D65 and the illuminant C represent an average daylight radiation. The first one to be standardized was the illuminant C but, along the time, as it was evidenced that it was not one hundred percent accurate, in 1964, it was replaced by the illuminant D65 to be the one which represents the daylight with a correlated temperature of 6500 K [26].

Figure 2.25 illustrates a graphical comparison between the SPDs of some illuminants.

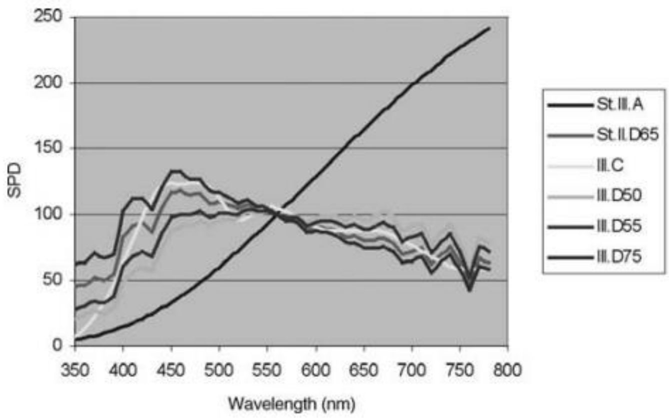

Figure 2.25 – Relative spectral power distribution of some CIE Illuminants [26]

2.3.4. CIE Standard Colorimetric Observer

CIE created two main standards systems to carachterize the way a standard observer perceives color:, CIE 1931 and CIE 1964. As mentioned before, our eyes have components stimulated in the presence of a specific range of wavelength radiation. These wavelengths correspond to the red, green, and blue zones of the visible spectrum. When this was discovered, a system that tried to replicate the way humans process the colors was created.

According to Grassman’s laws, a color stimulus can be matched by the additive mixture of three properly selected stimuli. Different amounts of each stimulus create different colors sensations.

In creating a colorimetric system, each stimulus must be wholly defined. This means that its units and the spectral power distribution need to be specified. A color match of an unknown stimulus can be obtained according to the formula represented in equation 2.18 [26]:

$$[C] \equiv R[R] + G[G] + B[B] \tag{2.18}$$

Where:

R, G, B – Amount of each red, green and blue stimulus respectively

$[R], [G], [B]$ – Units of matching stimuli

The amounts $R, G,$ and B are integrals that are called tristimulus values and are given by equations 2.19, 2.20, and 2.21 [26].

$$R = \int_{380}^{780} \bar{r}(\lambda)P(\lambda)d\lambda \qquad (2.19)$$

$$G = \int_{380}^{780} \bar{g}(\lambda)P(\lambda)d\lambda \qquad (2.20)$$

$$B = \int_{380}^{780} \bar{b}(\lambda)P(\lambda)d\lambda \qquad (2.21)$$

Where:

$\bar{r}$, $\bar{g}$, $\bar{b}$ – Color matching functions

$P(\lambda)$ – Function of nonmonochromatic test color stimulus

λ – Wavelength

CIE 1931 Standard Observer

For the 1931 system, the standard observer conditions were a 2º foveal field of observation and a dark surrounding, which is the angle that the eyes can distinguish colors better. Figure 2.26 illustrates how this system was created. The idea was to replicate the stimuli created by the test light, using the three primary colors, changing the intensity of each one of them. This experience showed that it is possible to create the same color stimuli using different combinations of each primary intensity.

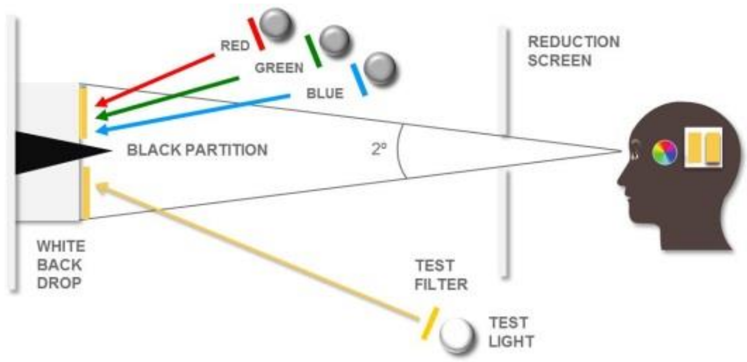

Figure 2.26 – CIE 1931 experiment [31]

However, as it is possible to see in figure 2.27, the RGB function has a negative lob, this means that it was needed to create a negative stimulus of one of the primaries to match some range of stimulus, which was not possible so, the first conclusion was that not all the stimuli could be matched, but in fact, there was a practical solution. It was to add that stimulus in the test light to make it like the combination of the primaries´ stimuli. Some years later, to facilitate the calculations, the $\bar{r}$, $\bar{g}$, and $\bar{b}$ functions were changed to a x, y, and z system by a linear transformation, in which the negative lobs were removed [26].

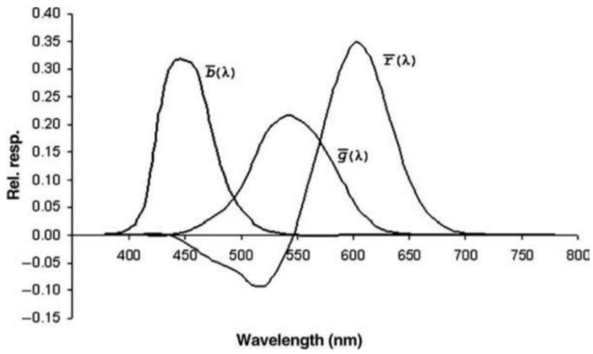

Figure 2.27 – r,g,b CMFs of the CIE 1931 standard colorimetric observer [7]

CIE 1964 Standard Observer

In CIE 1964, instead of a 2º foveal field of observation, a 10º field was used, which, despite not being the angle that the eyes have a better capacity to distinguish colors, is closer to what the observer perceives on a daily basis. In figure 2.28, it is possible to see the CIE 1931 and CIE 1964 CMF´s with the linear transformation meaning that there are no negative lobs [26].

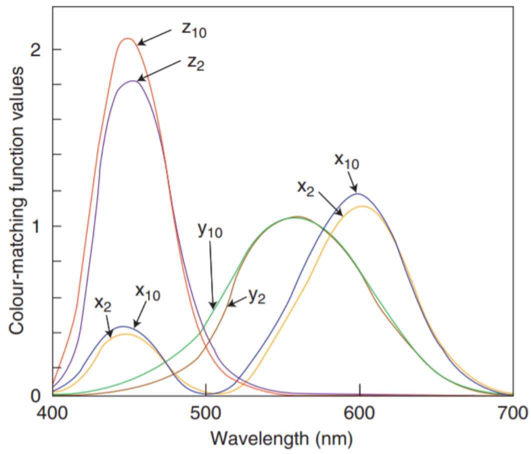

Figure 2.28 - CMF´s for 2º and 10º observers [34]

2.3.5. Chromaticity Coordiates

Using the tristimulus values to imagine a color stimuli is not easy, so usually it is not of interest knowing the tristimulus absolute values. In such scenarios, chormaticity coordinates are used to create a better perception of a color stimuli.

To calculate the chromaticity coordinates, it is firstly necessary to calculate the tristimulus values. Due to the linear transformation of the $\bar{r}$, $\bar{g}$, and $\bar{b}$ to x, y, and z the initial tristimulus values *RGB* are also converted to X, Y and, Z and are calculated following equations 2.22, 2.23, and 2.24:

$$X = K.\int_{380}^{780} \phi_\lambda(\lambda).\bar{x}(\lambda).\mathrm{d}\lambda \quad (2.22)$$

$$Y = K.\int_{380}^{780} \phi_\lambda(\lambda).\bar{y}(\lambda).\mathrm{d}\lambda \quad (2.23)$$

$$Z = K.\int_{380}^{780} \phi_\lambda(\lambda).\bar{z}(\lambda).\mathrm{d}\lambda \quad (2.24)$$

Where:

$\phi_\lambda -$ Color stimulus function of the light seen by the observer
$\bar{x}(\lambda), \bar{y}(\lambda), \bar{z}(\lambda) -$ CMF of the CIE 1931 standard observer.
$K -$ Maximum value of the luminous efficacy of radiation

According to the CIE recommendation, the integration can be carried out by numerical summation at wavelength step, Δλ, equal to 1 nm following equations 2.25, 2.26, and 2.27.

$$X = K.\sum_{380}^{780} \phi_\lambda(\lambda).\bar{x}(\lambda).\Delta\lambda \quad (2.25)$$

$$Y = K.\sum_{380}^{780} \phi_\lambda(\lambda).\bar{y}(\lambda).\Delta\lambda \quad (2.26)$$

$$Z = K.\sum_{380}^{780} \phi_\lambda(\lambda).\bar{z}(\lambda).\Delta\lambda \quad (2.27)$$

For stimulus reaching us from a reflected or transmitted surface, the color stimulus function, $\phi_\lambda(\lambda)$, is substituted by the relative color stimulus function, $\phi(\lambda)$ and is given by equations 2.28 or 2.29.

$$\phi(\lambda) = R(\lambda).S(\lambda) \quad (2.28)$$

$$\phi(\lambda) = T(\lambda).S(\lambda) \quad (2.29)$$

Where:

$R(\lambda)$ – Spectral reflectance

$T(\lambda)$ – Spectral transmittance

$S(\lambda)$ – Relative SPD of the illuminant

Chromaticity coordinates are defined by equations 2.30, 2.31, and 2.32:

$$x = \frac{X}{X+Y+Z} \quad (2.30)$$

$$y = \frac{Y}{X+Y+Z} \quad (2.31)$$

$$z = \frac{Z}{X+Y+Z} \quad (2.32)$$

As $x + y + z = 1$ it is possible to use only two coordinates to describe a chromaticity. Usually, it is x and y.

Figure 2.29 illustrates the chromaticity diagram for the CIE 1931 standard observer.

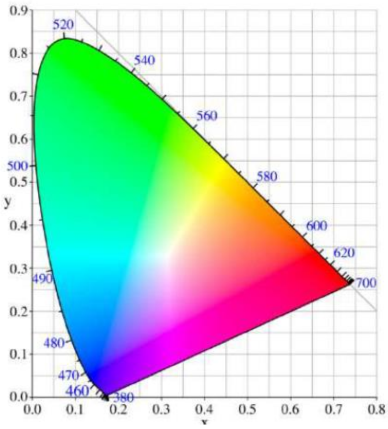

Figure 2.29 – x; y chromaticity diagram of the CIE 1931 trichromatic system [35]

2.3.6. CIELAB Color Space

Color stimuli are three dimensional, and since the beginning of the study of colorimetry, there was no system for color measurement that would be uniform. This means that distances seen in chromaticity diagrams or graphics didn´t represent the real differences perceived by the observer.

So, there was a need to create a system that would facilitate the comparison between objects with different colors, and in 1975 in a CIE meeting, it was agreed to create such color measurement system, the CIELAB.

The CIELAB system is defined by the $L*$, $a*$, and $b*$ coordinates. The $L*$ characterizes the luminance. $a*$ Is the coordinate that goes from red color stimuli to green, depending on its value, positive for red and negative for green. $b*$ Works the same way with the positive axis being in the direction of yellow stimuli and blue in case it is negative, as can be seen in figure 2.30 [26].

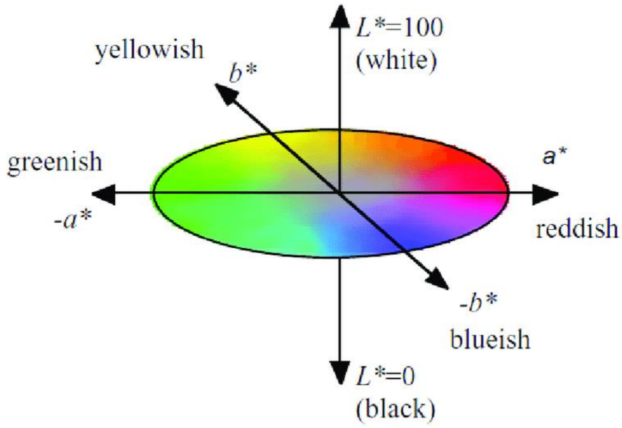

Figure 2.30 – CIELAB color space [36]

The coordinates of the CIELAB system are calculated from the tristimulus values, $X, Y,$ and Z, following the equations 2.33 to 4.24 below [37]:

$$L* = 116f\left(\frac{Y}{Y_n}\right) - 16 \tag{2.33}$$

$$a* = 500\left[f\left(\frac{X}{X_n}\right) - f\left(\frac{Y}{Y_n}\right)\right] \tag{2.34}$$

$$b* = 200\left[f\left(\frac{Y}{Y_n}\right) - f\left(\frac{Z}{Z_n}\right)\right] \tag{2.35}$$

Where:

$L*$ – CIELAB lightness

$a*$ – $a*$ coordinate from CIELAB

$b*$ – $b*$ coordinate from CIELAB

And:

$$f\left(\frac{X}{X_n}\right) = (X/X_n)^{\frac{1}{3}} \quad if \quad \left(\frac{X}{X_n}\right) > \left(\frac{24}{116}\right)^3 \tag{2.36}$$

$$f\left(\frac{X}{X_n}\right) = \left(\frac{841}{108}\right)\left(\frac{X}{X_n}\right) + \frac{16}{116} \quad if \quad \left(\frac{X}{X_n}\right) \leq \left(\frac{24}{116}\right)^3 \tag{2.37}$$

And:

$$f\left(\frac{Y}{Y_n}\right) = (Y/Y_n)^{\frac{1}{3}} \quad if \quad \left(\frac{Y}{Y_n}\right) > \left(\frac{24}{116}\right)^3 \tag{2.38}$$

$$f\left(\frac{Y}{Y_n}\right) = \left(\frac{841}{108}\right)\left(\frac{Y}{Y_n}\right) + \frac{16}{116} \quad if \quad \left(\frac{Y}{Y_n}\right) \leq \left(\frac{24}{116}\right)^3 \tag{2.39}$$

And:

$$f\left(\frac{Z}{Z_n}\right) = (Z/Z_n)^{\frac{1}{3}} \quad if \quad \left(\frac{Z}{Z_n}\right) > \left(\frac{24}{116}\right)^3 \tag{2.40}$$

$$f\left(\frac{Z}{Z_n}\right) = \left(\frac{841}{108}\right)\left(\frac{Z}{Z_n}\right) + \frac{16}{116} \quad if \quad \left(\frac{Z}{Z_n}\right) \leq \left(\frac{24}{116}\right)^3 \tag{2.41}$$

Where:

X_n, Y_n, Z_n – Tristimulus Values of a specified white object (perfect reflecting diffuser ideally)

From the L*, a* and b* it is possible to calculate the chroma, $C^*{}_{ab}$ and the hue angle, h_{ab} using equations 4.25 and 4.26.

$$C *_{ab}= (a^{*2}+b^{*2})^{\frac{1}{2}} \tag{2.42}$$

$$h_{ab} = \arctan\left(\frac{b^*}{a^*}\right) \tag{2.43}$$

Where:

$C^*{}_{ab}$ – CIELAB chroma

h_{ab} – CIELAB hue angle

In figure 2.31, it is possible to visualize and understand the chroma and the hue angle from 3D representation.

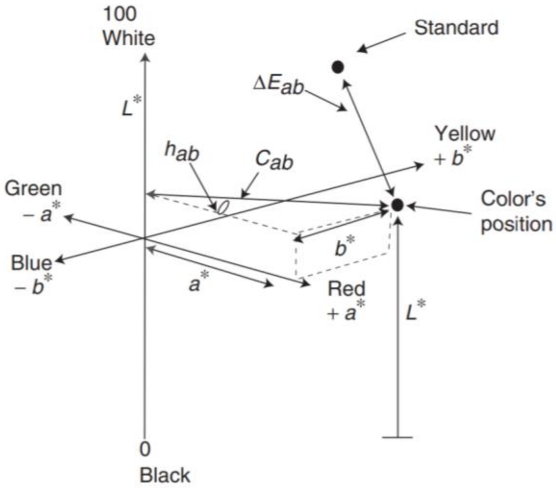

Figure 2.31 CIELAB parameters L*, a*, b*, $C^*{}_{ab}$, and h_{ab} of a given color and the $\Delta E^*{}_{ab}$ color difference [34]

To calculate the perceived magnitude color difference $\Delta E^*{}_{ab}$ between two object color stimuli of the same size and shape, viewed in identical white to middle–gray surroundings, the Euclidean distances are used in CIELAB color space, equations 2.44 to 2.51 [37].

$$\Delta E^*{}_{ab} = [(\Delta L^*)^2 + (\Delta a^*)^2 + (\Delta b^*)^2]^{\frac{1}{2}} \tag{2.44}$$

or

$$\Delta E^*{}_{ab} = [(\Delta L^*)^2 + (\Delta C^*{}_{ab})^2 + (\Delta H^*{}_{ab})^2]^{\frac{1}{2}} \quad (2.45)$$

Where:

$$\Delta H^*{}_{ab} = 2\left(C^*{}_{ab,1}.C^*{}_{ab,0}\right)^{\frac{1}{2}}.\sin\left(\frac{\Delta h_{ab}}{2}\right) \quad (2.46)$$

$$\Delta L = L^*{}_1 - L^*{}_0 \quad (2.47)$$

$$\Delta a^* = a^*{}_1 - a^*{}_0 \quad (2.48)$$

$$\Delta b^* = b^*{}_1 - b^*{}_0 \quad (2.49)$$

$$\Delta C^*{}_{ab} = C^*{}_{ab,1} - C^*{}_{ab,0} \quad (2.50)$$

$$\Delta h^*{}_{ab} = h^*{}_{ab,1} - h^*{}_{ab,0} \quad (2.51)$$

Where:

$\Delta E^*{}_{ab}$ – CIELAB color difference

$\Delta H^*{}_{ab}$ – CIELAB hue difference

$\Delta h^*{}_{ab}$ – CIELAB hue angle difference

$\Delta C^*{}_{ab}$ – CIELAB chroma difference

Δa^* – CIELAB *a** difference

Δb^* – CIELAB *b** difference

$L^*{}_{\frac{1}{0}}$ – CIELAB lightness from object $\frac{1}{2}$

$a^*{}_{\frac{1}{0}}$ – a* CIELAB coordinate from object $\frac{1}{2}$

$b^*{}_{\frac{1}{0}}$ – b* CIELAB coordinate from object $\frac{1}{2}$

$C^*{}_{ab,\frac{1}{0}}$ – Chroma from object $\frac{1}{2}$

$h^*{}_{ab,\frac{1}{0}}$ – Hue angle from object $\frac{1}{2}$

2.3.7. RAL Color system

RAL (*Reichs-Ausschuß für Lieferbedingungen und Gütesicherung* – Committee for Delivery and Quality Assurance***).*** color system is governed by the *RAL Deutsches Institut für Güte-sicherung und Kennzeichnung* (RAL German Institute for Quality Assurance and Labeling). The first RAL color standards were created in 1927, and are now part of the collection known as RAL Classic that includes 215 tones. The criteria used for including colors in this collection is based on its public interest. For example, the colors used in traffic signs or public authorities uniforms and vehicles belong to this collection due its importance for the community [38].

In RAL classic color system, colors are identified by a four digit number, where the first one stands for the tone (1: yellow, 2: orange, 3: red, 4: purple, 5: blue, 6: green, 7: grey, 8: brown and 9: white and black shades) and the other three for the chronological order of standardization.

There are other color collections belonging to RAL and each one has its own usage and its own color matching system. This work analysed samples that belong to the RAL Classic system.

3. Case Study

This chapter is dedicated to explaining the working conditions, how the data were collected and processed, and which results were obtained.

3.1. Materials and Surrounding Environment

The lab is climatized; thus, temperature and humidity were always controlled so that the measurements were all collected within the recommend conditions according to the manufacturers´ specifications, which is an interval between 10 % and 70 % for relative humidity and from 10 ºC to 35 ºC for the temperature. This data was collected by a digital Thermo Hygrometer model 1620 Dewk from Fluke Company with a resolution of 0,01 ºC for the temperature and 1 % for the relative humidity shown in figure 3.1. In all measurement performed in spectrophotometry, relative humidity and temperature were always collected. Consequently, we are enabled to conclude that in more than 95 % of them, the temperature was between 20 ºC a 23 ºC and the relative humidity between 40 % and 70 %, which is also the range that standardized samples should be measured to obtain results as close as possible from the certificate.

Figure 3.1 – Thermo hygrometer model 1620 Dewk from Fluke Company

The instrument used to collect the measurement results is the spectrophotometer model Lambda 950 from Perkin Elmer, which is a double beam type with two monochromators. It is connected to the computer, and with the assistance of the software UV Winlab also developed by Perkin Elmer, it is possible to read the results and change the kind of data collected. Screenshots of this software interface are displayed in figure 3.2.

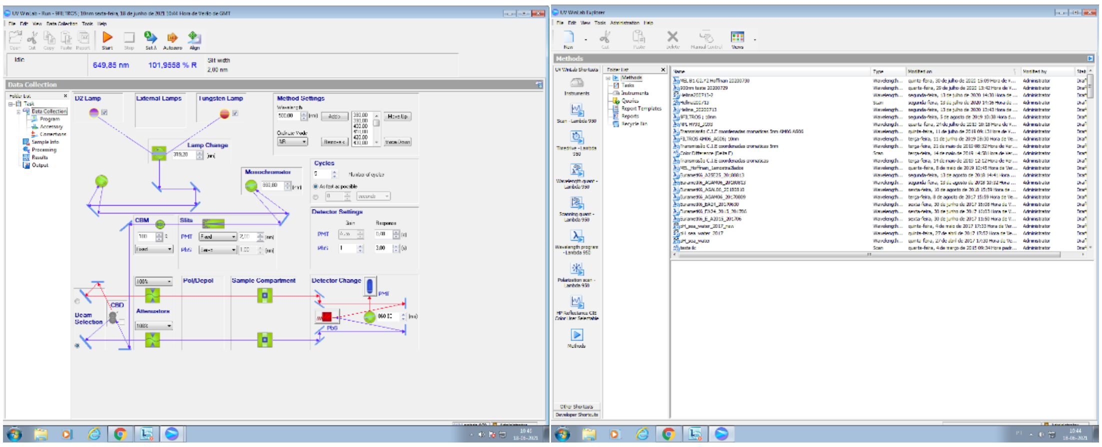

Figure 3.2 – UV Winlab interface

This spectrophotometer has the possibility to collect results in reflectance mode or transmission mode, and each one has its configuration. For the reflectance mode, it is used ceramic samples which are opaque, not letting the light pass through it and an integrated sphere that it shown in figure 3.3 (left), and in transmission mode, the integrated sphere is removed and placed in a compartment specifically to place transmission samples, figure 3.3 (right), these samples are filters that let a portion of light pass through it.

Figure 3.3 – Integrated sphere (left) transmission samples´ compartment (right)

There is also a bottle of compressed nitrogen, which is used to clean the samples before their measurement, a black blanket to cover the spectrophotometer from the external light, and latex gloves are used to handle the samples for them not to touch the hands directly, avoiding unexpected errors that can come from this procedure.

3.2. Procedure

The spectrophotometer is placed on a table so that outside vibrations are avoided, and effects from the air conditioner and external light are reduced to the minimum possible using a black blanket to cover the spectrophotometer. Before being measured the samples, are placed near the spectrophotometer so that their environment is the closest possible to the spectrophotometer.

After putting on the latex gloves to avoid the sample´s contamination, the next step is to pick the sample and clean it up by spraying compressed nitrogen for about 5 seconds. According to the *Procedimento Técnico de Calibração de Filtros com Espectrofotómetro Padrão* [21], this step is essential to reduce the errors from possible dust on the surface of the samples.

The following step is to place the sample in the compartment, close the spectrophotometer, cover it with the black blanket and wait at least 1 minute before collecting the data so that the environment inside the spectrophotometer can stabilize. Before any measurement, the spectrophotometer must be turned on one hour earlier so that the optic and electronics components can stabilize during that time.

Adopting *Procedimento Técnico de Calibração de Filtros com Espectrofotómetro Padrão* recommendations to reduce errors in the data collection, the following order of the sample's measurement was used:

$$T'_0(\lambda), T'_{100}(\lambda), T'_f(\lambda), T'_{100}(\lambda), T'_0(\lambda)$$

For transmittance, where:

$T'_0(\lambda)$ – 0 %Transmittance, obtained putting an opaque sample in the light path

$T'_{100}(\lambda)$ – 100 % Transmittance, obtained without any sample in the light path

$T'_{\mathrm{f}}(\lambda)$ – Transmittance of the sample intended to measure

And for reflectance:

$$R'_0(\lambda), R'_{ref}(\lambda), R'_c(\lambda), R'_{ref}(\lambda), R'_0(\lambda)$$

Where:

$R'_0(\lambda)$ – 0 % Reflectance, using a light trap, where photons are lost

$R'_{\mathrm{ref}}(\lambda)$ – 100 % Reflectance, using a certified sample where the light is totally reflected

$R'_c(\lambda)$ – Reflectance of the sample intended to measure

So that the conditions of reproducibility and repeatability could be fulfilled, the measurements were repeated on 2 different days. For each sample wavelength, the collection of the transmittance and reflectance values was repeated 5 times.

3.3. Procedure validation

The method used in this work can be validated by comparing the measurement results obtained for given samples with the results of the corresponding certificate.

First, the calibration of the spectrophotometer at the given configuration is performed by comparing the measured values with the values of the corresponding calibration certificate. This comparison enables to deduce the calibration function.

In this subsection, the procedure validation is performed for the transmission configuration. The transmittance reference values correspond to the certificates of the samples HY93, HZ93, JA93, JB93, JC93, JD93, JE93, JF93, and JG93, which are filters certified by the NPL in 2015. They are glass made with dimensions 56 mm × 12 mm × 12 mm and can be seen in figure 3.4.

Figure 3.4 – HY93, HZ93, JA93, JB93, JC93, JD93, JE93, JF93, JG93 samples

The wavelengths chosen to measure the transmittance were 400 nm, 500 nm, 600 nm, 700 nm, 800 nm, 900 nm, and 1000 nm. The values chosen for the spectral bandwidth and average time were 1 nm and 0,8 s, respectively, which were the same as those published in the NPL certificate.

3.3.1. Data Processing

The measurements were done in the order according to eq. 3.1, after obtaining the results from the 5 repetitions, the arithmetic mean and standard deviation were calculated. The results of each day are shown in tables 3.1 and 3.2 below.

Table 3.1 – Arithmetic mean and standard deviation in the first day of measurements

	λ / nm	400	500	600	700	800	900	1000
T0%_1	$T^*{}_f(\lambda)_1$/%	-0,005	-0,005	-0,005	-0,005	-0,005	0,114	0,137
	$s(\lambda)_1$/%	0,001	0,001	0,001	0,001	0,001	0,002	0,001
T100%_1	$T^*{}_f(\lambda)_1$/%	99,99	100,02	100,00	100,02	100,02	99,69	99,66
	$s(\lambda)_1$/%	0,01	0,01	0,01	0,02	0,02	0,02	0,03
HY93	$T^*{}_f(\lambda)_1$/%	91,13	91,38	91,50	91,65	91,72	91,83	91,92
	$s(\lambda)_1$/%	0,01	0,01	0,01	0,01	0,01	0,03	0,02
HZ93	$T^*{}_f(\lambda)_1$/%	70,543	71,71	70,845	72,508	67,62	61,50	56,94
	$s(\lambda)_1$/%	0,004	0,01	0,007	0,003	0,01	0,01	0,02
JA93	$T^*{}_f(\lambda)_1$/%	57,45	59,33	57,862	60,02	52,63	43,99	38,06
	$s(\lambda)_1$/%	0,01	0,01	0,002	0,01	0,01	0,01	0,01
JB93	$T^*{}_f(\lambda)_1$/%	28,780	31,166	30,375	38,52	38,60	33,70	29,71
	$s(\lambda)_1$/%	0,004	0,002	0,003	0,01	0,01	0,01	0,01
JC93	$T^*{}_f(\lambda)_1$	9,542	11,045	10,436	16,626	16,653	12,627	9,840
	$s(\lambda)_1$	0,002	0,001	0,001	0,002	0,003	0,002	0,004
JD93	$T^*{}_f(\lambda)_1$	2,076	3,517	3,5591	8,077	12,312	12,54	11,890
	$s(\lambda)_1$	0,001	0,001	0,0005	0,001	0,002	0,01	0,003
JE93	$T^*{}_f(\lambda)_1$	0,5266	1,077	1,0887	3,329	5,912	6,044	5,631
	$s(\lambda)_1$	0,0004	0,001	0,0005	0,001	0,001	0,003	0,004
JF93	$T^*{}_f(\lambda)_1$	0,153	0,375	0,3801	1,521	3,092	3,194	2,936
	$s(\lambda)_1$	0,001	0,001	0,0002	0,001	0,002	0,004	0,002
JG93	$T^*{}_f(\lambda)_1$	0,0440	0,133	0,1351	0,710	1,649	1,736	1,584
	$s(\lambda)_1$	0,0003	0,001	0,0003	0,001	0,002	0,003	0,003
T0%_2	$T^*{}_f(\lambda)_1$	-0,005	-0,0048	-0,0049	-0,004	-0,005	0,096	0,129
	$s(\lambda)_1$	0,001	0,0003	0,0002	0,000	0,002	0,004	0,003
T100%_2	$T^*{}_f(\lambda)_1$	99,9980	100,0217	100,0184	100,0323	100,0396	99,1831	99,0627
	$s(\lambda)_1$	0,0100	0,0104	0,0107	0,0085	0,0207	0,0208	0,0232

Table 3.2 – Arithmetic mean and standard deviation in the second day of measurements

	λ / nm	400	500	600	700	800	900	1000
T0%_1	$T^*{}_f(\lambda)_2$/%	-0,003	-0,0027	-0,002	-0,002	-0,002	0,104	0,139
	$s(\lambda)_2$/%	0,001	0,0003	0,001	0,000	0,001	0,001	0,002
T100%_1	$T^*{}_f(\lambda)_2$/%	97,29	99,96	99,99	100,01	100,01	100,26	100,16
	$s(\lambda)_2$/%	0,01	0,01	0,01	0,01	0,01	0,04	0,03
HY93	$T^*{}_f(\lambda)_2$/%	88,58	91,29	91,476	91,62	91,74	92,48	92,41
	$s(\lambda)_2$/%	0,01	0,01	0,005	0,01	0,01	0,03	0,02
HZ93	$T^*{}_f(\lambda)_2$/%	68,50	71,66	70,86	72,54	67,68	61,87	57,20
	$s(\lambda)_2$/%	0,01	0,01	0,01	0,01	0,01	0,01	0,01
JA93	$T^*{}_f(\lambda)_2$/%	55,94	59,30	57,870	60,03	52,67	44,46	38,46
	$s(\lambda)_2$/%	0,01	0,01	0,004	0,01	0,01	0,01	0,01
JB93	$T^*{}_f(\lambda)_2$/%	27,93	31,09	30,32	38,49	38,62	34,049	29,990
	$s(\lambda)_2$/%	0,01	0,01	0,01	0,01	0,01	0,002	0,003
JC93	$T^*{}_f(\lambda)_2$/%	9,32	11,031	10,411	16,605	16,663	12,79	10,01
	$s(\lambda)_2$/%	0,05	0,002	0,004	0,002	0,003	0,01	0,12
JD93	$T^*{}_f(\lambda)_2$/%	2,023	3,518	3,556	8,073	12,340	12,680	12,00
	$s(\lambda)_2$/%	0,001	0,001	0,002	0,002	0,001	0,003	0,01

Table 3.2 – Arithmetic mean and standard deviation in the second day of measurements (continuation)

	λ / nm	400	500	600	700	800	900	1000
JE93	$T^*_f(\lambda)_2/\%$	0,513	1,0757	1,085	3,322	5,916	6,112	5,674
	$s(\lambda)_2/\%$	0,002	0,0004	0,001	0,001	0,001	0,003	0,003
JF93	$T^*_f(\lambda)_2/\%$	0,151	0,375	0,378	1,5143	3,091	3,225	2,952
	$s(\lambda)_2/\%$	0,001	0,001	0,001	0,0004	0,002	0,002	0,006
JG93	$T^*_f(\lambda)_2/\%$	0,045	0,135	0,136	0,711	1,652	1,752	1,596
	$s(\lambda)_2/\%$	0,001	0,001	0,001	0,001	0,001	0,002	0,000
T0%_2	$T^*_f(\lambda)_2/\%$	-0,003	-0,004	-0,0033	-0,0027	-0,0031	0,096	0,124
	$s(\lambda)_2/\%$	0,0006	0,002	0,0003	0,0002	0,0011	0,003	0,005
T100%_2	$T^*_f(\lambda)_2/\%$	97,31	99,99	100,05	100,12	100,25	100,41	99,79
	$s(\lambda)_2/\%$	0,01	0,01	0,01	0,01	0,01	0,04	0,02

Where:

$s(\lambda)_1$ – Standard deviation of the values obtained on the first day of measurements for each sample

$s(\lambda)_2$ – Standard deviation of the values obtained on the second day of measurements for each sample

$T^*_f(\lambda)_1$ – Arithmetic mean of the transmittance measured on the first day of measurements

$T^*_f(\lambda)_2$ – Arithmetic mean of the transmittance measured on the second day of measurements

The following step is to calculate the arithmetic mean of the measurement results during the 2 days, which can be seen in Table 3.3 below:

Table 3.3 – Arithmetic mean of the measurement results of the two measurement days

	λ / nm	400	500	600	700	800	900	1000
T0%	$T^*_f(\lambda)/\%$	-0,004	-0,004	-0,004	-0,003	-0,004	0,102	0,132
T100%	$T^*_f(\lambda)/\%$	98,648	99,998	100,014	100,046	100,079	99,886	99,669
HY93	$T^*_f(\lambda)/\%$	89,859	91,336	91,490	91,632	91,726	92,153	92,165
HZ93	$T^*_f(\lambda)/\%$	69,523	71,684	70,855	72,523	67,648	61,682	57,066
JA93	$T^*_f(\lambda)/\%$	56,696	59,315	57,866	60,025	52,652	44,223	38,259
JB93	$T^*_f(\lambda)/\%$	28,356	31,127	30,348	38,508	38,608	33,877	29,856
JC93	$T^*_f(\lambda)/\%$	9,432	11,038	10,423	16,615	16,658	12,707	9,924
JD93	$T^*_f(\lambda)/\%$	2,049	3,518	3,557	8,075	12,326	12,611	11,945
JE93	$T^*_f(\lambda)/\%$	0,520	1,076	1,087	3,325	5,914	6,078	5,653
JF93	$T^*_f(\lambda)/\%$	0,152	0,375	0,379	1,518	3,091	3,209	2,944
JG93	$T^*_f(\lambda)/\%$	0,044	0,134	0,136	0,711	1,651	1,744	1,590

Where:

$T^*_f(\lambda)$ – Arithmetic mean of the transmittance measured in the two days of measurements

The next step is to calculate the transmittances using equation 3.1 so that errors due to stray light, noise, and the detectors non-linearity are minimized as much as possible.

$$T_f(\lambda) = \frac{T^*{}_f(\lambda) - T_0(\lambda)}{T_{100}(\lambda) - T_0(\lambda)} \quad (3.1)$$

Where:

$T^*{}_f(\lambda)$ – Arithmetic mean of the transmittance measured in the two days of measurements;

$T_0(\lambda)$ – Arithmetic mean of the two measurements days of the sample´s corresponding to 0 % transmittance;

$T_{100}(\lambda)$ – Arithmetic mean of the two measurements days of the sample´s corresponding to 100 % transmittance;

$T_f(\lambda)$ – Sample transmittance;

The results following equation 3.1 are presented in table 3.4.

Table 3.4 – Results obtained of the samples transmittance .

	λ / nm	400	500	600	700	800	900	1000
HY93	$T_f(\lambda)/\%$	91,091	91,338	91,477	91,590	91,653	92,251	92,462
HZ93	$T_f(\lambda)/\%$	70,478	71,686	70,846	72,491	67,596	61,715	57,199
JA93	$T_f(\lambda)/\%$	57,476	59,318	57,860	59,999	52,613	44,219	38,305
JB93	$T_f(\lambda)/\%$	28,748	31,130	30,344	38,489	38,584	33,846	29,856
JC93	$T_f(\lambda)/\%$	9,566	11,042	10,425	16,610	16,650	12,636	9,838
JD93	$T_f(\lambda)/\%$	2,082	3,522	3,561	8,074	12,321	12,540	11,869
JE93	$T_f(\lambda)/\%$	0,532	1,081	1,091	3,327	5,915	5,993	5,547
JF93	$T_f(\lambda)/\%$	0,159	0,380	0,383	1,520	3,094	3,118	2,826
JG93	$T_f(\lambda)/\%$	0,050	0,138	0,140	0,714	1,655	1,650	1,465

3.3.2. Uncertainty Calculation

In this subsection, the concepts and terms introduced in subsection 2.1.3.1 are used.

Calculating the uncertainties associated with the measurements of the samples, the combined standard uncertainty expressed by the equation 2.11 is used, and by applying it to this experiment using $T_f(\lambda)$ as $f(x_i)$ and $T^*{}_f(\lambda)$, $T_0(\lambda)$, $T_{100}(\lambda)$ as x_1, x_2, x_3 equation 3.2 is obtained.

$$u_{T_f(\lambda)} = \sqrt{u_{T_f^*}{}^2.\left(\frac{-100}{T_0 - T_{100}}\right)^2 + u_{T_0}{}^2.\left(\frac{100.\left(T_f^* - T_{100}\right)}{(T_0 - T_{100})^2}\right)^2 + u_{T_{100}}{}^2.\left(\frac{-100.\left(T_f^* - T_0\right)}{(T_{100} - T_0)^2}\right)^2} \quad (3.2)$$

Where:

$T^*{}_f(\lambda)$ – Arithmetic mean of the 2 measurements´ days of the sample transmittance;

$T_0(\lambda)$ – Arithmetic mean of the 2 measurements´ days of the sample corresponding to 0 % transmittance;

$T_{100}(\lambda)$ – Arithmetic mean of the 2 measurements´ days of the sample corresponding to 100 % transmittance;

$T_f(\lambda)$ – Sample transmittance
$u_{T_f^*}$ – Uncertainty associated to $T^*{}_f(\lambda)$
u_{T_0} – Uncertainty associated to $T_0(\lambda)$
$u_{T_{100}}$ – Uncertainty associated to $T_{100}(\lambda)$
u_{T_f} – Uncertainty associated to $T_f(\lambda)$

As all the three variables T_0, T_{100} and T^*_f were obtained by a repetitive experimental analysis, i.e. leading to uncertainties obtained by statistical method. Measurement uncertainties are also due to non-statistical method, namely due to imperfections of the spectrophotometer, deduced from the manufacturer´s specifications, for instance. This is synthetisezed in two kind of methods to calculate uncertainties that are type A and type B methods leading to combined uncetained expressed by equation 3.3.

$$u_{T_i} = \sqrt{u_A^2(T_i) + u_B^2(T_i)} \tag{3.3}$$

Where:
$u_A(T_i)$ – Type A method uncertainty, i.e. statistical method
$u_B(T_i)$ – Type B method uncertainty, i.e. non-statistical method
u_{T_i} – Uncertainty associated with a sample by combining type A and type B

Standard uncertainty calculated by type A method

In conditions of reproducibility and repeatability, as the measurements took place in the same laboratory, using the same method and instrument, by the same operator, and on different days, the standard uncertainty is equal to the standard deviation obtained in such statistical method, from the repeatability uncertainty, through equation 3.4:

$$S_{Ri=}\sqrt{\frac{n-1}{n}{S_{ri}}^2 + {S_{Mi}}^2} \tag{3.4}$$

Where:
S_{Ri} – Reproducibility uncertainty;
S_{ri} – Repeatability uncertainty;
S_{Mi} – Standard deviation of the mean
n – number of repetitions in each day of measurements

The repeatability uncertainty is calculated using equation 35:

$$S_{ri} = \sqrt{\frac{s(\lambda)_1{}^2 + s(\lambda)_2{}^2}{2}} \tag{3.5}$$

Where:

$s(\lambda)_1$ – Standard deviation of the values obtained on the first day of measurements for each sample

$s(\lambda)_2$ – Standard deviation of the values obtained on the second day of measurements for each sample

In table 3.5 below it is shown the results obtained for the values of S_{Ri}, S_{ri}, and S_{Mi}.

Table 3.5 – Values of S_{Ri}, S_{ri}, and S_{Mi}, for each sample.

0	λ / nm	400	500	600	700	800	900	1000
T0%	Sri (λ) /%	0,001	0,001	0,000	0,000	0,001	0,002	0,002
	SMi (λ) /%	0,002	0,001	0,002	0,002	0,002	0,004	0,001
	SRi (λ) /%	0,002	0,001	0,002	0,002	0,002	0,004	0,002
T100%	Sri (λ) /%	0,007	0,009	0,007	0,008	0,012	0,022	0,019
	SMi (λ) /%	1,906	0,029	0,008	0,029	0,069	0,633	0,434
	SRi (λ) /%	1,906	0,030	0,010	0,030	0,070	0,634	0,434
HY93	Sri (λ) /%	0,011	0,010	0,006	0,010	0,012	0,027	0,021
	SMi (λ) /%	1,803	0,068	0,020	0,024	0,015	0,457	0,348
	SRi (λ) /%	1,803	0,068	0,021	0,026	0,018	0,457	0,349
HZ93	Sri (λ) /%	0,008	0,012	0,006	0,009	0,009	0,007	0,015
	SMi (λ) /%	1,442	0,040	0,013	0,021	0,040	0,261	0,185
	SRi (λ) /%	1,442	0,041	0,015	0,022	0,041	0,261	0,186
JA93	Sri (λ) /%	0,009	0,007	0,003	0,006	0,007	0,012	0,008
	SMi (λ) /%	1,065	0,018	0,006	0,008	0,029	0,332	0,278
	SRi (λ) /%	1,065	0,019	0,007	0,010	0,029	0,332	0,278
JB93	Sri (λ) /%	0,007	0,004	0,005	0,007	0,006	0,005	0,007
	SMi (λ) /%	0,600	0,057	0,041	0,018	0,019	0,249	0,199
	SRi (λ) /%	0,600	0,057	0,042	0,019	0,019	0,249	0,199
JC93	Sri (λ) /%	0,038	0,002	0,003	0,002	0,003	0,007	0,087
	SMi (λ) /%	0,155	0,010	0,018	0,015	0,008	0,113	0,119
	SRi (λ) /%	0,158	0,010	0,018	0,015	0,008	0,113	0,142
JD93	Sri (λ) /%	0,001	0,001	0,001	0,002	0,002	0,005	0,005
	SMi (λ) /%	0,037	0,001	0,002	0,003	0,019	0,098	0,079
	SRi (λ) /%	0,037	0,001	0,003	0,003	0,019	0,098	0,079
JE93	Sri (λ) /%	0,001	0,001	0,001	0,001	0,001	0,003	0,004
	SMi (λ) /%	0,009	0,001	0,002	0,005	0,003	0,048	0,031
	SRi (λ) /%	0,010	0,001	0,003	0,005	0,003	0,048	0,031
JF93	Sri (λ) /%	0,001	0,001	0,001	0,000	0,002	0,003	0,004
	SMi (λ) /%	0,002	0,000	0,001	0,005	0,001	0,021	0,012
	SRi (λ) /%	0,002	0,001	0,001	0,005	0,002	0,021	0,012
JG93	Sri (λ) /%	0,001	0,001	0,001	0,001	0,001	0,003	0,002
	SMi (λ) /%	0,000	0,002	0,001	0,001	0,002	0,011	0,008
	SRi (λ) /%	0,001	0,002	0,001	0,001	0,003	0,011	0,008

Standard uncertainty calculated by type B method

As the spectrophotometer is an instrument with various components, with limited performance, although as good as possible, this non-statistical method to calculate uncertainties will need to characterize the different kinds of instrumental imperfections, deduced from the manufacturer´s specifications.

The standard uncertainty calculated by method type B is given by equation 3.6.

$$u_{\mathrm{B}}(T_i) = \sqrt{u_{\lambda}^2 + u_{\mathrm{phot.\ acc}}^2 + u_{\mathrm{nonlin}}^2 + u_{\mathrm{phot.\ rep}}^2 + u_{\mathrm{phot.noise}}^2 + u_{\mathrm{photo.lev}}^2 + u_{\mathrm{stray\ light}}^2} \qquad (3.6)$$

Where:

u_{λ} – Uncertainty associated to the wavelength;

$u_{\mathrm{phot.\ acc}}$ – Uncertainty associated to the photometric accuracy;

$u_{\mathrm{non.\ lin}}$ – Uncertainty associated to the non–linearity of the detectors;

$u_{\mathrm{phot.\ rep}}$ – Uncertainty associated to the photometric reproducibility;

$u_{\mathrm{phot.\ noise}}$ – Uncertainty associated to photometric noise

$u_{\mathrm{photo.\ lev}}$ – Uncertainty associated to photometric leveling

$u_{\mathrm{stray\ light}}$ – Uncertainty associated to the stray light

a. Uncertainty associated to the wavelength u_{λ}

The component of the spectrophotometer responsible for controlling the wavelength is the double monochromator. According to the specifications, there are three uncertainties related to it: resolution, accuracy, and reproducibility stated in tables 3.6 and 3.7 below. They are also dependent on the spectrum region.

Table 3.6 – Uncertainties associated to the wavelength in the UV/Vis region

Spectral region:	**UV/Vis**		
	Variability	Distribution	***u* / nm**
Resolution / nm:	0,05	rectangular	0,014
Accuracy / nm	0,16	rectangular	0,046
Reproducibility / nm:	0,020	rectangular	0,006

Table 3.7 – Uncertainties associated to the wavelength in the NIR region

Spectral region:	**NIR**		
	Variability	Distribution	***u* / nm**
Resolution / nm:	0,2	rectangular	0,058
Accuracy / nm	0,6	rectangular	0,173
Reproducibility / nm:	0,08	rectangular	0,023

The resulting uncertainty is given by equation 3.7.

$$u(\lambda) = \sqrt{u_{\mathrm{res}}^2 + u_{acc}^2 + u_{repr}^2} \quad (3.7)$$

Where:

u_{res} – Uncertainty of the wavelength associated to its resolution

u_{acc} – Uncertainty of the wavelength associated to its accuracy

u_{repr} – Uncertainty of the wavelength associated to its reproducibility

The results obtained by equation 3.7 are listed in table 3.8 below.

Table 3.8 – Resulting uncertainties by applying equation 3.7 to the values given in table 3.6 and 3.7

Spectral region:	Resulting uncertainty u(λ)/nm
UV/Vis	0,05
NIR	0,18

To finally reach the value of u_λ it is used equation 3.8.

$$u_\lambda = \frac{T_2 - T_1}{\lambda_2 - \lambda_1}\, u(\lambda) \quad (3.8)$$

Where:

T_i – Transmittance value of the sample measured wavelength i

λ_i – Wavelength i to be analyzed

b. Uncertainty associated to the photometric components

According to the equipment specifications, the uncertainties associated to the photometric components are due to the photometric accuracy, reproducibility, noise, leveling, the nonlinearity of the detectors, and the stray light. Some of the specifications are given as a function of the absorptance and not of the transmission. In those cases, it is needed to apply equation 3.9 so that it is possible to have a result as a function of the transmittance and to use a linear interpolation to obtain more accurate values.

$$u(T) = T.\ln(10).u(\mathrm{A}) \quad (3.9)$$

Where:

$u(T)$ – Uncertainty as a function of the transmittance

$u(A)$ – Uncertainty as a function of the absorbance

i. Photometric accuracy

According to the manufacturer the table 3.9 is used to calculate the photometric accuracy. In this case, it was needed to apply equation 3.9 so that the result is presented in the function of the transmittance.

Table 3.9 – Specifications associated to the calculation of the uncertainty resulting from the photometric accuracy

Absorbance	Variability	Distribution	$u(A)$	T / %	$u(T)$ /%
2	0,006	rectangular	0,0017	1,00	0,0040
1	0,006	rectangular	0,0017	10,00	0,0399
0,5	0,004	rectangular	0,0012	31,62	0,0841

It is also needed to use linear interpolation if the transmittance is $1{,}00\ \% < T \leq 31{,}62\ \%$, which is represented in the system of equations 3.10.

$$u_{phot.\ acc}(T) = \begin{cases} 0{,}0040\,, & T/\% \leq 1{,}00 \\ 0{,}0040 \times T, & 1{,}00 < T/\% \leq 10{,}00 \\ 0{,}0020 \times T + 0{,}01944\,, & 10{,}00 < T/\% \leq 31{,}62 \\ 0{,}0841, & 31{,}62 < T/\% \leq 100{,}00 \end{cases} \tag{3.10}$$

Where:

$u_{phot.\ acc}(T)$ – Uncertainty associated to the photometric accuracy

ii. Nonlinearity of the detectors

To calculate this uncertainty, again it is used a linear interpolation, equations 3.11 and 3.12, based on equation 3.9 using the values in tables 3.10 and 3.11 taken from the manufacturer´s specifications.

Table 3.10 – Specifications to calculate the uncertainty associated to the nonlinearity in the UV/Vis region

Spectral region:		**UV/Vis**			
Absorbance	Variability	Distribution	u / nm	T / %	$u(T)$ /%
3	0,012	rectangular	0,0035	0,10	0,0008
2	0,004	rectangular	0,0012	1,00	0,0027
1	0,002	rectangular	0,0006	10,00	0,0133

$$u_{nonlin}(T) = \begin{cases} 0{,}0008\,, & \mathrm{T} \leq 0{,}10 \\ 0{,}0021 \times \mathrm{T} + 0.0006, & 0{,}10 < \mathrm{T} \leq 1{,}00 \\ 0{,}0012 \times \mathrm{T} + 0{,}0015\,, & 1{,}00 < \mathrm{T} \leq 10{,}00 \\ 0{,}0133, & 10{,}00 < \mathrm{T} \leq 100{,}00 \end{cases} \tag{3.11}$$

Table 3.11– Specifications to calculate the uncertainty associated to the nonlinearity in the NIR region

Spectral region:		**NIR**			
Absorbance	Variability	Distribution	$u(A)$	T / %	$u(T)$ /%
2	0,014	rectangular	0,0040	1,00	0,0093
1	0,004	rectangular	0,0012	10,00	0,0266

$$u_{nonlin}(T) = \begin{cases} 0{,}0093, & T \leq 0{,}10 \\ 0{,}0019 \times T + 0{,}0074, & 1{,}00 < T \leq 10{,}00 \\ 0{,}0266, & 10{,}00 < T \leq 100{,}00 \end{cases} \quad (3.12)$$

iii. Photometric reproducibility

It is used a linear interpolation to calculate the photometric reproducibility uncertainty, equation 3.13, based on equation 3.9 using the values in table 3.12 taken from the manufacturer´s specifications.

Table 3.12 – Specifications to calculate the uncertainty associated to the photometric reproducibility.

Absorbance	Variability	Distribution	$u(A)$	T / %	$u(T)$ /%
1	0,00016	normal	0,00016	10,00	0,0037
0,5	0,00008	normal	0,00008	31,62	0,0058
0,3	0,00008	normal	0,00008	50,12	0,0092

$$u_{phot.\ rep.}(T) = \begin{cases} 0{,}0037\,, & T/\% \leq 10{,}00 \\ 0{,}0001 \times T + 0.0027, & 10{,}00 < T/\% \leq 31{,}62 \\ 0{,}0002 \times T, & 31{,}62 < T/\% \leq 50{,}12 \\ 0{,}0092, & 50{,}12 < T/\% \leq 100{,}00 \end{cases} \quad (3.13)$$

iv. Photometric noise

To calculate this uncertainty, again it is used a linear interpolation, equations 3.14 and 3.15, based on equation 3.9 using the values in tables 3.13 and 3.14 taken from the manufacturer´s specifications.

Table 3.13 – Specifications to calculate the uncertainty associated to the nonlinearity in the UV/Vis region

Spectral region:		**UV/Vis**			
Absorbance	Variability	Distribution	u / nm	T / %	$u(T)$ /%
4	0,001	rectangular	0,00029	0,01	0,0000
2	0,0002	rectangular	0,00006	1,00	0,0001
0	0,00005	rectangular	0,00001	100,00	0,0033

$$u_{nonlin}(T) = \begin{cases} 0{,}0093, & T/\% \leq 0{,}10 \\ 0{,}0019 \times T + 0{,}0074, & 1{,}00 < T/\% \leq 10{,}00 \\ 0{,}0266, & 10{,}00 < T/\% \leq 100{,}00 \end{cases} \quad (3.14)$$

Table 3.14 – Specifications to calculate the uncertainty associated to the nonlinearity in the NIR region

Spectral region:		NIR			
Absorbance	Variability	Distribution	$u(A)$	T / %	$u(T)$ /%
3	0,003	rectangular	0,00087	0,10	0,0002
2	0,0001	rectangular	0,00003	1,00	0,0001
0	0,00004	rectangular	0,00001	100,00	0,0027

$$u_{nonlin}(T) = \begin{cases} 0{,}0002, & T/\% \leq 0{,}10 \\ -0{,}0001 \times T + 0{,}0002, & 0{,}10 < T/\% \leq 1{,}00 \\ 0{,}00003 \times T + 0{,}00004, & 1{,}00 < T/\% \leq 100{,}00 \end{cases} \quad (3.15)$$

v. Photometric leveling

This uncertainty was calculated using equation 3.9 with $u(A) = 0{,}0005\,A$ constant in all the spectrum´s range.

vi. Stray light

This uncertainty was calculated using equation 3.16 based on the values of table 3.15 that refers to the specifications regarding the uncertainty due to the stray light.

Table 3.15 – Specifications associated to the calculation of the uncertainty resulting from the stray light

λ / nm	*S(T) / %*	Distribution	*u(t) / %*
220	0,00007	rectangular	0,00002
340	0,00007	rectangular	0,00002
370	0,00007	rectangular	0,00002
1420	0,00040	rectangular	0,00012
2365	0,00050	rectangular	0,00014

$$u_{nonlin}(T)/\,\% = \begin{cases} 0{,}00002, & \lambda \,/\, \mathrm{nm} \leq 370 \\ 6{,}3 \times 10^{-8} \times T + 6{,}4 \times 10^{-6}, & 370 < \lambda \,/\, \mathrm{nm} \leq 1420 \\ 0{,}00012, & 1420 \leq \lambda \,/\, \mathrm{nm} \end{cases} \quad (3.16)$$

c. Resulting standard uncertainty calculated by type B method

Table 3.16 displays the results of the calculation of the uncertainty by a type B using equation 3.6.

Table 3.16 –Standard uncertainties calculated by type B method for each sample

Sample	λ / nm	400	500	600	700	800	900	1000
T0(%)	$u_b(T_i)/\%$	0,0055	0,0055	0,0055	0,0055	0,0055	0,0108	0,0108
T100 (%)	$u_b(T_i)/\%$	0,1355	0,1366	0,1366	0,1366	0,1366	0,1384	*0,1382*
HY93	$u_b(T_i)/\%$	0,1283	0,1295	0,1296	0,1298	0,1298	0,1322	0,1322
HZ93	$u_b(T_i)/\%$	0,1132	0,1147	0,1141	0,1153	0,1119	0,1109	0,1078
JA93	$u_b(T_i)/\%$	0,1047	0,1064	0,1055	0,1068	0,1024	0,1015	0,0980
JB93	$u_b(T_i)/\%$	0,0843	0,0906	0,0888	0,0948	0,0948	0,0959	0,0910
JC93	$u_b(T_i)/\%$	0,0411	0,0458	0,0444	0,0580	0,0581	0,0550	0,0492
JD93	$u_b(T_i)/\%$	0,0100	0,0160	0,0162	0,0354	0,0486	0,0543	0,0530
JE93	$u_b(T_i)/\%$	0,0057	0,0064	0,0064	0,0152	0,0261	0,0317	0,0299
JF93	$u_b(T_i)/\%$	0,0055	0,0056	0,0056	0,0080	0,0143	0,0193	0,0182
JG93	$u_b(T_i)/\%$	0,0055	0,0055	0,0055	0,0059	0,0085	0,0134	0,0129

Uncertainty Results

With the calculated standard uncertainties by type A and type B methods, through equation 3.3, the resulting standard uncertainties can be obtained. values combining these two components, the uncertainty related to type A is the reproducibility uncertainty S_{Ri}, $(u_{\mathrm{A}} = S_{\mathrm{Ri}})$ and type B is given by equation 3.6. These values are applied in equation 3.2 to obtain the combined standard uncertainty of the measurements.

It is used the expanded uncertainty to have a confidence level above 95 %, with a coverage factor $k = 2$ expressed in equation 2.14. The results are shown in table 3.17 below.

Table 3.17 – Expanded uncertainty from each sample

		Wavelength λ(nm)						
Sample		400	500	600	700	800	900	1000
HY93	$UT_f(\lambda)\%$	5,0877	0,3887	0,3630	0,3679	0,3845	1,5322	1,1303
HZ93	$UT_f(\lambda)\%$	4,0066	0,3155	0,3009	0,3100	0,3159	0,9829	0,6785
JA93	$UT_f(\lambda)\%$	3,1083	0,2725	0,2642	0,2723	0,2673	0,9026	0,6882
JB93	$UT_f(\lambda)\%$	1,6577	0,2310	0,2132	0,2214	0,2269	0,6929	0,5181
JC93	$UT_f(\lambda)\%$	0,4974	0,0992	0,1005	0,1288	0,1282	0,3010	0,3160
JD93	$UT_f(\lambda)\%$	0,1132	0,0353	0,0359	0,0752	0,1116	0,2783	0,2210
JE93	$UT_f(\lambda)\%$	0,0326	0,0174	0,0181	0,0354	0,0567	0,1410	0,1021
JF93	$UT_f(\lambda)\%$	0,0176	0,0160	0,0163	0,0221	0,0322	0,0741	0,0554
JG93	$UT_f(\lambda)\%$	0,0163	0,0162	0,0160	0,0166	0,0217	0,0471	0,0402

Where:

$UT_f(\lambda)$ – Expanded uncertainty of the sample´s transmittance in the function of the wavelength

3.3.3. Calibration

Calibration is the "operation that, under specified conditions, in a first step, establishes a relation between the quantity values with measurement uncertainties provided by measurement standards and corresponding indications with associated measurement uncertainties and, in a second step, uses this information to establish a relation for obtaining a measurement result from an indication" [5].

To create the calibrate model used in this experience a calibration curve is utilized, which in this case it´s a straight-line function based on the method of the standard ISO/TS 28037:2010 [39].

In this scenario, it is needed to create two calibration functions, one for transmittances lower than 10 % and another for transmittances equal to or greater than 10 %. The samples HY93, HZ93, JA93, JB93, JC93, JD93, JE93, JF93, and JG93 were used because they verify this condition and have a certified value NPL, which is also required to create a valid calibration function.

The values are obtained in the formula expressed by equation 3.17 below.

$$T_c = a + b \times T_f \tag{3.17}$$

Where:

T_c – Corrected transmittance of the sample

T_f – Transmittance from the sample, calculated in table 3.4

a – Ordinate in the origin

b – Slope of the straight line

In tables 3.18 and 3.19, it is presented the results from the calibration function following the instructions in ISO/TS 28037:2010 for both transmittances under 10 % and equal or above 10 %, respectively.

Table 3.18 – Calibration function´s constants and uncertainties for T_f<10 %

λ / nm	Slope(b)	Ordinate (0,a)	*u(b)*	*u(a)*	*cov(a,b)*
400	1,0233	-0,0007	0,0367	0,0132	-0,0002
500	1,0153	-0,0019	0,0153	0,0134	-0,0001
600	1,0128	0,0001	0,0152	0,0134	-0,0001
700	1,0099	0,0050	0,0127	0,0225	-0,0002
800	1,0008	0,0080	0,0194	0,0521	-0,0009
900	0,9593	0,0090	0,0381	0,1007	-0,0034
1000	0,9516	0,0165	0,0291	0,0768	-0,0019

Table 3.19 – Calibration function´s constants and uncertainties for T_f ≥10 %

λ / nm	Slope(b)	Ordinate (0,a)	*u(b)*	*u(a)*	*cov(a,b)*
400	0,9962	0,7302	0,0657	3,1141	-0,1850
500	1,0044	0,1501	0,0048	0,1684	-0,0006
600	1,0036	0,0980	0,0047	0,1661	-0,0006
700	1,0030	0,1489	0,0056	0,2473	-0,0012
800	1,0042	0,0117	0,0055	0,2387	-0,0011
900	0,9959	-0,4460	0,0141	0,4580	-0,0050
1000	0,9931	-0,5084	0,0121	0,3979	-0,0038

Validation of the calibration process

Two conditions are necessary to validate this process of calibration. The first one is imposed by the standard ISO/TS 28037:2010, which requires that the "observed chi-squared, ${\chi_{obs}}^2$ value doesn´t exceed the 95 % quantile of the distribution of the chi-squared, ${\chi_{(0,95:\nu)}}^2$ and if it does, reject the straight-line model". This is a condition based on the confidence in the parameters of the fit given by tables 3.18 and 3.19.

The second condition, introduced in subsection 2.1.3.2, states that the relative error (equation 2.13), E_r, between the corrected measurement value and the reference value doesn´t exceed 5 %. This condition evidences the goodness of the fit to the calibration function.

In the following tables 3.20 and 3.21, it can be observed that the first condition is verified for T_f>10 % and $T_f \geq 10$ %.

Table 3.20 – Comparison between ${\chi_{obs}}^2$ and ${\chi_{(0,95:\nu)}}^2$ values obtained for $T_f < 10$ %

λ / nm	${\chi_{obs}}^2$	${\chi_{(0,95;\,\nu)}}^2$
400	0,009423	7,8147
500	0,080826	5,9915
600	0,02602	5,9915
700	0,027193	5,9915
800	0,005485	3,8415
900	0,000463	3,8415
1000	0,004617	5,9915

Table 3.21 – Comparison between ${\chi_{obs}}^2$ and ${\chi_{(0,95:\nu)}}^2$ values obtained for $T_f \geq 10$ %

λ / nm	${\chi_{obs}}^2$	${\chi_{(0,95;\,\nu)}}^2$
400	0,0171	5,9915
500	1,942	7,8147
600	1,5675	5,9915
700	1,4045	7,8147
800	0,7155	5,9915
900	0,3266	9,4877
1000	0,9454	5,9915

Table 3.22 displays the corrected transmittance values, T_c, obtained using the calibration function, equation 3.17, and the reference transmittance values, given by the NPL certificates, T_{NPL}, with the respective uncertainty. In order to check the goodness of the fitted calibration function, the relative error, E_r, corresponding to by the condition: $E_r(\lambda) \leq 5$ %, is also displayed.

Table 3.22 – T_c, T_{NPL}, U_{Tc}, $U_{T_{NPL}}$, and relative error, E_r, in function of the wavelength

		Wavelength λ(nm)						
Sample		400	500	600	700	800	900	1000
HY93	$T_c(\lambda)/\%$	91,47	91,89	91,89	92,02	92,05	91,43	91,32
	$T_{NPL}(\lambda)/\%$	91,30	91,48	91,54	91,66	91,79	91,87	91,94
	$UT_c(\lambda)/\%$	5,09	0,39	0,36	0,37	0,38	1,53	1,13
	$UT_{NPL}(\lambda)/\%$	0,4	0,40	0,40	0,40	0,40	0,50	0,50
	$E_r(\lambda)/\%$	0,19	0,44	0,40	0,39	0,28	0,48	0,68
HZ93	$T_c(\lambda)/\%$	70,94	72,15	72,15	72,86	67,89	61,02	56,30
	$T_{NPL}(\lambda)/\%$	71,35	72,47	71,54	73,16	68,11	61,17	56,23
	$UT_c(\lambda)/\%$	4,01	0,32	0,30	0,31	0,32	0,98	0,68
	$UT_{NPL}(\lambda)/\%$	0,32	0,3200	0,32	0,32	0,30	0,38	0,36
	$E_r(\lambda)/\%$	-0,58	-0,4422	-0,48	-0,41	0,33	0,25	0,12
JA93	$T_c(\lambda)/\%$	57,99	59,73	59,73	60,33	52,84	43,59	37,53
	$T_{NPL}(\lambda)/\%$	57,76	59,59	58,03	60,21	52,75	43,26	37,13
	$UT_c(\lambda)/\%$	3,11	0,27	0,26	0,27	0,27	0,90	0,69
	$UT_{NPL}(\lambda)/\%$	0,26	0,26	0,26	0,26	0,24	0,32	0,30
	$E_r(\lambda)/\%$	0,39	0,23	0,23	0,20	0,18	0,77	1,09
JB93	$T_c(\lambda)/\%$	29,37	31,42	31,42	38,75	38,76	33,26	29,14
	$T_{NPL}(\lambda)/\%$	29,38	31,67	30,72	38,94	38,88	33,11	28,96
	$UT_c(\lambda)/\%$	0,20	0,23	0,21	0,22	0,23	0,69	0,52
	$UT_{NPL}(\lambda)/\%$	1,66	0,20	0,20	0,22	0,22	0,30	0,28
	$E_r(\lambda)/\%$	-0,04	-0,80	-0,55	-0,48	0,32	0,46	0,63
JC93	$T_c(\lambda)/\%$	9,79	11,24	10,56	16,81	16,73	12,14	9,38
	$T_{NPL}(\lambda)/\%$	9,76	11,20	10,53	16,76	16,70	12,18	9,36
	$UT_c(\lambda)/\%$	0,50	0,04	0,10	0,13	0,13	0,30	0,32
	$UT_{NPL}(\lambda)/\%$	0,1	0,04	0,10	0,14	0,14	0,20	0,20
	$E_r(\lambda)/\%$	0,29	0,36	0,29	0,30	0,18	0,34	0,19
JD93	$T_c(\lambda)/\%$	2,13	3,57	3,57	8,16	12,38	12,04	11,28
	$T_{NPL}(\lambda)/\%$	2,14	3,58	3,61	8,17	12,38	12,11	11,38
	$UT_c(\lambda)/\%$	0,11	0,04	0,04	0,08	0,11	0,28	0,22
	$UT_{NPL}(\lambda)/\%$	0,03	0,04	0,04	0,08	0,12	0,22	0,24
	$E_r(\lambda)/\%$	-0,42	-0,17	-0,10	-0,13	0,03	0,56	0,89
JE93	$T_c(\lambda)/\%$	0,54	1,10	1,10	3,36	5,93	5,76	5,29
	$T_{NPL}(\lambda)/\%$	0,54	1,09	1,10	3,36	5,93	5,76	5,30
	$UT_c(\lambda)/\%$	0,03	0,02	0,02	0,04	0,06	0,14	0,10
	$UT_{NPL}(\lambda)/\%$	0,01	0,02	0,02	0,04	0,06	0,10	0,12
	$E_r(\lambda)/\%$	0,11	0,38	0,25	0,14	0,05	0,03	0,10
JF93	$T_c(\lambda)/\%$	0,16	0,38	0,38	1,54	3,10	3,00	2,71
	$T_{NPL}(\lambda)/\%$	0,16	0,38	0,39	1,54	3,10	3,00	2,71
	$UT_c(\lambda)/\%$	0,02	0,02	0,02	0,02	0,03	0,07	0,06
	$UT_{NPL}(\lambda)/\%$	0,00	0,02	0,01	0,02	0,03	0,06	0,06
	$E_r(\lambda)/\%$	0,13	0,14	0,01	0,13	0,09	0,05	0,05
JG93	$T_c(\lambda)/\%$	0,05	0,14	0,14	0,73	1,66	1,59	1,41
	$T_{NPL}(\lambda)/\%$	0,05	0,14	0,14	0,73	1,67	1,59	1,41
	$UT_c(\lambda)/\%$	0,02	0,02	0,02	0,02	0,02	0,05	0,04
	$UT_{NPL}(\lambda)/\%$	0,00	0,00	0,00	0,01	0,02	0,03	0,03
	$E_r(\lambda)/\%$	-0,32	-1,35	-0,65	-0,17	0,04	0,02	0,05

From the data displayed in tables 3.20, 3.21 and 3.22, it can be concluded that the calibration process is validated and be be used for any instrumental configuration of the spectrophotometer.

3.4. **Reflectance**

Using the validated method displayed in the previous chapter dedicated to the transmission configuration of the spectrophotometer, we now study colorimetry based on measuring reflectance of samples by spectrophotometry.

The samples, HV93, HT93 Pale Grey, HT93 Deep Grey, HT93 Deep Pink, HT93 Red, HT93 Orange, HT93 Bright Yellow, HT93 Cyan, HT93 Deep Blue, were chosen for the calibration of the spectrophotometer with 102 mm^2 area and 9 mm deep certified by the NPL in 2006 figure 3.5.

a) Orange (left) Bright Yellow (right); b) Deep Pink (left) Red (right); c) Cyan (left) Deep Blue (right); d) Pale Grey (left) Deep Grey (right)

Figure 3.5 – HT93 Samples and HV93 Samples

The samples were placed in the spectrophotometer with its identification on the top right corner facing the hole where the light beam hits it.

It is used a similar formula to the transmittance calculation to calculate each sample´s reflectance, shown in equation 3.18.

$$R_s(\lambda) = \rho'(\lambda) \times \frac{R_s^*(\lambda) - R_0(\lambda)}{R_{ref}(\lambda) - R_0(\lambda)} \qquad (3.18)$$

Where:

$R_s(\lambda)$ – Sample reflectance

$\rho'(\lambda)$ – Certified value of a sample with a reflectance near 100 %

$R_S^*(\lambda)$ – Arithmetic mean of the 2 measurements´ days of the sample reflectance

$R^*{}_0(\lambda)$ – Arithmetic mean of the 2 measurements´ days of the sample corresponding to 0 % R reflectance;

$R^*{}_{\text{ref}}(\lambda)$ – Arithmetic mean of the 2 measurements´ days of the sample corresponding to 100 % R reflectance

To obtain the $R_0(\lambda)$ and $R_{ref}(\lambda)$ values, it was needed to use a light trap and a sample that has a reflectance of nearly 100 %, which can be seen in figure 3.6 below.

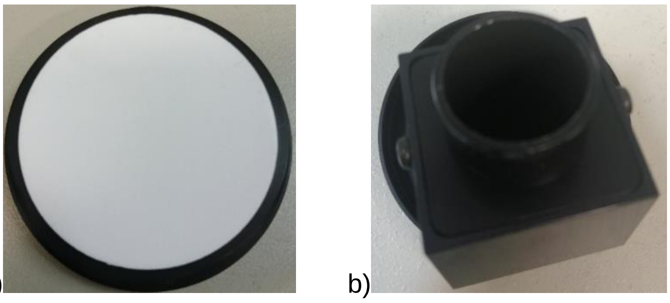

a) b)

Figure 3.6 – a) Light Trap; b) Fluoropolymer with R(%)≈100% made by Labsphere

3.4.1. Uncertainty Calculation of Reflectance

By applying the combined standard uncertainty equation 2.13 to equation 3.18, it is obtained equation 3.19 which is how the uncertainty in reflectance is calculated.

$$u_{R_s} = \sqrt{u_{R_S^*}{}^2 . \left(\frac{-\rho'}{R_0 - R_{ref}}\right)^2 + u_{R_o}^2 * \left(\frac{\rho' * (R_S^* - R_{100})}{\left(R_0 - R_{Ref}\right)^2}\right)^2 + u_{R_{ref}}{}^2 . \left(\frac{-\rho' * (R_S^* - R_0)}{(R_{ref} - R_0)^2}\right)^2 + u_{\rho'}{}^2 . \left(\frac{(R_S^* - R_0)}{(R_{ref} - R_0)}\right)^2} \qquad (3.19)$$

Where:

$\rho'(\lambda)$ – Certified value of a sample with a reflectance near 100 %

$R_S^*(\lambda)$ – Arithmetic mean of the 2 measurements´ days of the sample reflectance

$R^*{}_0(\lambda)$ – Arithmetic mean of the 2 measurements´ days of the sample´s corresponding to 0 % R reflectance;

$R^*{}_{\text{ref}}(\lambda)$ – Arithmetic mean of the 2 measurements´ days of the sample´s corresponding to 100 % R reflectance

$u_{R_S^*}$ – Uncertainty associated to $R_s(\lambda)$

u_{R_0} – Uncertainty associated to $R_0(\lambda)$

$u_{R_{\text{ref}}}$ – Uncertainty associated to $R_{ref}(\lambda)$

$u_{\rho'}$ – Uncertainty associated to ρ'

u_{R_s} – Combined standard uncertainty associated with the sample´s reflectance

The uncertainties calculated by methods type A and B in reflectance follow the same procedure used in section 3.3.2 for transmission but using the reflectance instead of the transmittance.

Because the study of colorimetry requires measurements along all the visible spectrum, table 3.23 shows only the reflectance and the expanded uncertainties with $k = 2$ of the samples in some wavelengths.

Table 3.23 – Reflectance and expanded uncertainty values of the samples, HV93, HT93 Pale Grey, HT93 Deep Grey, HT93 Deep Pink, HT93 Red, HT93 Orange, HT93 Bright Yellow, HT93 Cyan, HT93 Deep

Wavelength λ / nm		380	400	450	500	550	600	650	700	750	770
HV93	$R_s(\lambda)/\%$	4,79	4,82	4,83	4,81	4,75	4,49	4,47	7,58	5,28	8,39
	$UR_s(\lambda)/\%$	0,07	0,07	0,07	0,05	0,05	0,05	0,05	0,12	0,06	0,13
HT93 Pale grey	$R_s(\lambda)/\%$	58,32	61,23	63,51	63,95	64,20	63,81	63,77	62,90	63,95	62,48
	$UR_s(\lambda)/\%$	0,74	0,77	0,80	0,47	0,47	0,47	0,47	0,79	0,47	0,78
HT93 Deep grey	$R_s(\lambda)/\%$	8,47	8,63	8,53	8,57	8,91	8,49	8,69	18,73	11,49	20,89
	$UR_s(\lambda)/\%$	0,13	0,13	0,13	0,09	0,10	0,09	0,10	0,26	0,12	0,29
HT93 Deep pink	$R_s(\lambda)/\%$	18,39	17,99	13,51	10,45	11,57	20,36	37,88	54,19	51,41	53,45
	$UR_s(\lambda)/\%$	0,25	0,25	0,19	0,11	0,12	0,19	0,31	0,69	0,39	0,68
HT93 Red	$R_s(\lambda)/\%$	7,44	7,44	7,42	7,51	8,20	21,47	64,82	79,61	75,76	80,10
	$UR_s(\lambda)/\%$	0,11	0,11	0,11	0,08	0,09	0,22	0,48	0,99	0,54	1,00
HT93 Orange	$R_s(\lambda)/\%$	9,42	9,60	9,86	10,36	23,13	71,54	79,15	84,12	82,70	84,44
	$UR_s(\lambda)/\%$	0,14	0,14	0,15	0,11	0,23	0,52	0,57	1,04	0,59	1,05
HT93 Bright yellow	$R_s(\lambda)/\%$	5,92	6,03	7,80	31,51	72,36	78,79	81,72	83,73	83,52	84,65
	$UR_s(\lambda)/\%$	0,09	0,09	0,12	0,29	0,52	0,56	0,58	1,04	0,59	1,20
HT93 Cyan	$R_s(\lambda)/\%$	20,46	29,48	43,89	41,23	20,75	12,04	10,59	16,91	13,61	16,53
	$UR_s(\lambda)/\%$	0,29	0,40	0,56	0,33	0,19	0,12	0,11	0,24	0,14	0,23
HT93 Deep blue	$R_s(\lambda)/\%$	15,82	17,94	9,75	5,44	5,28	4,78	4,79	49,72	8,86	55,50
	$UR_s(\lambda)/\%$	0,22	0,25	0,15	0,06	0,06	0,05	0,05	0,64	0,10	0,70

$UR_s(\lambda)$ – Expanded uncertainty of the sample´s reflectance in function of the wavelength

3.4.2. Calibration in Reflectance

In reflectance, the construction of the calibration model also follows the procedures in ISO/TS 28037:2010 used in section 3.3.3., so there are two calibration lines to each wavelength, one for reflectance values under 10% ($R(\%) < 10\,\%$) and another for reflectance values equal or above 10 % ($R(\%) \geq 10\ \%$.

The calibration line follows equation 3.20 below.

$$R_c = a + b \times R_s \quad (3.20)$$

Where:

R_c – Corrected reflectance of the sample

R_s – Reflectance from the sample, calculated in table 3.23

a – Ordinate in the origin

b – Slope of the straight line

The values of the variables in equation 3.20 are exposed in table 3.24 for reflectance values under 10 % ($R(\%) < 10\,\%$) and in table 3.25 for reflectance values equal or above 10 % ($R(\%) \geq 10\,\%$). In table 3.24, the variables for wavelengths above 700 nm are not disposed because there weren´t three samples with a reflectance under 10% collected in those wavelengths. The values are disposed with a 50 nm interval, in annex C it is possible to observe them with a 10 nm interval .

.

Table 3.24 – Variables and uncertainties associated to eq 3.21 for *R* <10 %

wavelength λ / nm	Slope(b)	Ordinate (0,a)	u(b)	u(a)	cov(a,b)
400	0,9714	0,8150	0,0442	0,2700	-0,0115
450	1,0019	0,4813	0,0364	0,2411	-0,0084
500	1,0364	0,1187	0,0476	0,2713	-0,0126
550	1,0383	0,0898	0,0416	0,2387	-0,0096
600	1,0075	0,2507	0,0517	0,2618	-0,0132
650	0,9945	0,3605	0,0496	0,2519	-0,0121
700	1,0092	0,3802	0,0611	0,3625	-0,0216

Table 3.25 – Variables and uncertainties associated to eq 3.20 for $R \geq 10\%$

wavelength λ / nm	Slope(b)	Ordinate (0,a)	u(b)	u(a)	cov(a,b)
400	1,0038	0,5156	0,0256	0,6212	-0,0145
450	1,0098	0,3388	0,0200	0,5054	-0,0081
500	1,0088	0,2219	0,0109	0,2230	-0,0019
550	1,0039	0,4206	0,0110	0,2760	-0,0024
600	1,0009	0,5209	0,0092	0,2577	-0,0019
650	1,0041	0,3546	0,0077	0,2659	-0,0015
700	1,0020	0,3738	0,0071	0,2204	-0,0011
750	1,0015	0,6035	0,0100	0,3650	-0,0030
770	0,9950	1,0253	0,0102	0,3795	-0,0032

3.5. Colorimetric Analysis

The objective of this subchapter is to do a colorimetric analysis of the samples RAL 9006-HR White Aluminum, RAL 6018-GL Yellow green, RAL 9010-GL Pure White, RAL 8015 -GL Chestnut Brown, RAL 8001-GL Ochre Brown, RAL 7001-GL Silbergrau, RAL 4001-GL Rotlila, RAL 3000-GL Feuerrot, RAL 2003-GL Pastellorange, RAL 1021-GL Colza Yellow, from RAL Colours, dimensions: A5 sized (14.8 cm x 21.0 cm) and the color illustration A6-sized (10.5 cm x 14.8 cm). in figure 3.7 below [19].

RAL 9006-HR White Aluminum

RAL 6018-GL Yellow green

RAL 9010-GL Pure White

RAL 8015 -GL Chestnut Brown

RAL 8001-GL Ochre Brown

RAL 7001-GL Silbergrau

RAL 4001-GL Rotlila

RAL 3000-GL Feuerrot

RAL 2003-GL Pastellorange

1021-GL Colza Yellow

Figure 3.7 – Samples from RAL Colors

The first step is to measure the reflectance of the samples. The results for wavelengths and their uncertainties in 380 nm, 400 nm, 450 nm, 500 nm, 550 nm, 600 nm, 650 nm, 700 nm, 750 nm, and 770 nm are in table 3.26 below.

Table 3.26 – measurements´ results of the reflectance and its uncertainties of the samples from RAL Colours

Wavelength λ / nm		380	400	450	500	550	600	650	700	750	770
HR 9006 White Aluminum	$R_S(\lambda)/\%$	39,136	45,317	45,527	46,021	45,758	45,576	45,356	45,024	44,164	43,731
	$U_{R_S}(\lambda)/\%$	0,516	0,584	0,602	0,357	0,356	0,358	0,359	0,352	0,569	0,564
RAL 6018 Yellow green	$R_S(\lambda)/\%$	6,407	7,227	8,073	24,670	37,284	16,520	11,661	14,925	16,903	18,969
	$U_{R_S}(\lambda)/\%$	0,099	0,111	0,126	0,234	0,309	0,165	0,123	0,148	0,238	0,263
GL 9010 Pure White	$R_S(\lambda)/\%$	12,319	41,144	80,687	83,683	87,706	87,748	87,060	86,788	85,822	85,575
	$U_{R_S}(\lambda)/\%$	0,202	0,575	1,051	0,604	0,635	0,653	0,649	0,624	1,078	1,073
GL 8015 Chestnut Brown	$R_S(\lambda)/\%$	5,466	6,065	5,888	5,806	6,179	11,750	13,408	14,018	14,561	14,427
	$U_{R_S}(\lambda)/\%$	0,089	0,093	0,091	0,066	0,070	0,129	0,141	0,149	0,212	0,210
GL 8001 Ochre Brown	$R_S(\lambda)/\%$	5,740	6,258	7,690	8,760	18,827	30,405	29,530	29,446	29,744	29,419
	$U_{R_S}(\lambda)/\%$	0,088	0,096	0,121	0,099	0,184	0,295	0,292	0,433	0,419	0,411
RAL 7001-GL Silbergrau	$R_S(\lambda)/\%$	11,390	29,304	35,552	34,722	32,957	30,912	30,112	28,975	28,546	28,350
	$U_{R_S}(\lambda)/\%$	0,184	0,412	0,503	0,306	0,295	0,295	0,290	0,267	0,399	0,394
RAL 4001-GL Rotlila	$R_S(\lambda)/\%$	10,802	24,065	24,176	18,844	14,975	16,992	37,257	37,903	37,879	37,613
	$U_{R_S}(\lambda)/\%$	0,178	0,354	0,335	0,187	0,157	0,180	0,347	0,357	0,519	0,520
RAL 3000-GL Feuerrot	$R_S(\lambda)/\%$	5,889	6,334	5,862	5,827	6,419	27,120	51,006	57,810	61,598	60,898
	$U_{R_S}(\lambda)/\%$	0,091	0,097	0,093	0,066	0,072	0,299	0,404	0,461	0,797	0,780
RAL 2003-GL Pastellorange	$R_S(\lambda)/\%$	7,448	9,154	8,961	11,015	21,822	67,988	85,259	87,091	88,249	88,519
	$U_{R_S}(\lambda)/\%$	0,115	0,141	0,143	0,121	0,212	0,585	0,729	0,710	1,167	1,152
RAL 1021-GL Colza Yellow	$R_S(\lambda)/\%$	5,240	5,250	5,654	16,808	67,119	73,699	73,446	74,114	74,674	74,651
	$U_{R_S}(\lambda)/\%$	0,082	0,083	0,091	0,171	0,496	0,548	0,554	0,546	0,953	0,945

It is now applied the calibration line calculated in section 3.4.2. to the results of the reflectance obtained by measuring the samples from RAL Colours so that the values measured can be corrected.

According to ISO/TS 28037:2010, the uncertainty by applying the calibration model is given by equation 3.21.

$$u_{R_c}^2 = u_a^2 + R_s^2\, u_b^2 + 2\, R_s\, cov_{a,b} + b^2\, u_{R_s}^2 \tag{3.21}$$

Where:

u_{R_c} – Uncertainty associated to the corrected reflectance after the calibration model is applied

u_a – Uncertainty associated to the ordinate in the origin (*a*) of the calibration line in equation 3.21

u_b – Uncertainty associated to the slope (*b*) of the calibration line in equation 3.21

$cov_{a,b}$ – Covariance associated to the calibration model involving the variables *a* and *b* of equation 3.21

R_s – Sample´s reflectance

In table 3.27, it is possible to see the corrected reflectance and its uncertainty for the samples from RAL Colours displayed in figure 3.7.

Table 3.27 – Corrected reflectance and its uncertainty of the samples from RAL Colours

Wavelength λ / nm		380	400	450	500	550	600	650	700	750	770
HR 9006 White Aluminum	$R_c(\lambda)/\%$	39,9515	46,0065	46,3122	46,6479	46,3552	46,1392	45,8947	45,4866	44,8354	44,5370
	$u_{R_c}(\lambda)/\%$	0,7646	0,8735	0,8427	0,5066	0,4810	0,4471	0,4328	0,4177	44,8354	0,6171
RAL 6018 Yellow green	$R_c(\lambda)/\%$	7,1398	7,8354	8,5695	25,1084	37,8480	17,0565	12,0628	15,3287	17,5321	19,8995
	$u_{R_c}(\lambda)/\%$	0,1223	0,1419	0,1581	0,2901	0,3958	0,2349	0,2437	0,2201	17,5321	0,3610
GL 9010 Pure White	$R_c(\lambda)/\%$	0,2022	0,5745	1,0508	0,6036	0,6348	0,6530	0,6487	0,6239	1,0784	1,0727
	$u_{R_c}(\lambda)/\%$	12,9986	41,8174	81,8171	84,6403	88,4647	88,3505	87,7677	87,3340	1,0784	86,1717
GL 8015 Chestnut Brown	$R_c(\lambda)/\%$	6,2218	6,7061	6,3807	6,1359	6,5050	12,2818	13,8171	14,4199	15,1873	15,3803
	$u_{R_c}(\lambda)/\%$	0,1139	0,1151	0,1161	0,0928	0,0983	0,2256	0,2481	0,2220	0,3364	0,3439
GL 8001 Ochre Brown	$R_c(\lambda)/\%$	6,4891	6,8941	8,1860	9,1972	19,3201	30,9543	30,0045	29,8783	30,3929	30,2973
	$u_{R_c}(\lambda)/\%$	0,1120	0,1181	0,1486	0,1936	0,2464	0,3438	0,3469	0,4635	0,4704	0,4640
RAL 7001-GL Silbergrau	$R_c(\lambda)/\%$	12,0652	29,9319	36,2400	35,2493	33,5046	31,4613	30,5888	29,4058	29,1929	29,2331
	$u_{R_c}(\lambda)/\%$	0,3352	0,5193	0,6624	0,3959	0,3644	0,3448	0,3455	0,3127	0,4532	0,4497
RAL 4001-GL Rotlila	$R_c(\lambda)/\%$	11,4740	24,6732	24,7517	19,2312	15,4533	17,5290	37,7623	38,3516	38,5407	38,4503
	$u_{R_c}(\lambda)/\%$	0,3417	0,4402	0,4577	0,2367	0,2337	0,2447	0,4043	0,4057	0,5677	0,5670
RAL 3000-GL Feuerrot	$R_c(\lambda)/\%$	6,6340	6,9682	6,3540	6,1577	6,7543	27,6658	51,5675	58,2985	62,2965	61,6182
	$u_{R_c}(\lambda)/\%$	0,1136	0,1197	0,1175	0,0928	0,1031	0,3420	0,4870	0,5493	0,8861	0,8641
RAL 2003-GL Pastellorange	$R_c(\lambda)/\%$	8,1566	9,7069	9,4590	11,3334	22,3263	68,5723	85,9587	87,6372	88,9876	89,1010
	$u_{R_c}(\lambda)/\%$	0,1510	0,2109	0,1859	0,1929	0,2679	0,7380	0,8845	0,8622	1,3259	1,3081
RAL 1021-GL Colza Yellow	$R_c(\lambda)/\%$	6,0007	5,9146	6,1457	17,1776	67,7988	74,2877	74,0980	74,6340	75,3921	75,3024
	$u_{R_c}(\lambda)/\%$	0,1108	0,1113	0,1178	0,2214	0,7325	0,7412	0,6935	0,6781	1,0773	1,0647

3.5.1. Tristimulus Values

The following procedure is to calculate the tristimulus values according to equations 2.22, 2.23, and 2.24 where:

$$K = \frac{1}{\sum_{390}^{770} s(\lambda)\, \bar{y}(\lambda)\, \Delta\lambda} \tag{3.22}$$

And its uncertainties using the combined standard uncertainty, equations 3.23, 3.24, and 3.25:

$$u_X = \sqrt{u_{R_c}(\lambda)^2 \big(S(\lambda)\, \bar{x}(\lambda)\big)^2} = u_{R_c}(\lambda)\, S(\lambda)\, \bar{x}(\lambda) \tag{3.23}$$

$$u_Y = \sqrt{u_{R_c}(\lambda)^2\left(S(\lambda)\ \bar{y}(\lambda)\right)^2} = u_{R_c}(\lambda)\ S(\lambda)\ \bar{y}(\lambda) \tag{3.24}$$

$$u_Z = \sqrt{u_{R_c}(\lambda)^2\left(S(\lambda)\ \bar{z}(\lambda)\right)^2} = u_{R_c}(\lambda)\ S(\lambda)\ \bar{z}(\lambda) \tag{3.25}$$

Where:

u_X – Uncertainty associated to the tristimulus value X

u_Y – Uncertainty associated to the tristimulus value Y

u_Z – Uncertainty associated to the tristimulus value Z

The results for each illuminant and colorimetric system are presented in tables 3.28 to 3.31 below, for the samples RAL 9006-HR White Aluminum, RAL 8001-GL Ochre Brown, RAL 4001-GL Rotlila, RAL 1021-GL Colza Yellow. the other samples results are presented in Annex D.

Table 3.28 – Tristimulus values and uncertainties for Illuminants A, D 65, and C in the colorimetric systems 1931 and 1964 for RAL 9006-HR White Aluminum

RAL 9006-HR White Aluminum									
Illuminant	Illuminant A			Illuminant D65			Illuminant C		
1931	CIE tristimulus		*U i*	CIE tristimulus		*U i*	CIE tristimulus		*U i*
	X	50,69	0,14	*X*	43,91	0,12	*X*	45,31	0,13
	Y	46,27	0,13	*Y*	46,32	0,13	*Y*	46,32	0,13
	Z	16,49	0,10	*Z*	50,47	0,32	*Z*	54,78	0,36
1964	CIE tristimulus		*U i*	CIE tristimulus		*U i*	CIE tristimulus		*U i*
	X	51,31	0,14	*X*	43,84	0,12	*X*	44,98	0,12
	Y	46,28	0,12	*Y*	46,34	0,12	*Y*	46,34	0,12
	Z	16,33	0,10	*Z*	49,81	0,32	*Z*	53,87	0,35

Table 3.29 – Tristimulus values and uncertainties for Illuminants A, D 65, and C in the colorimetric systems 1931 and 1964 for RAL 8001-GL Ochre Brown

RAL 8001-GL Ochre Brown									
Illuminant	Illuminant A			Illuminant D65			Illuminant C		
1931	CIE tristimulus		*U i*	CIE tristimulus		*U i*	CIE tristimulus		*U i*
	X	30,22	0,11	*X*	22,63	0,08	*X*	23,17	0,08
	Y	23,46	0,08	*Y*	20,69	0,07	*Y*	20,86	0,07
	Z	2,97	0,03	*Z*	8,86	0,07	*Z*	9,59	0,09
1964	*CIE tristimulus*		*U i*	CIE tristimulus		*U i*	CIE tristimulus		*U i*
	X	30,19	0,11	*X*	22,16	0,07	*X*	22,58	0,07
	Y	23,01	0,08	*Y*	19,81	0,07	*Y*	19,92	0,07
	Z	2,89	0,04	*Z*	8,63	0,07	*Z*	9,32	0,06

Table 3.30 – Tristimulus values and uncertainties for Illuminants A, D 65, and C in the colorimetric systems 1931 and 1964 for RAL 4001-GL Rotlila

RAL 4001-GL Rotlila									
Illuminant	Illuminant A			Illuminant D65			Illuminant C		
1931	CIE tristimulus		*U i*	CIE tristimulus		*U i*	CIE tristimulus		*U i*
	X	25,51	0,09	*X*	20,75	0,07	*X*	21,52	0,07
	Y	18,85	0,07	*Y*	17,76	0,06	*Y*	17,81	0,06
	Z	8,30	0,05	*Z*	26,15	0,17	*Z*	28,49	0,20
1964	*CIE tristimulus*		*U i*	CIE tristimulus		*U i*	CIE tristimulus		*U i*
	X	25,11	0,09	*X*	20,28	0,07	*X*	20,91	0,07
	Y	18,97	0,06	*Y*	18,08	0,06	*Y*	18,14	0,06
	Z	8,36	0,06	*Z*	26,17	0,17	*Z*	28,39	0,18

Table 3.31 – Tristimulus values and uncertainties for Illuminants A, D 65, and C in the colorimetric systems 1931 and 1964 for RAL 1021-GL Colza Yellow

RAL 1021-GL Colza Yellow									
Illuminant	Illuminant A			Illuminant D65			Illuminant C		
1931	CIE tristimulus		*U i*	CIE tristimulus		*U i*	CIE tristimulus		*U i*
	X	76,54	0,23	*X*	56,63	0,17	*X*	57,78	0,17
	Y	64,36	0,19	*Y*	58,09	0,18	*Y*	58,39	0,18
	Z	3,27	0,02	*Z*	8,52	0,06	*Z*	9,08	0,08
1964	*CIE tristimulus*		*U i*	CIE tristimulus		*U i*	CIE tristimulus		*U i*
	X	76,99	0,23	*X*	55,91	0,17	*X*	56,78	0,17
	Y	62,65	0,18	*Y*	54,62	0,16	*Y*	54,72	0,16
	Z	2,91	0,04	*Z*	7,88	0,06	*Z*	8,41	0,05

3.5.2. Chromaticity Coordinates

With the tristimulus values obtained, it is now possible to calculate the chromaticity coordinates using equations 2.30, 2.31, and 2.32 and its uncertainties following equations 3.26, 3.27, and 3.28 by applying the combined standard uncertainty.

$$u_x = \sqrt{u_X^2.\left(\frac{Y+Z}{(X+Y+Z)^2}\right)^2 + u_Y^2.\left(\frac{-X}{(X+Y+Z)^2}\right)^2 + u_Z^2.\left(\frac{Y+Z}{(X+Y+Z)^2}\right)^2} \tag{3.26}$$

$$u_y = \sqrt{u_X^2.\left(\frac{-Y}{(X+Y+Z)^2}\right)^2 + u_Y^2.\left(\frac{X+Z}{(X+Y+Z)^2}\right)^2 + u_Z^2.\left(\frac{-Y}{(X+Y+Z)^2}\right)^2} \tag{3.27}$$

$$u_z = \sqrt{u_X^2.\left(\frac{-Z}{(X+Y+Z)^2}\right)^2 + u_Y^2.\left(\frac{-Z}{(X+Y+Z)^2}\right)^2 + u_Z^2.\left(\frac{Y+Z}{(X+Y+Z)^2}\right)^2} \tag{3.28}$$

Where:

X, Y, Z – Tristimulus values

u_x, u_y, u_z – Uncertainties associated to the chromaticity coordinates

u_X, u_Y, u_Z – Uncertainties associated to the tristimulus values

In tables 3.32 to 3.35, it is shown the results of the calculation of the chromaticity coordinates and its uncertainties using the expanded uncertainty with a $K = 2$ for the samples RAL 9006-HR White Aluminum, RAL 8001-GL Ochre Brown, RAL 4001-GL Rotlila, RAL 1021-GL Colza Yellow the other samples results are presented in Annex E.

Table 3.32 – Chromaticity coordinates and uncertainties for Illuminants A, D 65, and C in the colorimetric systems 1931 and 1964 for RAL 9006-HR White Aluminum

RAL 9006-HR White Aluminum									
Illuminant	Illuminant A			Illuminant D65			Illuminant C		
1931	Chromaticity Coord.		*U i*	Chromaticity Coord.		*U i*	Chromaticity Coord.		*U i*
	x	0,45	0,00	*x*	0,31	0,00	*x*	0,31	0,00
	y	0,41	0,00	*y*	0,33	0,00	*y*	0,32	0,00
	z	0,15	0,00	*z*	0,36	0,00	*z*	0,37	0,00
1964	Chromaticity Coord.		*U i*	Chromaticity Coord.		*U i*	Chromaticity Coord.		*U i*
	x	0,45	0,00	*x*	0,31	0,00	*x*	0,31	0,00
	y	0,41	0,00	*y*	0,33	0,00	*y*	0,32	0,00
	z	0,14	0,00	*z*	0,36	0,00	*z*	0,37	0,00

Table 3.33 – Chromaticity coordinates and uncertainties for Illuminants A, D 65, and C in the colorimetric systems 1931 and 1964 for RAL 4001-GL Ochre Brown

RAL 8001-GL Ochre Brown									
Illuminant	Illuminant A			Illuminant D65			Illuminant C		
1931	Chromaticity Coord.		*U i*	Chromaticity Coord.		*U i*	Chromaticity Coord.		*U i*
	x	0,533	0,001	*x*	0,434	0,001	*x*	0,432	0,001
	y	0,414	0,001	*y*	0,396	0,001	*y*	0,389	0,001
	z	0,053	0,001	*z*	0,170	0,001	*z*	0,179	0,001
1964	Chromaticity Coord.		*U i*	Chromaticity Coord.		*U i*	Chromaticity Coord.		*U i*
	x	0,538	0,001	*x*	0,438	0,001	*x*	0,436	0,001
	y	0,410	0,001	*y*	0,391	0,001	*y*	0,384	0,001
	z	0,051	0,001	*z*	0,171	0,001	*z*	0,180	0,001

Table 3.34 – Chromaticity coordinates and uncertainties for Illuminants A, D 65, and C in the colorimetric systems 1931 and 1964 for RAL 4001-GL Rotlila

RAL 4001-GL Rotlila									
Illuminant	Illuminat A			Illuminat D65			Illuminat C		
1931	Chromaticity Coord.		*U i*	Chromaticity Coord.		*U i*	Chromaticity Coord.		*U i*
	x	0,48	0,00	*x*	0,32	0,00	*x*	0,32	0,00
	y	0,36	0,00	*y*	0,27	0,00	*y*	0,26	0,00
	z	0,16	0,00	*z*	0,40	0,00	*z*	0,42	0,00
1964	Chromaticity Coord.		*U i*	Chromaticity Coord.		*U i*	Chromaticity Coord.		*U i*
	x	0,48	0,00	x	0,31	0,00	x	0,31	0,00
	y	0,36	0,00	y	0,28	0,00	y	0,27	0,00
	z	0,16	0,00	z	0,41	0,00	z	0,42	0,00

Table 3.35 – Chromaticity coordinates and uncertainties for Illuminants A, D 65, and C in the colorimetric systems 1931 and 1964 for RAL 1021-GL Colza Yellow

RAL 1021-GL Colza Yellow									
Illuminant	Illuminant A			Illuminant D65			Illuminant C		
1931	Chromaticity Coord.		*U i*	Chromaticity Coord.		*U i*	Chromaticity Coord.		*U i*
	x	0,531	0,001	*x*	0,460	0,001	*x*	0,461	0,001
	y	0,446	0,001	*y*	0,471	0,001	*y*	0,466	0,001
	z	0,023	0,001	*z*	0,069	0,001	*z*	0,072	0,001
1964	Chromaticity Coord.		*U i*	Chromaticity Coord.		*U i*	Chromaticity Coord.		*U i*
	x	0,540	0,001	*x*	0,472	0,001	*x*	0,474	0,001
	y	0,439	0,001	*y*	0,461	0,001	*y*	0,456	0,001
	z	0,020	0,001	*z*	0,067	0,001	*z*	0,070	0,001

3.5.3. CIELAB Coordinates

Equations from 2.33 to 2.41 should be used to calculate the CIELAB color space coordinates. For the uncertainties of the values L*, a* and b* the following equations from 3.29 to 3.31 are used [25], [40]:

$$u_{L^*} = \sqrt{\left(V_{(L*,a*,b*)}\right)_{11}} \tag{3.29}$$

$$u_{a^*} = \sqrt{\left(V_{(L*,a*,b*)}\right)_{22}} \tag{3.30}$$

$$u_{b^*} = \sqrt{\left(V_{(L*,a*,b*)}\right)_{33}} \tag{3.31}$$

Where:

$u_{L^*}, u_{a^*}, u_{b^*}$ – Uncertainties associated to L*, a* and b* values of the CIELAB color space

$V_{(L*,a*,b*)}$ – Variance and covariance matrix of CIELAB color space

The covariance matrix $V_{(L*,a*,b*)}$ is calculated following equations 3.32 to 3.40:

$$V_{(L*,a*,b*)} = J V_{(X,Y,Z)} J^T \tag{3.32}$$

Where:

$$J = \begin{pmatrix} \frac{\partial L^*}{\partial X} & \frac{\partial L^*}{\partial Y} & \frac{\partial L^*}{\partial Z} \\ \frac{\partial a^*}{\partial X} & \frac{\partial a^*}{\partial Y} & \frac{\partial a^*}{\partial Z} \\ \frac{\partial b^*}{\partial X} & \frac{\partial b^*}{\partial Y} & \frac{\partial b^*}{\partial Z} \end{pmatrix} = \begin{pmatrix} 0 & \frac{116}{Y_n} f'\left(\frac{Y}{Y_n}\right) & 0 \\ \frac{500}{X_n} f'\left(\frac{X}{X_n}\right) & -\frac{500}{Y_n} f'\left(\frac{Y}{Y_n}\right) & 0 \\ 0 & \frac{200}{Y_n} f'\left(\frac{Y}{Y_n}\right) & -\frac{200}{Z_n} f'\left(\frac{Z}{Z_n}\right) \end{pmatrix} = \tag{3.33}$$

$$= \begin{pmatrix} 0 & \frac{116}{3} Y_n^{-\frac{1}{3}} Y^{-\frac{2}{3}} & 0 \\ \frac{500}{3} X_n^{-\frac{1}{3}} X^{-\frac{2}{3}} & -\frac{500}{3} Y_n^{-\frac{1}{3}} Y^{-\frac{2}{3}} & 0 \\ 0 & \frac{200}{3} Y_n^{-\frac{1}{3}} Y^{-\frac{2}{3}} & -\frac{200}{3} Z_n^{-\frac{1}{3}} Z^{-\frac{2}{3}} \end{pmatrix}$$

And:

$$V_{(X,Y,Z)} = \begin{pmatrix} u^2(X) & u(X,Y) & u(X,Z) \\ u(X,Y) & u^2(Y) & u(Y,Z) \\ u(X,Z) & u(Y,Z) & u^2(Z) \end{pmatrix} \tag{3.34}$$

Where:

$$u(X,Y) = u_X\, u_Y \quad (3.35)$$

$$u(X,Z) = u_X\, u_Z \quad (3.36$$

$$u(Y,Z) = u_Y\, u_Z \quad (3.37)$$

$$u^2(X) = u_X\, u_X \quad (3.38)$$

$$u^2(Y) = u_Y\, u_Y \quad (3.39)$$

$$u^2(Z) = u_Z\, u_Z \quad (3.40)$$

Where:

$V_{(X,Y,Z)}$ – Variance and covariance matrix of the tristimulus values

J – Jacobian matrix associated to the CIELAB color space

u_X, u_Y, u_Z – Uncertainties associated to the tristimulus values

The following tables 3.36 to 3.39 show the results and the uncertainties as expanded uncertainty with $k = 2$ obtained for the L*, a*, and b* coordinates of the CIELAB color space for the samples RAL 9006-HR White Aluminum, RAL 8001-GL Ochre Brown, RAL 4001-GL Rotlila, RAL 1021-GL Colza Yellow, the other samples results are presented in Annex F.

Table 3.36 – CIELAB values *L**, *a** and *b** and uncertainties for Illuminants A, D 65, and C in the colorimetric systems 1931 and 1964 for RAL 9006-HR White Aluminum

RAL 9006-HR White Aluminum									
Illuminant	Illuminant A			Illuminant D65			Illuminant C		
1931	CIELAB Coordinates		U i	CIELAB Coordinates		U i	CIELAB Coordinates		U i
	L*	73,70	0,23	L*	73,74	0,16	L*	73,73	0,20
	a*	-0,32	0,78	a*	-0,30	0,67	a*	-0,29	0,59
	b*	-0,15	0,57	b*	-0,07	0,74	b*	-0,07	0,80
1964	CIELAB Coordinates		U i	CIELAB Coordinates		U i	CIELAB Coordinates		U i
	L*	73,70	0,22	L*	73,74	0,17	L*	73,76	0,20
	a*	-0,31	0,74	a*	-0,30	0,64	a*	2,73	0,57
	b*	-0,14	0,62	b*	-0,06	0,75	b*	-3,42	0,80

Table 3.37 – CIELAB values *L**, *a** and *b** and uncertainties for Illuminants A, D 65, and C in the colorimetric systems 1931 and 1964 for RAL 8001-GL Ochre Brown

RAL 8001-GL Ochre Brown									
Illuminant	Illuminant A			Illuminant D65			Illuminant C		
1931	CIELAB Coordinates		U i	CIELAB Coordinates		U i	CIELAB Coordinates		U i
	L*	55,53	0,29	L*	52,59	0,20	L*	52,78	0,17
	a*	16,83	0,76	a*	14,23	0,76	a*	12,59	0,72
	b*	35,86	0,47	b*	31,59	0,39	b*	32,00	0,49
1964	CIELAB Coordinates		U i	CIELAB Coordinates		U i	CIELAB Coordinates		U i
	L*	55,07	0,26	L*	51,60	0,19	L*	51,75	0,20
	a*	17,42	0,72	a*	16,52	0,73	a*	17,66	0,73
	b*	35,66	0,75	b*	30,25	0,37	b*	28,67	0,30

Table 3.38 – CIELAB values *L**, *a** and *b** and uncertainties for Illuminants A, D 65, and C in the colorimetric systems 1931 and 1964 for RAL 4001-GL Rotlila

RAL 4001-GL Rotlila									
Illuminant	Illuminant A			Illuminant D65			Illuminant C		
1931	CIELAB Coordinates		U i	CIELAB Coordinates		U i	CIELAB Coordinates		U i
	L*	50,50	0,23	L*	49,19	0,20	L*	49,25	0,25
	a*	20,64	0,67	a*	20,07	0,47	a*	20,30	0,35
	b*	-8,48	0,48	b*	-11,92	0,69	b*	-11,98	0,78
1964	CIELAB Coordinates		U i	CIELAB Coordinates		U i	CIELAB Coordinates		U i
	L*	50,64	0,20	L*	49,57	0,20	L*	49,67	0,23
	a*	17,19	0,63	a*	16,28	0,45	a*	18,78	0,38
	b*	-8,95	0,57	b*	-11,85	0,69	b*	-14,55	0,73

Table 3.39 – CIELAB values *L**, *a** and *b** and uncertainties for Illuminants A, D 65, and C in the colorimetric systems 1931 and 1964 for RAL 1021-GL Colza Yellow

RAL 1021-GL Colza Yellow									
Illuminant	Illuminant A			Illuminant D65			Illuminant C		
1931	CIELAB Coordinates		U i	CIELAB Coordinates		U i	CIELAB Coordinates		U i
	L*	84,13	0,37	L*	80,77	0,32	L*	80,93	0,31
	a*	11,61	1,01	a*	3,59	1,10	a*	1,31	1,08
	b*	82,32	0,43	b*	81,31	0,34	b*	82,10	0,44
1964	CIELAB Coordinates		U i	CIELAB Coordinates		U i	CIELAB Coordinates		U i
	L*	83,24	0,36	L*	78,80	0,31	L*	78,88	0,32
	a*	14,56	0,96	a*	10,55	1,04	a*	12,16	1,04
	b*	83,94	0,73	b*	79,75	0,34	b*	78,42	0,25

3.5.4. Color Difference Magnitude

As the CIELAB color space is a colorimetric system that facilitates the process of the colors´ visualization and thus its differences, it was done a practical example between the samples RAL 8001-GL Ochre Brown and RAL 4001-GL Rotlila following equations 2.42 to 2.51. Table 3.40 shows the values of each of these samples for the variables *L**, *a**, *b**, *h* (º), and *C*.

Table 3.40 – *L**, *a**, *b**, *h* (º), and *C* values of Ochre Brown and Rotlila

RAL 8001-GL Ochre Brown		RAL 4001-GL Rotlila	
L^*_1	55,528	L^*_0	50,641
a^*_1	16,827	a^*_0	17,189
b^*_1	35,860	b^*_0	-8,955
h_1	63,960	h_0	-27,518
C_1	39,691	C_0	19,382

Table 3.41 illustrates the color difference magnitudes between these 2 samples.

Table 3.41 – Color's difference magnitude of the samples RAL 8001-GL Ochre Brown and RAL 4001-GL Rotlila

Δ RAL 8001-GL Ochre Brown, RAL 4001-GL Rotlila	$\Delta L_{1,0}$	$\Delta a_{1,0}$	$\Delta b_{1,0}$	$\Delta h_{1,0}$	$\Delta C_{1,0}$	$\Delta H_{1,0}$	$\Delta E_{1,0}$
	4,425	0,236	44,141	91,477	20,310	39,828	44,926

3.6. Results Discussion

In the first stage of the experience, the calibration model ISO/TS 28037:2010 was tested on the samples HY93, HZ93, JA93, JB93, JC93, JD93, JE93, JF93, and JG93 certified by the NPL, for spectrophotometry in transmission configuration. The transmittance on the wavelengths 380 nm, 400 nm, 500 nm, 600 nm, 700 nm, 800 nm, 900 nm, and 1000 nm was measured, and its uncertainty was calculated. With the help of a function developed in Microsoft Excel, following the indications of the standard ISO/TS 28037:2010, the calibration function was calculated, and the obtained results were compared with the certified values of the samples.

The obtained values were according to what was predicted, and the maximum relative error was 1,34 %, which was found to be satisfying and allowed us to validate the procedure for spectrophotometric measurements.

The second stage consisted of calculating a calibration function of a spectrophotometer for the samples measured in reflection configuration . It was utilized the same validated procedure. The reflectance of the samples HV93, HT93 Pale Grey, HT93 Deep Grey, HT93 Deep Pink, HT93 Red, HT93 Orange, HT93 Bright Yellow, HT93 Cyan, HT93 Deep Blue certified by the NPL were measured on the wavelengths from 380 nm to 770 nm with a 10 nm interval and its uncertainties calculated. The calibration function was deduced from the data collected.

The third stage was applying the calibration function calculated in the second stage to the reflectance along the wavelengths 380 nm to 770 nm in a 10 nm interval of the samples RAL 9006-HR White Aluminum, RAL 6018-GL Yellow green, RAL 9010-GL Pure White, RAL 9005-GL Jet Black, RAL 8015 -GL Chestnut Brown, RAL 8001-GL Ochre Brown, RAL 7001-GL Silbergrau, RAL 5013-GL Kobaltblau, RAL 4001-GL Rotlila, RAL 3000-GL Feuerrot, RAL 2003-GL Pastellorange, and RAL 1021-GL Colza Yellow so that the values could be corrected and more accurate.

The fourth stage consisted on performing a colorimetric analysis and certification of the samples from RAL Colours, according to CIE standards. After obtaining the corrected reflectance values, the tristimulus values were calculated to three different Illuminants: A, D65, and C, and to 1931 and 1964 colorimetric systems. The next step was to calculate the chromaticity coordinates and the CIELAB values for each illuminant and colorimetric system.

4. Conclusions

Along this work, spectrophotometric measurements and calibrations in reflectance configuration were performed to certify color illustrations A6-sized samples from RAL Colours. A double monochromater, double beam spectrophotometer Lambda 950 by Perkin Elmer in the spectrophotometry laboratory of IPQ was the measuring instrument.

Uncertainties were calculated following *Evaluation of measurement data — Guide to the expression of uncertainty in measurement*, using type A uncertainties for data obtained experimentally and type B uncertainties for data obtained by certificates and manufacturer´s specifications. Then the combined uncertainty was calculated, followed by the expanded uncertainty with a coverage factor k=2.

The ISO/TS 28037:2010 standard was used to calculate the calibration function of spectrophotometric measurement. In a first stage, the procedure was tested and validated for regular transmittance measurement. Then, regular reflectance measurements were performed. For the first time, a correspondence between RAL classification and CIE colorimetric coordinates was obtained. A straightforward application of this work is the publication in standards with only RAL system classification, the corresponding CIE colorimetric references.

Albeit the demonstrated validation of the method, other intervals for the determination of the linear calibration function (used in the ISO/TS 28037:2010) or different calibration functions may be studied to improve the performance of the method.

Using CIE recommendations, the samples' tristimulus values and chromaticity coordinates were calculated for both 1931 and 1964 colorimetric systems and for the illuminants A, D65, and C.

The CIELAB color space was explored, the RAL Colors´ samples were analyzed and certified in this color measuring system, its coordinates and respective uncertainties were calculated for each sample. As it is a color space that privileges color comparison, it was done a practical comparison between two samples.

The calculations along all this work were done in Microsoft Office Excel. A document that pre-existed which automatically generates the results and uncertainties for each system was improved and used.

The model can be used in industries that require high accuracy color control for quality control purposes, as the tools used can guarantee high-quality measurement results.

It might be interesting in future works to compare certification models in colorimetry that use a different color measuring system and evaluate which can be more accurate.

Bibliography

[1] "INSTITUTO PORTUGUÊS DA QUALIDADE." http://www1.ipq.pt/PT/IPQ/Pages/IPQ.aspx.

[2] Joint Committee for Guides in Metrology (JCGM), *International vocabulary of metrology – Basic and general concepts and associated terms (VIM)*. 2012.

[3] F. Redgrave and P. Howarth, *Metrology – In Short 3rd Edition*. 2008.

[4] "Sistema Português da Qualidade." http://www1.ipq.pt/PT/SPQ/Pages/SPQ.aspx.

[5] Joint Committee for Guides in Metrology (JCGM), *Evaluation of measurement data — Guide to the expression of uncertainty in measurement*, no. September. 2008.

[6] N. I. of S. and Technology, "Spectrophotometry," 2009. https://www.nist.gov/programs-projects/spectrophotometry (accessed Jun. 16, 2021).

[7] P. Bouguer, *Essai D'Optique, Sur La Gradation De La Lumière*. 1729.

[8] R. Di Capua, F. Offi, and F. Fontana, "Check the Lambert-Beer-Bouguer law: A simple trick to boost the confidence of students toward both exponential laws and the discrete approach to experimental physics," *Eur. J. Phys.*, vol. 35, no. 4, 2014, doi: 10.1088/0143-0807/35/4/045025.

[9] A. Santos and C. Alves, "Calibração de Filtros de Fator de Transmissão Regular em Espectrofotometria," 2015.

[10] "Continuum, Absorption & Emission Spectra," *Astronomy Department of the New Mexico State Univeristy*. http://astronomy.nmsu.edu/geas/lectures/lecture19/slide02.html (accessed Jun. 16, 2021).

[11] A. Mehta, "Introduction to the Electromagnetic Spectrum and Spectroscopy," *pharmaxchange.info*, 2011. .

[12] T. E. of E. Britannica, "Electromagnetic spectrum," *Encyclopedia Britannica*. 2019, [Online]. Available: https://www.britannica.com/science/electromagnetic-spectrum.

[13] G. Butcher, *Tour Of The Electromagnetic Spectrum*, 3rd ed. National Aeronautics and Space Administration, 2016.

[14] "Electromagnetic spectrum," *Wikipedia*. https://en.wikipedia.org/wiki/Electromagnetic_spectrum (accessed Jun. 16, 2021).

[15] Explicatorium, "Propagação da luz." http://explicatorium.com/cfq-8/propagacao-da-luz.html (accessed Jun. 16, 2021).

[16] A. Ryer, *Light Measurement Handbock*. 1998.

[17] A. Höpe, "Chapter 6 - Diffuse Reflectance and Transmittance," in *Experimental Methods in the Physical Sciences*, Volume 46., T. A. Germer, J. C. Zwinkels, and B. K. Tsai, Eds. 2014, pp. 179–219.

[18] Sheffield Hallam University, "Beer´s Law." https://teaching.shu.ac.uk/hwb/chemistry/tutorials/molspec/beers1.htm (accessed Jun. 16, 2021).

[19] Biochemistry Den, “Spectrophotometer Instrumentation: Principle and Applications,” 2021. https://biochemden.com/spectrophotometer-instrumentation-principle/ (accessed Jun. 16, 2021).

[20] HITACHI, “UV-Vis/NIR Spectrophotometer Basic Course.” https://www.hitachi-hightech.com/global/products/science/tech/ana/uv/basic/course7.html (accessed Jun. 16, 2021).

[21] L. Eusébio, *Procedimento Técnico de Calibração de Filtros com Espectrofotómetro Padrão*. Faculdade de Ciências da Universidade de Lisboa, 2007.

[22] Shimadzu, “Fundamentals of UV-Vis-NIR Spectroscopy.” https://www.ssi.shimadzu.com/products/uv-vis-spectrophotometers/faqs/instrument-design.html (accessed Jun. 16, 2021).

[23] Berthold, “GLOSSARY BIOANALYTIC.” https://www.berthold.com/en/bioanalytic/knowledge/glossary/monochromator/ (accessed Jul. 09, 2021).

[24] M. L.C. Passos and M. L. M.F.S. Saraiva, “Detection in UV-visible spectrophotometry: Detectors, detection systems, and detection strategies,” *Meas. J. Int. Meas. Confed.*, vol. 135, pp. 896–904, 2019, doi: 10.1016/j.measurement.2018.12.045.

[25] https://electropedia.org/ (accessed Jul. 09, 2021)

[26] J. Schanda, *Colorimetry : Understanding the CIE System*. 2007.

[27] Y. Ohno, “CIE Fundamentals for Color Measurements,” *Int. Conf. Digit. Print. Technol.*, vol. 2000, pp. 540–545, 2000.

[28] R. Mukamal, “How Humans See In Color,” *American Academy of Ophtalmology*, 2017. https://www.aao.org/eye-health/tips-prevention/how-humans-see-in-color (accessed Jun. 11, 2021).

[29] A. Tan, “No How does the human eye work?,” 2013. https://www.quora.com/How-does-the-human-eye-work (accessed Jun. 16, 2021).

[30] ZEISS, “O olho humano,” 2017. https://www.zeiss.pt/vision-care/melhor-visao/compreender-a-visao/o-olho-humano.html.

[31] R. Nave, “Additive Color Mixing,” *Hyperphysics*. http://hyperphysics.phy-astr.gsu.edu/hbase/vision/addcol.html (accessed Jun. 14, 2021).

[32] R. Nave, “Subtractive Color Mixing,” *Hyperphysics*. http://hyperphysics.phy-astr.gsu.edu/hbase/vision/subcol.html#c1 (accessed Jun. 14, 2021).

[33] Hubblesite, “The Eletromagnetic Spectrum,” 2019. https://hubblesite.org/contents/articles/the-electromagnetic-spectrum (accessed Jun. 16, 2021).

[34] C. L. Chakrabarti, “Atomic spectroscopy, historical perspective,” *Encycl. Spectrosc. Spectrom.*, vol. 1, pp. 105–106, 2016, doi: 10.1016/B978-0-12-803224-4.00103-5.

[35] “Chromaticity,” *Wikipedia*. https://en.wikipedia.org/wiki/Chromaticity (accessed Jun. 16, 2021).

[36] C. Andersen, “Daytime Color Appearance of Retroreflective Traffic Control Sign Materials,” *U.S Dep. Transp.*, no. April 2013, pp. 1–65, 2013.

[37] “ISO 11664-4:2011 Colorimetry - Part 4: CIE 1976 L*a*b* Colour space,” 2011.

[38] R. Institute, “RAL COLOURS.” https://www.ral.de/en/ (accessed Aug. 03, 2021).

[39] “ISO/TS 28037:2010 Determination and use of straight-line calibration functions.” 2010.

[40] G. Wübbeler, J. Campos Acosta, and C. Elster, “Evaluation of uncertainties for CIELAB color coordinates,” *Color Res. Appl.*, vol. 42, no. 5, pp. 564–570, 2017, doi: 10.1002/col.22109.

Annexes

Annex A – $\bar{x}(\lambda)$, $\bar{y}(\lambda)$, $\bar{z}(\lambda)$ values with a 5 nm interval, for the two colorimetric systems, CIE 1931 and CIE 1964.

λ/nm	$\bar{x}_{1931}(\lambda)$	$\bar{y}_{1931}(\lambda)$	$\bar{z}_{1931}(\lambda)$	$\bar{x}_{1964}(\lambda)$	$\bar{y}_{1964}(\lambda)$	$\bar{z}_{1964}(\lambda)$
380	0,001368	0,000039	0,00645	0,00016	0,000017	0,000705
385	0,002236	0,000064	0,01055	0,000662	0,000072	0,002928
390	0,004243	0,00012	0,02005	0,002362	0,000253	0,010482
395	0,00765	0,000217	0,03621	0,007242	0,000769	0,032344
400	0,01431	0,000396	0,06785	0,01911	0,002004	0,086011
405	0,02319	0,00064	0,1102	0,0434	0,004509	0,19712
410	0,04351	0,00121	0,2074	0,084736	0,008756	0,389366
415	0,07763	0,00218	0,3713	0,140638	0,014456	0,65676
420	0,13438	0,004	0,6456	0,204492	0,021391	0,972542
425	0,21477	0,0073	1,03905	0,264737	0,029497	1,2825
430	0,2839	0,0116	1,3856	0,314679	0,038676	1,55348
435	0,3285	0,01684	1,62296	0,357719	0,049602	1,7985
440	0,34828	0,023	1,74706	0,383734	0,062077	1,96728
445	0,34806	0,0298	1,7826	0,386726	0,074704	2,0273
450	0,3362	0,038	1,77211	0,370702	0,089456	1,9948
455	0,3187	0,048	1,7441	0,342957	0,106256	1,9007
460	0,2908	0,06	1,6692	0,302273	0,128201	1,74537
465	0,2511	0,0739	1,5281	0,254085	0,152761	1,5549
470	0,19536	0,09098	1,28764	0,195618	0,18519	1,31756
475	0,1421	0,1126	1,0419	0,132349	0,21994	1,0302
480	0,09564	0,13902	0,81295	0,080507	0,253589	0,772125
485	0,05795	0,1693	0,6162	0,041072	0,297665	0,57006
490	0,03201	0,20802	0,46518	0,016172	0,339133	0,415254
495	0,0147	0,2586	0,3533	0,005132	0,395379	0,302356
500	0,0049	0,323	0,272	0,003816	0,460777	0,218502
505	0,0024	0,4073	0,2123	0,015444	0,53136	0,159249
510	0,0093	0,503	0,1582	0,037465	0,606741	0,112044
515	0,0291	0,6082	0,1117	0,071358	0,68566	0,082248
520	0,06327	0,71	0,07825	0,117749	0,761757	0,060709
525	0,1096	0,7932	0,05725	0,172953	0,82333	0,04305
530	0,1655	0,862	0,04216	0,236491	0,875211	0,030451
535	0,22575	0,91485	0,02984	0,304213	0,92381	0,020584
540	0,2904	0,954	0,0203	0,376772	0,961988	0,013676

λ/ nm	$\bar{x}_{1931}(\lambda)$	$\bar{y}_{1931}(\lambda)$	$\bar{z}_{1931}(\lambda)$	$\bar{x}_{1964}(\lambda)$	$\bar{y}_{1964}(\lambda)$	$\bar{z}_{1964}(\lambda)$
545	0,3597	0,9803	0,0134	0,451584	0,9822	0,007918
550	0,43345	0,99495	0,00875	0,529826	0,991761	0,003988
555	0,51205	1	0,00575	0,616053	0,99911	0,001091
560	0,5945	0,995	0,0039	0,705224	0,99734	0
565	0,6784	0,9786	0,00275	0,793832	0,98238	0
570	0,7621	0,952	0,0021	0,878655	0,955552	0
575	0,8425	0,9154	0,0018	0,951162	0,915175	0
580	0,9163	0,87	0,00165	1,01416	0,868934	0
585	0,9786	0,8163	0,0014	1,0743	0,825623	0
590	1,0263	0,757	0,0011	1,11852	0,777405	0
595	1,0567	0,6949	0,001	1,1343	0,720353	0
600	1,0622	0,631	0,0008	1,12399	0,658341	0
605	1,0456	0,5668	0,0006	1,0891	0,593878	0
610	1,0026	0,503	0,00034	1,03048	0,527963	0
615	0,9384	0,4412	0,00024	0,95074	0,461834	0
620	0,85445	0,381	0,00019	0,856297	0,398057	0
625	0,7514	0,321	0,0001	0,75493	0,339554	0
630	0,6424	0,265	0,00005	0,647467	0,283493	0
635	0,5419	0,217	0,00003	0,53511	0,228254	0
640	0,4479	0,175	0,00002	0,431567	0,179828	0
645	0,3608	0,1382	0,00001	0,34369	0,140211	0
650	0,2835	0,107	0	0,268329	0,107633	0
655	0,2187	0,0816	0	0,2043	0,081187	0
660	0,1649	0,061	0	0,152568	0,060281	0
665	0,1212	0,04458	0	0,11221	0,044096	0
670	0,0874	0,032	0	0,081261	0,0318	0
675	0,0636	0,0232	0	0,05793	0,022602	0
680	0,04677	0,017	0	0,040851	0,015905	0
685	0,0329	0,01192	0	0,028623	0,01113	0
690	0,0227	0,00821	0	0,019941	0,007749	0
695	0,01584	0,005723	0	0,013842	0,005375	0
700	0,011359	0,004102	0	0,009577	0,003718	0
705	0,008111	0,002929	0	0,006605	0,002565	0
710	0,00579	0,002091	0	0,004553	0,001768	0
715	0,004109	0,001484	0	0,003145	0,001222	0
720	0,002899	0,001047	0	0,002175	0,000846	0
725	0,002049	0,00074	0	0,001506	0,000586	0
730	0,00144	0,00052	0	0,001045	0,000407	0
735	0,001	0,000361	0	0,000727	0,000284	0
740	0,00069	0,000249	0	0,000508	0,000199	0
745	0,000476	0,000172	0	0,000356	0,00014	0
750	0,000332	0,00012	0	0,000251	0,000098	0
755	0,000235	0,000085	0	0,000178	0,00007	0
760	0,000166	0,00006	0	0,000126	0,00005	0
765	0,000117	0,000042	0	0,00009	0,000036	0
770	0,000083	0,00003	0	0,000065	0,000025	0
775	0,000059	0,000021	0	0,000046	0,000018	0
780	0,000042	0,000015	0	0,000033	0,000013	0

Annex B – SPD of the CIE Illuminants

λ/ nm	CIE Illuminant A	CIE Illuminant D65	Illuminant C	Illuminant D50	Illuminant D55	Illuminant D75
380	9,795	49,976	33	24,488	32,584	66,703
385	10,9	52,312	39,92	27,179	35,335	68,333
390	12,085	54,648	47,4	29,871	38,087	69,963
395	13,354	68,702	55,17	39,589	49,518	85,946
400	14,708	82,755	63,3	49,308	60,949	101,929
405	16,148	87,12	71,81	52,91	64,751	106,911
410	17,675	91,486	80,6	56,513	68,554	111,894
415	19,291	92,459	89,53	58,273	70,065	112,346
420	20,995	93,432	98,1	60,034	71,577	112,798
425	22,788	90,057	105,8	58,926	69,746	107,945
430	24,671	86,682	112,4	57,818	67,914	103,092
435	26,643	95,774	117,75	66,321	76,76	112,145
440	28,703	104,865	121,5	74,825	85,605	121,198
445	30,851	110,936	123,45	81,036	91,799	127,104
450	33,086	117,008	124	87,247	97,993	133,01
455	35,407	117,41	123,6	88,93	99,228	132,682
460	37,812	117,812	123,1	90,612	100,463	132,355
465	40,3	116,336	123,3	90,99	100,188	129,838
470	42,869	114,861	123,8	91,368	99,913	127,322
475	45,517	115,392	124,09	93,238	101,326	127,061
480	48,242	115,923	123,9	95,109	102,739	126,8
485	51,042	112,367	122,92	93,536	100,409	122,291
490	53,913	108,811	120,7	91,963	98,078	117,783
495	56,854	109,082	116,9	93,843	99,379	117,186
500	59,861	109,354	112,1	95,724	100,68	116,589
505	62,932	108,578	106,98	96,169	100,688	115,146
510	66,064	107,802	102,3	96,613	100,695	113,702
515	69,253	106,296	98,81	96,871	100,341	111,181
520	72,496	104,79	96,9	97,129	99,987	108,659
525	75,79	106,239	96,78	99,614	102,098	109,552
530	79,133	107,689	98	102,099	104,21	110,445
535	82,519	106,047	99,94	101,427	103,156	108,367
540	85,947	104,405	102,1	100,755	102,102	106,289
545	89,412	104,225	103,95	101,536	102,535	105,596
550	92,912	104,046	105,2	102,317	102,968	104,904
555	96,442	102,023	105,67	101,159	101,484	102,452
560	100	100	105,3	100	100	100
565	103,582	98,167	104,11	98,868	98,608	97,808
570	107,184	96,334	102,3	97,735	97,216	95,616
575	110,803	96,061	100,15	98,327	97,482	94,914
580	114,436	95,788	97,8	98,918	97,749	94,213

λ/ nm	CIE Illuminant A	CIE Illuminant D65	Illuminant C	Illuminant D50	Illuminant D55	Illuminant D75
585	118,08	92,237	95,43	96,208	94,59	90,605
590	121,731	88,686	93,2	93,499	91,432	86,997
595	125,386	89,346	91,22	95,593	92,926	87,112
600	129,043	90,006	89,7	97,688	94,419	87,227
605	132,697	89,803	88,83	98,478	94,78	86,684
610	136,346	89,599	88,4	99,269	95,14	86,14
615	139,988	88,649	88,19	99,155	94,68	84,861
620	143,618	87,699	88,1	99,042	94,22	83,581
625	147,235	85,494	88,06	97,382	92,334	81,164
630	150,836	83,289	88	95,722	90,448	78,747
635	154,418	83,494	87,86	97,29	91,389	78,587
640	157,979	83,699	87,8	98,857	92,33	78,428
645	161,516	81,863	87,99	97,262	90,592	76,614
650	165,028	80,027	88,2	95,667	88,854	74,801
655	168,51	80,121	88,2	96,929	89,586	74,562
660	171,963	80,215	87,9	98,19	90,317	74,324
665	175,383	81,246	87,22	100,597	92,133	74,873
670	178,769	82,278	86,3	103,003	93,95	75,422
675	182,118	80,281	85,3	101,068	91,953	73,499
680	185,429	78,284	84	99,133	89,956	71,576
685	188,701	74,003	82,21	93,257	84,817	67,714
690	191,931	69,721	80,2	87,381	79,677	63,852
695	195,118	70,665	78,24	89,492	81,258	64,464
700	198,261	71,609	76,3	91,604	82,84	65,076
705	201,359	72,979	74,36	92,246	83,842	66,573
710	204,409	74,349	72,4	92,889	84,844	68,07
715	207,411	67,977	70,4	84,872	77,539	62,256
720	210,365	61,604	68,3	76,854	70,235	56,443
725	213,268	65,745	66,3	81,683	74,768	60,343
730	216,12	69,886	64,4	86,511	79,301	64,242
735	218,92	72,486	62,8	89,546	82,147	66,697
740	221,667	75,087	61,5	92,58	84,993	69,151
745	224,361	69,34	60,2	85,405	78,437	63,89
750	227	63,593	59,2	78,23	71,88	58,629
755	229,585	55,005	58,5	67,961	62,337	50,623
760	232,115	46,418	58,1	57,692	52,793	42,617
765	234,589	56,612	58	70,307	64,36	51,985
770	237,008	66,805	58,2	82,923	75,927	61,352
775	239,37	65,094	58,5	80,599	73,872	59,838
780	241,675	63,383	59,1	78,274	71,818	58,324

Annex C – Calibration function values and uncertainties

For $R < 10\%$:

Wavelength λ / nm	Slope(b)	Ordinate (0,a)	u(b)	u(a)	cov(a,b)
380	0,976	0,8855	0,045284	0,274541	-0,012007
390	0,974	0,8610	0,044704	0,272512	-0,011759
400	0,971	0,8150	0,044162	0,269987	-0,011504
410	0,977	0,7347	0,043945	0,269175	-0,011410
420	0,979	0,6961	0,043792	0,268985	-0,011361
430	0,986	0,6343	0,043572	0,269266	-0,011312
440	0,990	0,5784	0,042965	0,268082	-0,011097
450	1,002	0,4813	0,036430	0,241115	-0,008404
460	1,009	0,3677	0,037121	0,244945	-0,008713
470	1,008	0,3411	0,039054	0,250782	-0,009425
480	1,039	0,1822	0,054138	0,318638	-0,016809
490	1,040	0,1686	0,054022	0,313731	-0,016508
500	1,036	0,1187	0,047586	0,271344	-0,012579
510	1,038	0,0922	0,047002	0,267067	-0,012220
520	1,040	0,0878	0,045998	0,261588	-0,011699
530	1,038	0,0894	0,044339	0,253417	-0,010904
540	1,045	0,0495	0,042906	0,246524	-0,010244
550	1,038	0,0898	0,041555	0,238698	-0,009589
560	1,032	0,1233	0,040302	0,229031	-0,008904
570	1,034	0,1157	0,038741	0,217132	-0,008088
580	1,038	0,1227	0,034837	0,196391	-0,006517
590	1,012	0,2554	0,051507	0,262559	-0,013152
600	1,008	0,2507	0,051720	0,261763	-0,013171
610	1,003	0,2866	0,052273	0,263284	-0,013397
620	1,004	0,3003	0,051872	0,261807	-0,013213
630	1,027	0,1050	0,064532	0,412770	-0,025536
640	0,991	0,3649	0,049737	0,252506	-0,012195
650	0,994	0,3605	0,049595	0,251867	-0,012126
660	0,991	0,4059	0,049350	0,251725	-0,012057
670	0,982	0,4509	0,047909	0,248122	-0,011523
680	0,982	0,4637	0,045341	0,244361	-0,010710
690	-0,290	6,7108	0,034129	0,157228	-0,005063
700	1,009	0,3802	0,061100	0,362497	-0,021645

For $R \geq 10\%$:

Wavelength λ / nm	Slope(b)	Ordinate (0,a)	u(b)	u(a)	cov(a,b)
380	1,005	0,6174	0,026423	0,540173	-0,013355
390	1,009	0,5187	0,025737	0,578379	-0,013933
400	1,004	0,5156	0,025633	0,621158	-0,014523
410	1,005	0,4639	0,024051	0,584700	-0,012661
420	1,007	0,3845	0,022266	0,523280	-0,010275
430	1,007	0,4005	0,020487	0,451936	-0,007930
440	1,009	0,3801	0,018943	0,383773	-0,005997
450	1,010	0,3388	0,019971	0,505421	-0,008138
460	1,007	0,3139	0,019156	0,467072	-0,007042
470	1,004	0,4515	0,015191	0,289300	-0,003482
480	1,009	0,3368	0,014817	0,255967	-0,003096
490	1,013	0,2742	0,014440	0,261637	-0,003056
500	1,009	0,2219	0,010921	0,223027	-0,001906
510	1,010	0,1906	0,010550	0,222764	-0,001815
520	1,009	0,1785	0,010355	0,222941	-0,001772
530	1,006	0,2444	0,010366	0,227180	-0,001818
540	1,003	0,3819	0,010693	0,246394	-0,002088
550	1,004	0,4206	0,010959	0,276014	-0,002450
560	1,007	0,3596	0,010550	0,283983	-0,002399
570	1,006	0,3530	0,010002	0,279464	-0,002195
580	1,004	0,4014	0,009655	0,275876	-0,002061
590	1,001	0,5465	0,009103	0,229672	-0,001616
600	1,001	0,5209	0,009165	0,257728	-0,001860
610	1,002	0,4588	0,008816	0,267713	-0,001835
620	1,005	0,3886	0,008377	0,267514	-0,001702
630	1,004	0,3920	0,008032	0,265249	-0,001583
640	1,004	0,3703	0,007818	0,264472	-0,001516
650	1,004	0,3546	0,007692	0,265941	-0,001488
660	1,005	0,3675	0,007632	0,270086	-0,001495
670	1,003	0,3835	0,007608	0,276724	-0,001533
680	1,002	0,3534	0,007647	0,286715	-0,001612
690	1,000	0,3603	0,006951	0,204192	-0,000986
700	1,002	0,3738	0,007116	0,220404	-0,001121
710	0,999	0,4616	0,007097	0,205126	-0,001078
720	1,000	0,4686	0,007495	0,244876	-0,001432
730	0,999	0,4505	0,007694	0,274108	-0,001687
740	1,001	0,4295	0,007789	0,293331	-0,001850
750	1,002	0,6035	0,010025	0,365044	-0,002971
760	1,009	0,5226	0,010106	0,375171	-0,003086
770	0,995	1,0253	0,010173	0,379490	-0,003151

Annex D – Samples Tristimulus Values and its uncertainties

RAL 6018 Yellow green									
Illuminant	Illuminant A			Illuminant D65			Illuminant C		
1931	CIE tristimulus		*U i*	CIE tristimulus		*U i*	CIE tristimulus		*U i*
	X	21,29	0,08	*X*	18,66	0,07	*X*	19,05	0,07
	Y	26,79	0,09	*Y*	28,95	0,10	*Y*	28,64	0,09
	Z	4,37	0,03	*Z*	11,76	0,08	*Z*	12,57	0,10
1964	*CIE tristimulus*		*U i*	CIE tristimulus		*U i*	CIE tristimulus		*U i*
	X	22,32	0,08	*X*	19,30	0,07	*X*	19,56	0,07
	Y	26,45	0,08	*Y*	28,02	0,09	*Y*	27,65	0,09
	Z	4,02	0,04	*Z*	11,00	0,08	*Z*	11,76	0,07

GL 9010 Pure White									
Illuminant	Illuminant A			Illuminant D65			Illuminant C		
1931	CIE tristimulus		*U i*	CIE tristimulus		*U i*	CIE tristimulus		*U i*
	X	96,52	0,28	*X*	82,46	0,24	*X*	85,02	0,24
	Y	87,92	0,25	*Y*	87,55	0,26	*Y*	87,55	0,25
	Z	29,02	0,19	*Z*	88,14	0,61	*Z*	95,71	0,67
1964	*CIE tristimulus*		*U i*	CIE tristimulus		*U i*	CIE tristimulus		*U i*
	X	97,67	0,28	*X*	82,21	0,23	*X*	84,30	0,24
	Y	87,77	0,24	*Y*	87,20	0,25	*Y*	87,18	0,25
	Z	28,60	0,19	*Z*	86,57	0,61	*Z*	93,72	0,66

GL 8015 Chestnut Brown									
Illuminant	Illuminant A			Illuminant D65			Illuminant C		
1931	CIE tristimulus		*U i*	CIE tristimulus		*U i*	CIE tristimulus		*U i*
	X	12,31	0,07	*X*	9,46	0,05	*X*	9,73	0,05
	Y	9,21	0,04	*Y*	8,27	0,04	*Y*	8,31	0,04
	Z	2,25	0,02	*Z*	6,91	0,06	*Z*	7,50	0,08
1964	*CIE tristimulus*		*U i*	CIE tristimulus		*U i*	CIE tristimulus		*U i*
	X	12,22	0,07	*X*	9,24	0,05	*X*	9,45	0,05
	Y	9,14	0,04	*Y*	8,14	0,03	*Y*	8,17	0,03
	Z	2,23	0,04	*Z*	6,83	0,06	*Z*	7,39	0,05

RAL 7001-GL Silbergrau									
Illuminant	Illuminant A			Illuminant D65			Illuminant C		
1931	CIE tristimulus		*U i*	CIE tristimulus		*U i*	CIE tristimulus		*U i*
	X	34,94	0,11	*X*	31,03	0,09	*X*	32,07	0,10
	Y	32,63	0,10	*Y*	33,17	0,10	*Y*	33,14	0,10
	Z	12,76	0,08	*Z*	39,18	0,25	*Z*	42,56	0,28
1964	*CIE tristimulus*		*U i*	CIE tristimulus		*U i*	CIE tristimulus		*U i*
	X	35,46	0,11	*X*	31,07	0,09	*X*	31,92	0,09
	Y	32,72	0,09	*Y*	33,34	0,10	*Y*	33,33	0,10
	Z	12,66	0,08	*Z*	38,73	0,25	*Z*	41,92	0,27

RAL 3000-GL Feuerrot									
Illuminant	Illuminant A			Illuminant D65			Illuminant C		
1931	CIE tristimulus		*U i*	CIE tristimulus		*U i*	CIE tristimulus		*U i*
	X	30,92374	0,111023	*X*	20,49	0,07	*X*	20,99	0,08
	Y	17,69343	0,061047	*Y*	13,46	0,05	*Y*	13,59	0,05
	Z	2,249114	0,022752	*Z*	6,90	0,06	*Z*	7,50	0,08
1964	*CIE tristimulus*		*U i*	CIE tristimulus		*U i*	CIE tristimulus		*U i*
	X	29,78	0,11	*X*	19,29	0,07	*X*	19,67	0,07
	Y	17,47	0,06	*Y*	13,04	0,04	*Y*	13,13	0,04
	Z	2,23	0,04	*Z*	6,83	0,06	*Z*	7,39	0,05

RAL 2003-GL Pastellorange									
Illuminant	Illuminant A			Illuminant D65			Illuminant C		
1931	CIE tristimulus		*U i*	CIE tristimulus		*U i*	CIE tristimulus		*U i*
	X	68,49	0,23	*X*	47,77	0,16	*X*	48,87	0,16
	Y	45,83	0,14	*Y*	37,05	0,11	*Y*	37,50	0,12
	Z	3,62	0,03	*Z*	10,73	0,09	*Z*	11,61	0,11
1964	*CIE tristimulus*		*U i*	CIE tristimulus		*U i*	CIE tristimulus		*U i*
	X	67,36	0,22	*X*	45,92	0,15	*X*	46,78	0,15
	Y	44,87	0,14	*Y*	35,22	0,11	*Y*	35,55	0,11
	Z	3,50	0,04	*Z*	10,46	0,08	*Z*	11,29	0,08

Annex E – Samples Chromaticity Coordinates and its uncertainties

RAL 6018 Yellow green									
Illuminant	Illuminat A			Illuminat D65			Illuminat C		
1931	Chromaticity Coord.		*U i*	Chromaticity Coord.		*U i*	Chromaticity Coord.		*U i*
	x	0,406	0,001	*x*	0,314	0,001	*x*	0,316	0,001
	y	0,511	0,001	*y*	0,488	0,001	*y*	0,475	0,001
	z	0,083	0,001	*z*	0,198	0,001	*z*	0,209	0,001
1964	Chromaticity Coord.		*U i*	Chromaticity Coord.		*U i*	Chromaticity Coord.		*U i*
	x	0,423	0,001	x	0,331	0,001	x	0,332	0,001
	y	0,501	0,001	y	0,480	0,001	y	0,469	0,001
	z	0,076	0,001	z	0,189	0,001	z	0,199	0,001

GL 9010 Pure White									
Illuminant	Illuminant A			Illuminant D65			Illuminant C		
1931	Chromaticity Coord.		*U i*	Chromaticity Coord.		*U i*	Chromaticity Coord.		*U i*
	x	0,452	0,001	*x*	0,319	0,001	*x*	0,317	0,001
	y	0,412	0,001	*y*	0,339	0,001	*y*	0,326	0,001
	z	0,136	0,001	*z*	0,341	0,002	*z*	0,357	0,002
1964	Chromaticity Coord.		*U i*	Chromaticity Coord.		*U i*	Chromaticity Coord.		*U i*
	x	0,456	0,001	*x*	0,321	0,001	*x*	0,318	0,001
	y	0,410	0,001	*y*	0,341	0,001	*y*	0,329	0,001
	z	0,134	0,001	*z*	0,338	0,002	*z*	0,353	0,002

GL 8015 Chestnut Brown									
Illuminant	Illuminat A			Illuminat D65			Illuminat C		
1931	Chromaticity Coord.		*U i*	Chromaticity Coord.		*U i*	Chromaticity Coord.		*U i*
	x	0,518	0,002	*x*	0,384	0,002	*x*	0,381	0,002
	y	0,387	0,002	*y*	0,336	0,002	*y*	0,325	0,002
	z	0,095	0,001	*z*	0,280	0,002	*z*	0,294	0,002
1964	Chromaticity Coord.		*U i*	Chromaticity Coord.		*U i*	Chromaticity Coord.		*U i*
	x	0,518	0,002	x	0,382	0,002	x	0,378	0,001
	y	0,387	0,002	y	0,336	0,001	y	0,327	0,001
	z	0,094	0,002	z	0,282	0,002	z	0,296	0,001

RAL 7001-GL Silbergrau									
Illuminant	Illuminant A			Illuminant D65			Illuminant C		
1931	Chromaticity Coord.		*U i*	Chromaticity Coord.		*U i*	Chromaticity Coord.		*U i*
	x	0,435	0,001	*x*	0,300	0,001	*x*	0,298	0,001
	y	0,406	0,001	*y*	0,321	0,001	*y*	0,308	0,001
	z	0,159	0,001	*z*	0,379	0,002	*z*	0,395	0,002
1964	Chromaticity Coord.		*U i*	Chromaticity Coord.		*U i*	Chromaticity Coord.		*U i*
	x	0,439	0,001	*x*	0,301	0,001	*x*	0,298	0,001
	y	0,405	0,001	*y*	0,323	0,001	*y*	0,311	0,001
	z	0,157	0,001	*z*	0,375	0,002	*z*	0,391	0,002

RAL 3000-GL Feuerrot									
Illuminant	Illuminat A			Illuminat D65			Illuminat C		
1931	Chromaticity Coord.		*U i*	Chromaticity Coord.		*U i*	Chromaticity Coord.		*U i*
	x	0,608	0,001	*x*	0,502	0,001	*x*	0,499	0,001
	y	0,348	0,001	*y*	0,329	0,001	*y*	0,323	0,001
	z	0,044	0,001	*z*	0,169	0,001	*z*	0,178	0,001
1964	Chromaticity Coord.		*U i*	Chromaticity Coord.		*U i*	Chromaticity Coord.		*U i*
	x	0,602	0,001	x	0,493	0,001	x	0,489	0,001
	y	0,353	0,001	y	0,333	0,001	y	0,327	0,001
	z	0,045	0,001	z	0,174	0,001	z	0,184	0,001

RAL 2003-GL Pastellorange									
Illuminant	Illuminant A			Illuminant D65			Illuminant C		
1931	Chromaticity Coord.		*U i*	Chromaticity Coord.		*U i*	Chromaticity Coord.		*U i*
	x	0,581	0,001	*x*	0,500	0,001	*x*	0,499	0,001
	y	0,389	0,001	*y*	0,388	0,001	*y*	0,383	0,001
	z	0,031	0,001	*z*	0,112	0,001	*z*	0,118	0,001
1964	Chromaticity Coord.		*U i*	Chromaticity Coord.		*U i*	Chromaticity Coord.		*U i*
	x	0,582	0,001	*x*	0,501	0,001	*x*	0,500	0,001
	y	0,388	0,001	*y*	0,385	0,001	*y*	0,380	0,001
	z	0,030	0,001	*z*	0,114	0,001	*z*	0,121	0,001

Annex F – Samples CIELAB *L** ,*a** and b* values and its uncertainties

RAL 6018 Yellow green									
Illuminant	Illuminant A			Illuminant D65			Illuminant C		
1931	CIELAB Coordinates		*U i*	CIELAB Coordinates		*U i*	CIELAB Coordinates		*U i*
	*L**	58,76	0,26	*L**	60,72	0,20	*L**	60,44	0,19
	*a**	-32,93	0,97	*a**	-40,11	1,12	*a**	-39,95	1,06
	*b**	29,46	0,41	*b**	37,04	0,32	*b**	37,03	0,40
1964	CIELAB Coordinates		*U i*	CIELAB Coordinates		*U i*	CIELAB Coordinates		*U i*
	*L**	58,44	0,25	*L**	59,89	0,20	*L**	59,57	0,20
	*a**	-28,12	0,91	*a**	-33,06	1,04	*a**	-30,53	1,01
	*b**	31,35	0,62	*b**	37,28	0,33	*b**	35,05	0,28

GL 9010 Pure White									
Illuminant	Illuminant A			Illuminant D65			Illuminant C		
1931	CIELAB Coordinates		*U i*	CIELAB Coordinates		*U i*	CIELAB Coordinates		*U i*
	*L**	95,10	0,31	*L**	94,94	0,18	*L**	94,95	0,23
	*a**	-0,08	1,03	*a**	-1,38	0,91	*a**	-1,51	0,82
	*b**	4,67	0,73	*b**	4,89	0,94	*b**	4,86	1,00
1964	CIELAB Coordinates		*U i*	CIELAB Coordinates		*U i*	CIELAB Coordinates		*U i*
	*L**	95,04	0,30	*L**	94,80	0,19	*L**	94,82	0,24
	*a**	0,17	0,98	*a**	-0,91	0,86	*a**	2,73	0,78
	*b**	4,85	0,77	*b**	4,93	0,96	*b**	0,81	1,02

GL 8015 Chestnut Brown									
Illuminant	Illuminant A			Illuminant D65			Illuminant C		
1931	CIELAB Coordinates		*U i*	CIELAB Coordinates		*U i*	CIELAB Coordinates		*U i*
	*L**	36,37	0,28	*L**	34,53	0,06	*L**	34,61	0,16
	*a**	15,30	0,73	*a**	13,93	0,60	*a**	13,25	0,50
	*b**	10,64	0,49	*b**	7,35	0,45	*b**	7,48	0,63
1964	CIELAB Coordinates		*U i*	CIELAB Coordinates		*U i*	CIELAB Coordinates		*U i*
	*L**	36,24	0,23	*L**	34,26	0,06	*L**	34,34	0,12
	*a**	14,31	0,67	*a**	13,38	0,58	*a**	14,63	0,60
	*b**	10,37	0,85	*b**	6,82	0,43	*b**	5,19	0,31

RAL 7001-GL Silbergrau									
Illuminant	Illuminant A			Illuminant D65			Illuminant C		
1931	CIELAB Coordinates		*U i*	CIELAB Coordinates		*U i*	CIELAB Coordinates		*U i*
	*L**	63,84	0,22	*L**	64,28	0,16	*L**	64,26	0,20
	*a**	-2,90	0,76	*a**	-1,76	0,65	*a**	-1,51	0,57
	*b**	-4,46	0,52	*b**	-3,84	0,69	*b**	-3,92	0,76
1964	CIELAB Coordinates		*U i*	CIELAB Coordinates		*U i*	CIELAB Coordinates		*U i*
	*L**	63,92	0,21	*L**	64,42	0,16	*L**	64,43	0,19
	*a**	-2,88	0,73	*a**	-2,02	0,62	*a**	0,87	0,56
	*b**	-4,44	0,58	*b**	-3,68	0,70	*b**	-6,83	0,74

RAL 3000-GL Feuerrot									
Illuminant	Illuminant A			Illuminant D65			Illuminant C		
1931	CIELAB Coordinates		*U i*	CIELAB Coordinates		*U i*	CIELAB Coordinates		*U i*
	*L**	49,11	0,27	*L**	43,43	0,12	*L**	43,63	0,10
	*a**	47,00	0,60	*a**	43,60	0,49	*a**	42,06	0,41
	*b**	32,58	0,51	*b**	22,72	0,44	*b**	23,04	0,59
1964	CIELAB Coordinates		*U i*	CIELAB Coordinates		*U i*	CIELAB Coordinates		*U i*
	*L**	48,83	0,24	*L**	42,80	0,12	*L**	42,96	0,15
	*a**	42,80	0,57	*a**	40,53	0,48	*a**	41,60	0,50
	*b**	32,10	0,86	*b**	21,56	0,41	*b**	20,07	0,31

RAL 2003-GL Pastellorange									
Illuminant	Illuminant A			Illuminant D65			Illuminant C		
1931	CIELAB Coordinates		*U i*	CIELAB Coordinates		*U i*	CIELAB Coordinates		*U i*
	*L**	73,41	0,36	*L**	67,29	0,26	*L**	67,63	0,24
	*a**	41,67	0,84	*a**	38,47	0,78	*a**	35,88	0,76
	*b**	60,75	0,50	*b**	51,23	0,43	*b**	51,92	0,50
1964	CIELAB Coordinates		*U i*	CIELAB Coordinates		*U i*	CIELAB Coordinates		*U i*
	*L**	72,79	0,34	*L**	65,90	0,25	*L**	66,17	0,25
	*a**	40,32	0,81	*a**	39,53	0,75	*a**	40,57	0,75
	*b**	60,46	0,71	*b**	49,20	0,43	*b**	47,73	0,38